

1-1-2012

# Frp Bond Strength Degradation: An Experimental Study Using Pull-Off Testing

Clarisse Mikami

*Wayne State University,*

Follow this and additional works at: [http://digitalcommons.wayne.edu/oa\\_theses](http://digitalcommons.wayne.edu/oa_theses)

---

## Recommended Citation

Mikami, Clarisse, "Frp Bond Strength Degradation: An Experimental Study Using Pull-Off Testing" (2012). *Wayne State University Theses*. Paper 213.

This Open Access Thesis is brought to you for free and open access by DigitalCommons@WayneState. It has been accepted for inclusion in Wayne State University Theses by an authorized administrator of DigitalCommons@WayneState.

**FRP BOND STRENGTH DEGRADATION: AN EXPERIMENTAL STUDY USING PULL-OFF  
TESTING**

by

**CLARISSE MACHADO MIKAMI**

**THESIS**

Submitted to the Graduate School

of Wayne State University,

Detroit, Michigan

in partial fulfillment of the requirements

for the degree of

**MASTER OF SCIENCE**

2012

MAJOR: CIVIL ENGINEERING

Approved by:

---

Advisor

Date



**© COPYRIGHT BY**

**CLARISSE MACHADO MIKAMI**

**2012**

**All Rights Reserved**

## DEDICATION

*To my husband,*

*my son,*

*my daughter,*

*my father,*

*and my mother.*

## ACKNOWLEDGMENTS

*I would like to thank the following people for their support and help during my studies at Wayne State:*

*Dr. Hwai-Chung Wu, my committee chair and academic advisor. I am deeply grateful for his help, advice, guidance, and expertise.*

*Dr. Christopher Eamon, my committee member.*

*Dr. Xin Wu, my committee member.*

*Dr. Abulgasem Elarbi, for his time, help, and contribution during my lab work. I am deeply thankful for all his help.*

*Dr. John Gruber and Mr. John Lamb, for their time and help during my study. I sincerely appreciate their willingness to help.*

*Mr. Syed Ahsan, for his support and encouragement to pursue this degree.*

*I would also like to thank all the staff members of the Civil and Environmental Engineering Department at Wayne State University.*

*Finally, I would like to express my deep appreciation to my husband Eduardo, my son Felliipe and my daughter Emily for all the support and understanding, and to my parents, Luiz and Vera, for their support and encouragement during my studies.*

## TABLE OF CONTENTS

Dedication	ii
Acknowledgments	iii
List of Tables	ix
List of Figures	xi
Chapter 1 Introduction	1
1.1 General Overview	1
1.2 Material Properties and Durability	3
1.2.1 Concrete	3
1.2.2 Fiber Reinforced Polymer (FRP)	6
1.3 Objectives	10
Chapter 2 Literature Review	11
2.1 Performance of FRP Systems	11
2.2 Pull-off test	12
2.3 Environmental Effects on Bond	14
2.4 Conclusion	19
Chapter 3 Experimental Study	20
3.1 Test Specimens	20

3.1.1 Concrete Specimens Preparation and Properties	20
3.1.2 FRP Application and Properties	24
3.2 Environmental Conditioning	27
3.3 Test Procedures	30
Chapter 4 Experimental Results	41
4.1 Introduction	41
4.2 Experimental Results	42
4.2.1 Beam Conditioned to Room Temperature and Relative Humidity (in air)	42
4.2.1.1 Beam Conditioned to Room Temperature and Relative Humidity: 40 Cycles	42
4.2.1.2 Beam Conditioned to Room Temperature and Relative Humidity: 100 Cycles	44
4.2.1.3 Beam Conditioned to Room Temperature and Relative Humidity: 250 Cycles	46
4.2.2 Beam Conditioned to Room Temperature and Immersion in Distilled Water	48
4.2.2.1 Beam Conditioned to Room Temperature and Immersion in Distilled Water: 40 Cycles	48
4.2.2.2 Beam Conditioned to Room Temperature and Immersion in Distilled Water: 100 Cycles	50
4.2.2.3 Beam Conditioned to Room Temperature and Immersion in Distilled Water: 250 Cycles	52
4.2.3 Beam Conditioned to Room Temperature and Immersion in Salt Water	53
4.2.3.1 Beam Conditioned to Room Temperature and Immersion in Salt Water: 40 Cycles	53
4.2.3.2 Beam Conditioned to Room Temperature and Immersion in Salt Water: 100 Cycles	55

4.2.3.3 Beam Conditioned to Room Temperature and Immersion in Salt Water: 250 Cycles_____	56
4.2.4 Beam conditioned to 180°C and 0% relative humidity_____	58
4.2.4.1 Beam conditioned to 180°C and 0% relative humidity: 40 Cycles_____	58
4.2.4.2 Beam conditioned to 180°C and 0% relative humidity: 100 Cycles _____	60
4.2.4.3 Beam conditioned to 180°C and 0% relative humidity: 250 Cycles_____	62
4.2.5 Beam conditioned to 180°C and 100% relative humidity (in air)_____	64
4.2.5.1 Beam conditioned to 180°C and 100% relative humidity: 40 Cycles_____	65
4.2.5.2 Beam conditioned to 180°C and 100% relative humidity: 100 Cycles_____	67
4.2.5.3 Beam conditioned to 180°C and 100% relative humidity: 250 Cycles_____	68
4.2.6 Beam conditioned to 180°C and distilled water_____	70
4.2.6.1 Beam conditioned to 180°C and distilled water: 40 Cycles _____	70
4.2.6.2 Beam conditioned to 180°C and distilled water: 100 Cycles_____	72
4.2.6.3 Beam conditioned to 180°C and distilled water: 250 Cycles_____	74
4.2.7 Beam conditioned to 100°C and 0% relative humidity _____	76
4.2.7.1 Beam conditioned to 100°C and 0% relative humidity: 40 Cycles_____	76
4.2.7.2 Beam conditioned to 100°C and 0% relative humidity: 100 Cycles_____	78
4.2.7.3 Beam conditioned to 100°C and 0% relative humidity: 250 Cycles_____	79
4.2.8 Beam conditioned to 100°C and 100% relative humidity (in air)_____	81

4.2.8.1 Beam conditioned to 100°C and 100% relative humidity: 40 Cycles	81
4.2.8.2 Beam conditioned to 100°C and 100% relative humidity: 100 Cycles	82
4.2.8.3 Beam conditioned to 100°C and 100% relative humidity: 250 Cycles	84
4.2.9 Beam conditioned to 100°C and distilled water	85
4.2.9.1 Beam conditioned to 100°C and distilled water: 40 Cycles	85
4.2.9.2 Beam conditioned to 100°C and distilled water: 100 Cycles	87
4.2.9.3 Beam conditioned to 100°C and distilled water: 250 Cycles	89
4.2.10 Beam conditioned to 100°C and salt water	90
4.2.10.1 Beam conditioned to 100°C and salt water: 40 Cycles	90
4.2.10.2 Beam conditioned to 100°C and salt water: 100 Cycles	92
4.2.10.3 Beam conditioned to 100°C and salt water: 250 Cycles	93
4.3 Observations	96
Chapter 5 Conclusion	103
5.1 Conclusions	103
5.1.1 Effect of High Temperatures	103
5.1.2 Effect of Humidity	105
5.1.3 Effect of Immersion in Distilled Water	105
5.1.4 Effect of Immersion in Salt Water	106

5.2 Future Work	107
References	108
Abstract	115
Autobiographical Statement	116



## LIST OF TABLES

Table 3.1: Mix compositions of concrete [11].....	20
Table 3.2: SikaWrap® Hex 113C fiber properties [13].....	24
Table 3.3: Tyfo® S Saturant Epoxy properties [14].....	25
Table 3.4: Cured laminate properties from SikaWrap® Hex 113C [13].....	25
Table 3.5: Capacity of Positest® pull-off Adhesion Tester AT-A [45] .....	32
Table 4.1: Results for 40 cycles of room temperature and relative humidity.....	43
Table 4.2: Results for 100 cycles of room temperature and relative humidity.....	45
Table 4.3: Results for 250 cycles of room temperature and relative humidity.....	46
Table 4.4: Results for 40 cycles of room temperature and immersion in distilled water.....	48
Table 4.5: Results for 100 cycles of room temperature and immersion in distilled water.....	51
Table 4.6: Results for 250 cycles of room temperature and immersion in distilled water.....	52
Table 4.7: Results after 40 cycles of room temperature and immersion in salt water.....	54
Table 4.8: Results after 100 cycles of room temperature and immersion in salt water.....	55
Table 4.9: Results after 250 cycles of room temperature and immersion in salt water.....	57
Table 4.10: Results after 40 cycles of 180°C of temperature and 0% relative humidity.....	59
Table 4.11: Results after 100 cycles of 180°C of temperature and 0% relative humidity.....	61
Table 4.12: Results after 250 cycles of 180°C of temperature and 0% relative humidity.....	63

Table 4.13: Results after 40 cycles of 180°C of temperature and 100% relative humidity.....	65
Table 4.14: Results after 100 cycles of 180°C of temperature and 100% relative humidity .....	67
Table 4.15: Results after 250 cycles of 180°C of temperature and 100% relative humidity .....	69
Table 4.16: Results after 40 cycles of 180°C and immersion in distilled water.....	71
Table 4.17: Results after 100 cycles of 180°C and immersion in distilled water.....	73
Table 4.18: Results after 100 cycles of 180°C and immersion in distilled water.....	75
Table 4.19: Results after 100 cycles of 100°C and 0% relative humidity.....	77
Table 4.20: Results after 100 cycles of 100°C and 0% relative humidity.....	78
Table 4.21: Results after 250 cycles of 100°C and 0% relative humidity.....	80
Table 4.22: Results after 40 cycles of 100°C and 100% relative humidity .....	81
Table 4.23: Results after 100 cycles of 100°C and 100% relative humidity .....	83
Table 4.24: Results after 250 cycles of 100°C and 100% relative humidity .....	84
Table 4.25: Results after 40 cycles of 100°C and immersion in distilled water.....	86
Table 4.26: Results after 100 cycles of 100°C and immersion in distilled water.....	87
Table 4.27: Results after 250 cycles of 100°C and immersion in distilled water.....	89
Table 4.28: Test results after 40 cycles of 100°C and salt water.....	91
Table 4.29: Test results after 100 cycles of 100°C and salt water.....	92
Table 4.30: Test results after 250 cycles of 100°C and salt water.....	94

## LIST OF FIGURES

Figure 1.1: Factors affecting the durability of concrete repair systems. [5]	2
Figure 1.2: Examples of cracks in a concrete structure. [6]	5
Figure 1.3: Typical glass transition temperature for an epoxy characterized by a DSC scan [12]	8
Figure 3.1: digital scale (model # SL 3000) and table vibrator	21
Figure 3.2: Concrete mixers used	22
Figure 3.3: Molds used for all beam specimens	22
Figure 3.4: Compressive strength test using MTS-290 machine	23
Figure 3.5: Compressive strength test using Forney compression testing machine	23
Figure 3.6: Concrete surface preparation	26
Figure 3.7: SikaWrap® Hex 113C used	26
Figure 3.8: Mixing resin with drill	27
Figure 3.9: Application of carbon fiber to concrete beam	27
Figure 3.10: Tenney environmental chamber (model # T10RC-1.5SPL) used to provide high temperatures and 100% relative humidity	28
Figure 3.11: Lab oven (Quincy Lab, model # 21-350) used to provide high temperatures and 0% relative humidity	29
Figure 3.12: Conditioning performed during experimental program	30
Figure 3.13: Failure locations	31
Figure 3.14: Positest® pull-off Adhesion Tester AT-A [45]	33



Figure 4.8: Pull-off tests on beam after 250 cycles of room temperature and relative humidity.....	47
Figure 4.9: Dollies show cohesive failures and single mixed failure after 250 cycles of room temperature and relative humidity.....	47
Figure 4.10: Beam conditioned to 40 cycles (80 hours) of room temperature and distilled water.....	49
Figure 4.11: Pull-off test being performed on beam conditioned to 40 cycles of room temperature and distilled water.....	49
Figure 4.12: Dollies detached during pull-off tests.....	50
Figure 4.13: Beam conditioned to 100 cycles of room temperature and distilled water.....	51
Figure 4.14: Beam after testing with detached dollies.....	51
Figure 4.15: Beam conditioned to 250 cycles (500 hours) of room temperature and distilled water.....	52
Figure 4.16: Pull-off on beam after 250 cycles of room temperature and distilled water.....	53
Figure 4.17: Beam conditioned to 40 cycles (80 hours) of room temperature and salt water.....	54
Figure 4.18: Beam tested after 40 cycles in room temperature and salt water.....	54
Figure 4.19: Beam conditioned to 100 cycles (200 hours) of room temperature and salt water.....	55
Figure 4.20: Pull-off tests performed in beam conditioned to 100 cycles of room temperature and salt water.....	56
Figure 4.21: Beam after 250 cycles (500 hours) of conditioning under room temperature and salt water.....	57
Figure 4.22: Beam tested after 250 cycles of conditioning under room temperature and salt water. An error in the fixture attachment produced an invalid result, observed by an adhesive failure at the dolly.....	58
Figure 4.23: Beam after 40 cycles (80 hours) of 180°C of temperature and 0% relative humidity.....	59
Figure 4.24: Delamination in beam after 40 cycles of 180°C of temperature and 0% relative humidity.....	60
Figure 4.25: Dollies from beam exposed to 40 cycles of 180°C of temperature and 0% relative humidity.....	60
Figure 4.26: Beam exposed to 100 cycles of 180°C of temperature and 0% relative humidity...	61

Figure 4.27: Pull-off tests locations in beam exposed to 100 cycles of 180°C of temperature and 0% relative humidity.....	62
Figure 4.28: Dollies pulled after 100 cycles of 180°C of temperature and 0% relative humidity.....	62
Figure 4.29: Beam exposed to 250 cycles of 180°C of temperature and 0% relative humidity...	63
Figure 4.30: Beam after pull-off tests were performed.....	64
Figure 4.31: Dollies from beam exposed to 250 cycles of 180°C of temperature and 0% relative humidity .....	64
Figure 4.32: Beam after exposure to 40 cycles of 180°C of temperature and 100% relative humidity.....	65
Figure 4.33: Pull-off testing locations on beam exposed to 40 cycles of 180°C of temperature and 100% relative humidity.....	66
Figure 4.34: Pulled dollies at their respective testing locations.....	66
Figure 4.35: Failure planes on each dolly for 40 cycles of 180°C of temperature and 100% relative humidity exposure.....	66
Figure 4.36: Beam after exposure to 100 cycles of 180°C of temperature and 100% relative humidity.....	67
Figure 4.37: Dollies pulled after 100 cycles of 180°C of temperature and 100% relative humidity.....	68
Figure 4.38: Beam after exposure to 250 cycles of 180°C of temperature and 100% relative humidity.....	69
Figure 4.39: Dollies pulled at their respective locations on the beam exposed to 250 cycles of 180°C of temperature and 100% relative humidity.....	70
Figure 4.40: Beam exposed to 40 cycles of 180°C of temperature and immersion in distilled water.....	71
Figure 4.41: Dollies at their testing locations on beam exposed to 40 cycles of 180°C of temperature and immersion in distilled water.....	72
Figure 4.42: View of the failure plane at dollies from the beam exposed to 40 cycles of 180°C of temperature and immersion in distilled water.....	72
Figure 4.43: Beam exposed to 100 cycles of 180°C of temperature and immersion in distilled water.....	73
Figure 4.44: Dollies at their testing locations on beam exposed to 100 cycles of 180°C of temperature and immersion in distilled water.....	74

Figure 4.45: Variability in failure modes at dollies from the beam exposed to 100 cycles of 180°C of temperature and immersion in distilled water.....	74
Figure 4.46: Beam after exposure to 250 cycles of 180°C of temperature and immersion in distilled water.....	75
Figure 4.47: Closer view of the beam exposed to 250 cycles of 180°C of temperature and immersion in distilled water.....	76
Figure 4.48: Dollies at their respective test locations showing mixed failures.....	76
Figure 4.49: Beam exposed to 40 cycles of 100°C of temperature and 0% relative humidity before testing.....	77
Figure 4.50: Beam exposed to 40 cycles of 100°C of temperature and 0% relative humidity after testing.....	78
Figure 4.51: Beam exposed to 100 cycles of 100°C and 0% relative humidity before testing.....	79
Figure 4.52: Beam exposed to 100 cycles of 100°C and 0% relative humidity after testing.....	79
Figure 4.53: Beam exposed to 250 cycles of 100°C and 0% relative humidity before testing.....	80
Figure 4.54: Beam exposed to 250 cycles of 100°C and 0% relative humidity after testing.....	80
Figure 4.55: Beam exposed to 40 cycles of 100°C and 100% relative humidity.....	82
Figure 4.56: Dollies pulled from beam exposed to 40 cycles of 100°C and 100% relative humidity.....	82
Figure 4.57: Beam exposed to 100 cycles of 100°C of temperature and 100% relative humidity.....	83
Figure 4.58: Pull-off tests on beam exposed to 100 cycles of 100°C and 100% relative humidity.....	83
Figure 4.59: Beam exposed to 250 cycles of 100°C and 100% relative humidity.....	84
Figure 4.60: Pull-off tests on beam exposed to 250 cycles of 100°C and 100% relative humidity.....	85
Figure 4.61: Failure modes on dollies after 250 cycles of 100°C and 100% relative humidity....	85
Figure 4.62: Beam tested after exposure to 40 cycles of 100°C and immersion in distilled water.....	86

Figure 4.63: Dollies from testing the beam subjected to 40 cycles of 100°C and immersion in distilled water.....	86
Figure 4.64: Beam exposed to 100 cycles of 100°C and immersion in distilled water .....	88
Figure 4.65: Beam exposed to 100 cycles of 100°C and immersion in distilled water with the tested dollies close to their testing locations.....	88
Figure 4.66: Face of dollies removed from beam exposed to 100 cycles of 100°C, 100% relative humidity and immersion in distilled water.....	88
Figure 4.67: Beam exposed to 250 cycles of 100°C and immersion in distilled water .....	88
Figure 4.68: Dollies from the beam exposed to 250 cycles of 100°C and immersion in distilled water.....	90
Figure 4.69: Faces of dollies removed from beam exposed to 250 cycles of 100°C and immersion in distilled water.....	90
Figure 4.70: Beam after conditioning .....	91
Figure 4.71: Conditioned and tested beam with dollies close to their testing locations.....	91
Figure 4.72: Beam after conditioning.....	92
Figure 4.73: Dollies from beam exposed to 100 cycles of 100°C and salt water.....	93
Figure 4.74: Beam after conditioning .....	94
Figure 4.75: Visible delamination of fiber after beam was exposed to 250 cycles of 100°C and immersed in salt water .....	95
Figure 4.76: Dollies removed during testing at each test site.....	95
Figure 4.77: Dollies showing the failure modes from beam exposed to 250 cycles of 100°C and immersed in salt water .....	96
Figure 4.78: Comparison of average pull-off strength values for all conditions at room temperature and relative humidity.....	96
Figure 4.79: Average pull-off strength values at 0% relative humidity.....	97
Figure 4.80: Average pull-off strength values at 100% relative humidity (in air).....	98



Figure 4.81 Average pull-off strength values at 180°C of temperature.....	99
Figure 4.82: Average pull-off strength values at 100°C of temperature.....	100
Figure 4.83: Average pull-off strength values showing the effect of immersion in distilled water.....	101
Figure 4.84: Average pull-off strength values showing the effect of immersion in salt water.....	102

## CHAPTER 1: INTRODUCTION

### 1.1 General Overview

All materials have a lifetime, and even though we expect them to perform well during their entire service life, periodic inspection assures that any maintenance required, either aesthetically or structurally, will not be neglected. Structural repair or strengthening may be necessary when a structure was not properly designed or constructed, when its original intended usage has changed over time, or when the structure has deteriorated due to environmental effects [11]. In repairing or strengthening concrete, steel is the traditional material used, but fiber reinforced polymer (FRP) has been employed efficiently to rehabilitate deteriorated structures and delay their overall replacement [24, 47].

Fiber reinforced polymer (FRP) is a composite material consisting of high strength fibers embedded in a polymeric resin. It offers several advantages when strengthening concrete structures, including ease of installation, corrosion resistance, negligible addition in dead load, and potential long-term durability [25, 28, 38]. Environmental factors, however, affect the durability performance of FRP [21, 24]. These conditions may consist of high temperatures, high humidity, salt water, chemicals, and freeze-thaw cycles [38].

According to FRP manufacturers, such as Sika and Fyfe Co., FRP should not be applied if raining, snowing, or dew condensation is expected on site. Application temperatures of saturant epoxy must range between 4°C (40°F) and 38°C (100°F). Concrete surfaces must be dry and free of surface moisture and frost, as well as sound and free of bond inhibiting materials [7, 8]. When hot temperature combined with high humidity or chloride exposure is expected during the service life of the structure, FRP application may be affected in a very detrimental manner [32]. Hygrothermal conditions have been linked with debonding between the FRP and the concrete substrate [17]. Bond durability is critical to the overall integrity of the strengthening

system, and consequently, its long-term performance [17, 21, 28]. Preventive measures must be carried out to assure good bond. For instance, proper substrate preparation and on site tests should be executed to verify that each resin batch has sufficient bond with the concrete substrate [7, 8, 9]. As shown in figure 1.1, the success of a concrete repair system is affected by the service and exposure conditions, the properties of the substrate materials, the repair method, including surface preparation, application and bond, and the repair system itself, regarding its materials properties, design and production. All these factors directly affect the durability of the concrete repair system [5].

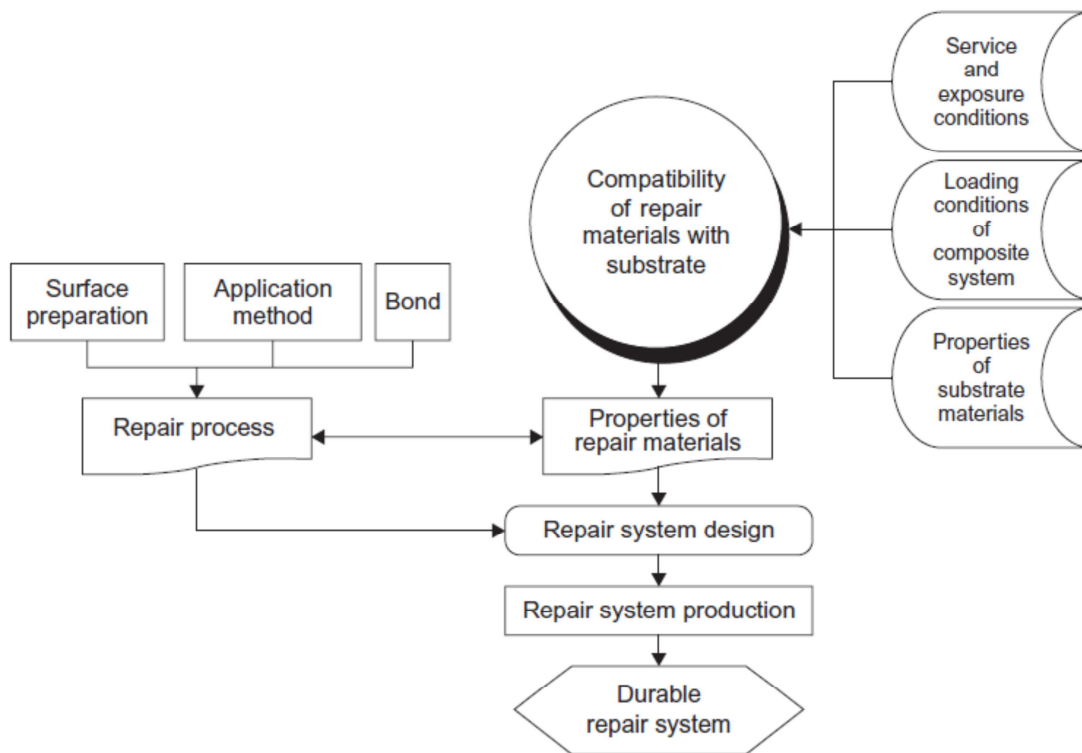


Figure 1.1: Factors affecting the durability of concrete repair systems [5].

The intrinsic variability of FRP materials combined to specific exposure conditions contributes to the continuous need of data on bond to characterize the long-term durability of structures rehabilitated with FRP systems [22, 28]. The current study intends to provide

quantitative data on bond degradation due to specific hygrothermal conditions by developing an experimental program using CFRP strengthened concrete members exposed to accelerated tests in the laboratory and assessed by pull-off tests.

## **1.2 Material Properties and Durability**

The understanding of each material's properties and aging performance provides us with a background that will lead into an efficient and economical usage of the material, as well as a better prediction on its durability. As degradation occurs; a quick, economical, efficient and durable solution is required. Fiber Reinforced Polymer (FRP) offers a practical solution for retrofitting concrete structures. Its short-term performance has been found satisfactory. However, its long-term weather durability performance is yet to be evaluated.

### **1.2.1 Concrete**

Concrete is basically composed of a hydraulic cementing material, fine and coarse aggregates and water. Other materials, known as additives, may also be added to the concrete mixture to obtain special properties [4]. Portland cement is the major cementing material used in concrete. It is composed mainly of calcium silicates, calcium aluminates, and calcium aluminoferrites, where the calcium silicates are primarily responsible for the strength that the cement will develop upon hydration. Aggregates comprise of roughly 75% of the volume of the concrete [1]. They provide dimensional stability and wear resistance. In general, aggregates are much stronger than the cement paste, and focus are placed on their soundness, grading, shape, and moisture content [1]. Adequate materials and mix design, as well as proper casting and curing will ensure the quality and durability of the concrete.

The durability of concrete is also affected by the transport of fluids into the concrete, which can be water, pure or carrying aggressive ions, carbon dioxide and oxygen [2]. The hydrated cement paste of concrete is a porous binder with an interconnected pore system

randomly distributed [6]. These interconnected capillary pores are responsible for the permeability of the hardened cement paste. The paste pore structure almost always governs the rates at which fluid movements occur through concrete [6]. Aggregates pores are usually discontinuous, and do not contribute to the permeability of the concrete [2]. Still, aggregates affect the movement of fluids into concrete by creating a tortuous path, which reduces the effective area for flow [2]. Therefore, the type of pores present in the concrete affects more its permeability than the total volume of pores in the concrete, or its porosity [2]. Discontinuous pores will cause a low permeability, even if porosity is high [2].

Permeability is a function of the water/cement ratio, the degree of cement hydration, and the properties of the cement. For instance, permeability is lower when the cement content is higher [2]. A water/cement ratio below 0.4 will produce a paste with very low permeability since the capillaries become segmented [2]. Permeability decreases with degree of hydration, and providing a wet cure will help reduce even more the water permeability. Additionally, the finer the cement, the lower the porosity of the hardened cement paste. Decreased permeability is desirable, since it improves concrete's resistance to saturation, sulfate attack, chemical attack and chloride penetration [1, 2].

In general, the strength of hardened concrete is inversely proportional to its porosity, which is directly related to the amount of mixing water used. The larger the amount of mixing water, the greater the porosity, and consequently, the concrete will have a higher permeability and lower strength [2, 3]. In good quality concrete, water can penetrate into the concrete to a certain depth, but there is no flow of water through the concrete [1].

Besides the movement of fluids in concrete by flow through the porous system, this movement also occurs by diffusion and sorption [2]. While permeability refers to flow under a

pressure differential, in the diffusion process the fluid moves under a concentration gradient [2, 15]. Sorption, on the other hand, is the result of capillary movement in the pores in concrete [2].

The water tightness of concrete is affected by cracking. Cracks must be avoided and controlled as they impair durability, structural integrity and it is undesirable aesthetically [2]. Non-structural cracks in concrete may be due to shrinkage, thermal movement, and corrosion of reinforcement, while structural cracks may be caused by overload [6]. Figure 1.2 exemplifies visually these types of cracks.

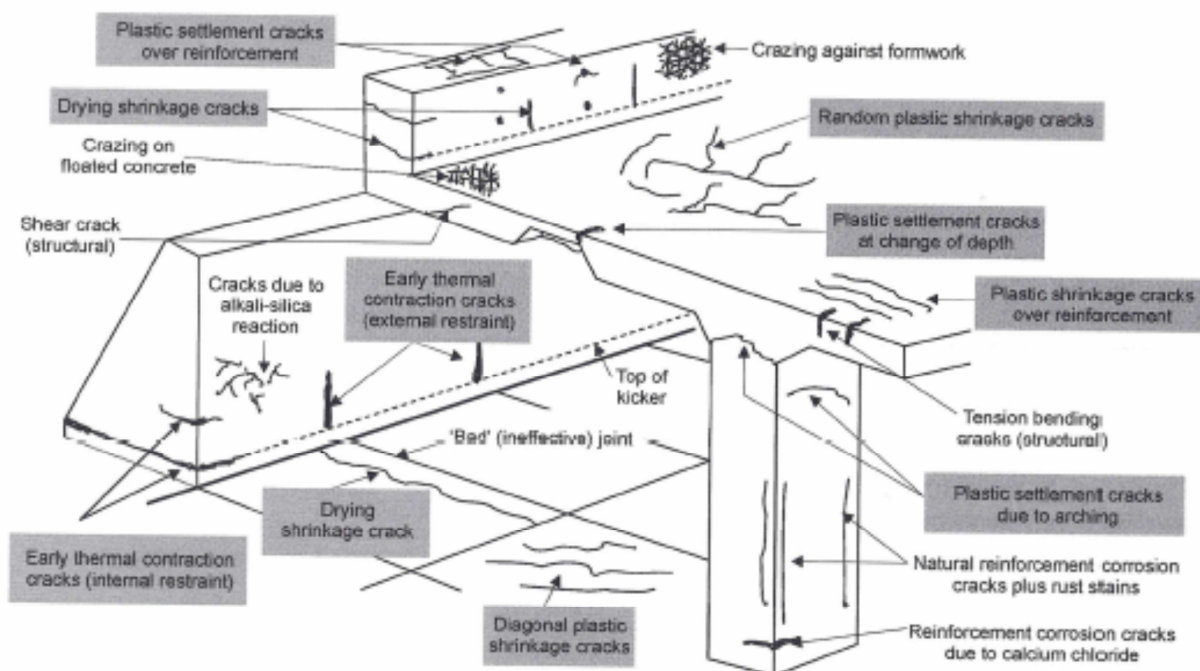


Figure 1.2: Examples of cracks in a concrete structure [6].

Shrinkage can occur when concrete is setting or after hardening [5]. Plastic shrinkage cracks occur when fresh concrete loses surface water by evaporation. Tensile stresses are developed when the water evaporates faster than the bleeding water reaches the surface [6]. Temperature, ambient relative humidity and wind influence this process, so controlling these factors during early curing, and consequently reducing this excessive evaporation will prevent this type of shrinkage [2, 5, 6]. Drying shrinkage cracks, on the other hand, is due to tensile

stresses that develop when the restrained hardened concrete loses water. Restrain is provided by reinforcing steel embedded in concrete, by the subbase or by other adjacent structural members. Drying shrinkage is affected by water/cement ratio, aggregate size, relative humidity, size of member and time. In order to control drying shrinkage, some preventive measures should be taken into account, including reducing the amount of water content in concrete, using larger aggregates, improving curing, and providing adequate reinforcement and control joints. Drying shrinkage will continue to occur at a decreasing rate during many years [2, 5, 6].

Thermal movements, if restrained, will also cause cracks. As temperature rises, concrete expands slightly, and it contracts as temperature falls. Similarly, concrete expands slightly with an increase in moisture, and contracts with a loss in moisture [1, 3]. Large concrete elements may have thermal cracks due to internal or external restrains. Internal restraint occurs when the core and the surface of the concrete heats and cools at different rates, while external restraint is commonly provided by adjacent members previously cast [2, 6].

Corrosion of reinforcement is an expansive process, which leads to internal stresses, concrete spalling, reduction of cross-sectional area of steel rebar, and possible structural failure [2]. A low permeability paste, adequate cover, suitable drainage, the use of epoxy-coated reinforcing bars, and corrosion inhibiting admixtures are some of the procedures that help minimize this problem [5].

### **1.2.2 Fiber Reinforced Polymer (FRP)**

Fiber reinforced plastic (FRP) is an advanced composite material comprised of high strength continuous fibers and a polymer resin matrix. The resin functions as an adhesive to bind the fibers together and to the substrate, as a protective layer against environmental attack, and as a medium to transfer the loads to be carried by the fibers [10, 11]. The properties of these materials may vary widely, and should be obtained from each manufacturer.

Glass and carbon fibers are the principal synthetic fiber materials used to manufacture FRP products used in structural engineering. The polymer resins most used are thermosetting epoxies, polyesters and vinyl-esters.

Glass fibers are mainly composed of silica dioxide. Individual filaments are coated by a sizing for protection and bonding enhancement between the glass fiber and the polymer resin used to make the glass-reinforced FRP composite material. Glass fibers are excellent thermal and electrical insulators, and are the most inexpensive of the high-performance fibers. However, glass fibers are affected by moisture, and susceptible to creep rupture and loss of strength under sustained stresses [10].

Carbon fibers can be formed from a natural cellulosic rayon textile fiber, a synthetic polyacrylonitrile textile fiber or pitch. These fibers are also sized to improve bonding with the resin. Carbon fibers are very durable and perform well in hot and moist environments and when subjected to fatigue loads [10]. Comparing carbon fibers to glass fibers, carbon fibers exhibit higher strength and stiffness [27]. They also have excellent chemical resistance and temperature performance, but they have low abrasion resistance and when in contact to metallic materials, a galvanic cell can develop, which may lead to degradation of the polymer resin in the FRP composite and corrosion of the metallic material [10, 27].

The polymer resin, also called matrix or binder, is the non fibrous part of the FRP composite material. It consists of macromolecules held together by covalent bonds in chains [10]. Polymers can be classified as thermosetting or thermoplastic. Thermosetting polymers are cross-linked, where the molecular chains are joined to form a continuous three-dimensional network by strong covalently bonded atoms, so once solid, it cannot be heated and softened to be reformed. Thermoplastic polymers, conversely, are not cross-linked, and the molecular



chains are held together by weak van der Waals forces or by hydrogen bonds, which can be reshaped when heated [9, 10].

Polymers are semicrystalline solids containing noncrystalline amorphous regions [10]. They undergo other thermal transitions at temperatures below their melting point. At a temperature called glass transition temperature,  $T_g$ , the mobility of the polymer chains increases and the material changes from rigid (or glassy) to a viscous (or rubbery) state [12]. This characteristic is extremely important in the performance of the FRP composite. Operating temperatures must be below the glass transition temperature of the polymer. At temperatures above  $T_g$ , the modulus of the resin and the strength of the FRP decreases [10]. The glass transition temperature of a polymer can be measured using differential scanning calorimetry (DSC). In this method, the glass transition temperature is defined as the midpoint temperature of an endothermic transition region in the heat flow [12]. Figure 1.3 shows a typical glass transition temperature for an epoxy [12].

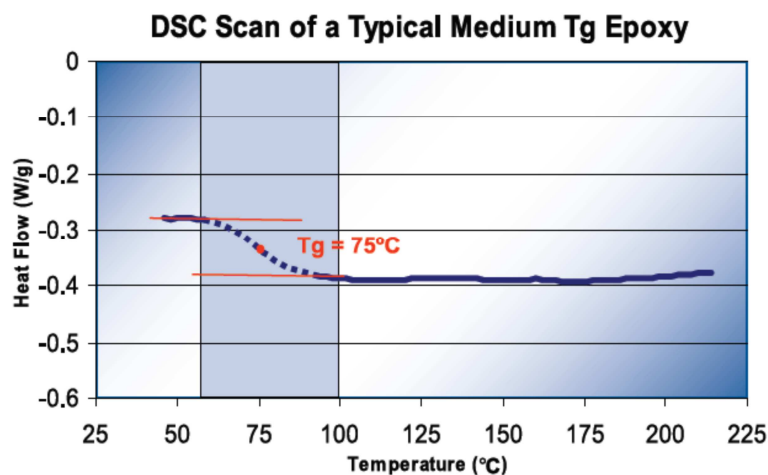


Figure 1.3: Typical glass transition temperature for an epoxy characterized by a DSC scan [12].

Polymer resins exhibit viscoelastic behavior, showing elastic or glassy behavior at ambient temperatures, and viscous behavior with a corresponding change in the time dependence of the modulus when exposed to moisture at elevated temperatures [27]. They creep under sustained stresses and relax under constant strains [10]. Polymer resins are good insulators and do not conduct heat or electricity provided that they have low void ratios [10]. Thermosetting resins are not suitable for use at temperatures greater than 180°C (350°F) and in fires if not protected or combined with fire-retarding additives, while thermoplastic polymers have been developed for high temperatures up to 450°C (800°F) [10].

Fiber reinforced plastic (FRP) is used to increase the load-carrying capacity and ductility of a deficient or deteriorated structure. When FRP is applied to the underside (tension face) of a beam, it increases the flexural capacity of the beam, and when it is applied to the side of the beam, it increases its shear capacity. Columns, on the other hand, need to be confined or wrapped by the fibers to enhance their axial capacity and ductility [9].

There are primarily two methods to attach FRP composite materials to a concrete structure for retrofitting purposes: using pre-manufactured rigid FRP strips or bars adhesively bonded to the surface of the member, or using flexible dry fiber fabrics or sheets and liquid polymers to attach the FRP on the surface of the structural member. Pre-manufactured systems are produced in the factory using carbon or glass fibers and thermosetting resins, such as epoxy or vinyl-ester, cured at high temperatures and then bonded to concrete on site at ambient temperature using an epoxy adhesive. The formed-in-place system, also known as hand layup or wet layup, uses dry fibers sheets or fabrics saturated by a thermosetting resin in the field at ambient temperature at the time it is installed. In this method, the FRP composite is formed by laying up layers of fibers impregnated by a liquid polymer resin, which then cures in place to form a solid FRP composite element [1, 10].

The general procedures for the hand layup method start by preparing the surface. A primer sealant is then applied. Putty may be used to fill any surface depressions. The surface is coated with a thin layer of the liquid resin using a fabric roller. An appropriate length of the fiber sheet is cut and applied. Hand rollers are used to press the fiber sheet into the resin, removing air bubbles and excess resin from the composite. More resin can be applied if not enough was applied initially. Additional layers of impregnated fibers will be applied as designed. The rate of installation depends on the pot life of the resin. Typically, epoxy has a pot life of 1 to 4 hours between 15°C and 27°C (60°F and 80°F) before beginning to gel and cure. At higher temperatures, the pot life decreases, and at low temperatures, some resins may not cure. Finished application should be protected from environmental conditions while curing, but direct contact between finished application and protective sheeting should not be allowed [8, 10].

The quality of the composite depends on the adhesive polymer used, the preparation of the concrete surface prior to the application of FRP, and the correct installation. Proper bond is essential to guarantee a good performance of the FRP strengthening system.

### **1.3 Objectives**

A concrete repair must resist structural loading and environmental conditions without degradation and deterioration [1]. As bond at the interfacial region between FRP and concrete is essential for the durability of the FRP repair or strengthening system, the focus of this study is on bond. Therefore, an experimental program was developed to study the effect of long-term environmental exposure on bond strength. Pull-off testing was used to generate quantitative data on the CFRP bond degradation, as well as a continuation and comparison to previous work performed at Wayne State University. Besides cyclic hygrothermal (temperature and humidity) conditions, the possibility of further degradation with the presence of distilled water and salt water was also investigated.

## CHAPTER 2: LITERATURE REVIEW

### 2.1 Performance of FRP systems

The mechanical properties of an FRP system are prone to degradation under high temperatures, high humidity, salt water, chemicals, ultraviolet (UV) light, freeze-and-thaw cycles, and alkaline environments [18, 38]. During installation of an FRP system, daily inspection should be conducted. ACI 440.2R [16] recommends keeping records for a minimum of 10 years of the current ambient conditions on the site, including temperature, relative humidity and general weather observations. Additionally, the surface condition, such as dryness, cleanliness and preparation, the installation procedures, batch characteristics, and the location and size of any air voids or delaminations must be documented [16].

Pull-off test results and tests of field sample panels or witness panels are used to evaluate the installed FRP system. Tension adhesion testing should be conducted according to ACI 503R [39] or ASTM D4541 [41]. Tension strengths should exceed 1.4 MPa (200psi) and exhibit a failure of the concrete substrate [16]. Witness panels are used to evaluate the tensile strength and modulus, lap splice strength, hardness, and  $T_g$  of the FRP. Tests on the FRP materials, such as tensile strength,  $T_g$ , and adhesive shear strength, can be sent to a laboratory, while pot life of resins and curing hardness may be conducted on site [16].

Performance of FRP strengthened structures depends on the efficiency of the bond, which is directly affected by the roughness of the surface [11]. Therefore, proper preparation of the concrete substrate is necessary to ensure a good bonding interface between fiber and substrate. Voids or uneven areas require proper care before epoxy is applied.

Moisture entrapment is another performance concern. FRP systems should not be applied to concrete surfaces that are subject to moisture vapor transmission [16]. If the movement of vapor in the concrete becomes trapped at the interface of a permeable concrete

and an impermeable barrier, it will lead to debonding [1]. Adequate means should be provided to allow moisture to escape from the concrete structure [16]. The manufacturer of the carbon fiber used in this research (SikaWrap® Hex 113C), for example, specifies in its data sheet that this system is a vapor barrier, and consequently, concrete should not be encapsulated in areas of freeze and thaw [13].

Furthermore, other effects of environmental conditions must also be addressed with care. FRP systems in contact with moisture and temperature cycles, for instance, are expected to have a lower durability due to the deterioration of the bond [17]. Many studies exist on bond characterization, and on the effects of environmental exposure on FRP strength [17, 23]. Still, long term behavior of FRP strengthening is not fully understood. The performance of the strengthened structure must be guaranteed during the entire service life, which can be reached through constant on site inspection of this material over time and further research.

## **2.2 Pull-off test**

The pull-off test is one of the most common tensile test methods used to measure the bond strength between FRP and concrete [23, 34]. It is a partially destructive test that produces a localized damage, which does not weaken the member to any significant extent [15]. This test is used both to measure the strength of the concrete substrate before application of the FRP system, and after the FRP is installed to evaluate if the bond is satisfactory.

According to Malhotra et al. [15], the tensile force required to pull a metal disk with a layer of concrete from the surface to which it is attached is related to the compressive strength of the concrete. Bonaldo et al. [34] also observed that the strength of the substrate plays a major role in the pull-off strength, and when fracture occurs in the concrete substrate, the pull-off strength is related to the tensile strength of the concrete.

The pull-off test is conducted by bonding a metal fixture (dolly) to the surface of FRP, and using a loading device to apply an increasing tensile force until the fixture is pulled off of the concrete [20, 23, 34]. Usually a partial core is cut through the coating down to the surface of the concrete substrate before testing [42]. Coring into the concrete is done by a rotary core cutting drill with diamond bits. It is important to ensure uniform pressure when the core is being drilled [34]. Results may be affected if proper coring is not performed. Orthogonality of the core drilling relative to the substrate and accuracy in positioning the metal fixture on top of the partial core are essential to reduce the eccentricity of loading [34]. Increasing the deepness of the core drilling may produce an increase in the load eccentricity and core damage generated by the vibration of the cutting drill machine [22, 34].

Typical equipments used for this test provide the tensile force necessary to pull the metal disk from the surface, and the pull-off tensile strength has to be calculated based on the diameter of the fixture.

This test is easy and simple to perform, as well as quick and convenient, and it does not cause any major damage to the surface. ACI 440 [16] recommends avoiding high-stress or splicing areas as pull-off test sites. Furthermore, cored hole can be filled with repair mortar or putty, and even repaired by an overlapping FRP sheet patch of equivalent plies immediately after taking the core sample [16].

Disadvantages of this test method may include the curing time of the adhesive, limitation of the test to each location and depth, and the inability to compare results from different equipments [15, 34]. On site tests are usually performed 24 hours after attachment of the dolly to allow for curing of the adhesive used, which may lead into an insignificant result if there is any error in installation or unexpected environmental condition [15].

### 2.3 Environmental effects on bond

Many studies have been done to evaluate the environmental effects on bond. The pull-off adhesion test offers a standard method to investigate such behaviors, but even though it has been used in a similar manner several times, due to the different equipments used, the expected variability in each equipment's results, and even the variability of the materials in each case study, results cannot be directly compared, and only trends drawn from each study are analyzed.

Malvar et al. [20], for instance, used pull-off tests to evaluate the short term effects of temperature, moisture, chloride content, and the use of primer on the CFRP adhesion. It was shown that high temperature (35°C or 95°F) and relative humidity (95%) reduce significantly the bond strength [20]. Since failure in the concrete substrate was not the goal in this study, and the tensile strengths of concrete are usually lower than adhesive strengths, the authors in this study decided to use aluminum plates as substrate instead of concrete. 13-mm aluminum dollies were then bonded to aluminum plates. Bonding of dollies was performed inside the environmental chamber. The presence of moisture during the mixing of epoxy was linked to the reaction of the water vapor with the phenolic ether (part A) and reduction of the strength of the epoxy adhesive. Test results showed that humidity reduces the epoxy adhesive strength, but on average, strengths remained above the minimum proposed by ACI 440 of 1.4 MPa (200psi). Significant decrease in bond strength was also observed in another set of experiments that used 20-mm dollies bonded to brushed concrete cube surfaces and subjected to the high temperature (38°C or 100°F) and humidity conditions (95%). At last, the chloride effect was studied by attaching 20-mm dollies to concrete piles exposed to marine environment, and it was concluded that adhesion of the epoxy without primer decreased as the surface chloride concentration increased, especially for a region subjected to splashing. Hydroblasting and the use of primer in this condition showed an improvement in adhesive strength of epoxy [20].

In 2004, Grace [18] studied the durability of externally bonded CFRP plates and fabrics exposed to independent environmental conditions, such as 100% humidity, dry heat, alkaline solution, saltwater solution, freezing-and-thawing cycles, and thermal expansion cycles. It was concluded that short-term exposure of CFRP fabrics to dry-heat (60°C) slightly increased the load-carrying capacity of the beams. Humidity and salt water had an adverse effect, causing a decrease in the load-carrying capacity of the beams, but the duration of the exposure had no significant effect. Thermal expansion cycles had no significant effect on the load carrying capacity of the beams, while freezing-and-thawing cycles reduced the load-carrying capacity by 13% [18].

The long-term structural degradation of concrete beams strengthened with GFRP and CFRP fabrics was investigated by Li et al. [24] through the use of short-term accelerated conditioning tests. High temperature and high moisture content environments were used to predict a longer-term behavior in an ambient environment. Boiling water provided the highest temperature and moisture content possible and ultraviolet (UV) radiation was added to enhance the damaging effect of temperature and moisture [24]. It was found that both water absorption at elevated temperature and intensive ultraviolet radiation reduce considerably the mechanical strength and stiffness of the FRP fabrics, but it was noted that deterioration was mainly in the polymer matrix, not on the fibers. Penetration of water into the FRP is believed to occur by diffusion through the matrix resin and capillary flow via microcracks and voids, resulting in the development of residual stress and plasticization of the resin. The elevated temperature accelerates the water diffusion process and leads to rapid degradation of FRP [24]. Therefore, the authors recommended increasing the water and aging resistance of the polymer to enhance the long-term performance of the FRP strengthened concrete structures [24].

Benzarti et al. [21] evaluated the durability of the adhesive bond between concrete and CFRP under accelerated aging conditions (40°C and 95%RH). Two sets of experiments were



investigated, where both were exposed to saturated humidity at 40°C. The first set was evaluated only using pull-off tests. It was observed that pull-off strength was significantly reduced under hygrothermal aging, and that failure mode changed over time from an initial cohesive failure within the concrete substrate towards an increasing number of mixed or adhesive failures, which was considered consistent with the substantial deterioration seen on the adhesive bond. Regarding the concrete surface preparation, bond strength values were higher with sand-blasted concrete surfaces, which is a rougher surface finish compared to the grinding finish also used. By comparing strengthened specimens prepared from carbonated concrete to non-carbonated specimens, authors concluded that carbonated specimens had a decrease in porosity of the superficial concrete layer, leading to an improvement in the mechanical properties of the substrate, a consequently higher pull-off strength values. Deterioration was caused by moisture diffusion from the concrete surface towards the adhesively bonded joint, which was restricted in carbonated samples.

In the second set of experiments from Benzarti et al. [21] paper, one of the intentions was to characterize the adhesive bond by using two different methods, pull-off and shear loading tests. In addition to that, two types of strengthening systems, carbon fiber sheets and CFRP plates, as well as the properties of each constitutive material were assessed. After exposure to 40°C and 95% humidity, concrete showed a slight increase in compressive strength, associated to the continuation of the hydration process, and the epoxy adhesive showed further cross-linking with the elevation of the temperature, but due to the moisture ingress, plasticization occurred and  $T_g$  dropped drastically after a few hours of aging, with a re-increase of  $T_g$  as sorption slows down and cross linking continues. Comparing the results from pull-off and shear tests, shear loading provided an evolution of failure modes from cohesive within the concrete substrate to a cohesive failure within the polymer joint for CFRP plate specimens, and to an interfacial failure in carbon fiber sheet specimens. These results were

attributed to the effect of aging on the polymer plasticization and bond degradation induced by water diffusion. The authors also discuss the effect of the test method used when measuring bond and their test results suggest that the shear test is a more sensitive method than the pull-off test.

Nishizaki and Kato [22] found that the adhesive pull-off strength in a carbon fiber sheet system decreased only slightly after fourteen years of outdoor exposure. Since all failures were in the concrete substrate, the authors suspected that the pull-off adhesive strength did not necessarily indicated that the properties of the bond had changed, but it could be due to a change in the mechanical properties of the concrete substrate [22].

Temperature cycles, moisture, salt fog and immersion in five percent salt water (50g/l water) were also studied by Silva and Biscaia [17] using beams strengthened with GFRP and CFRP. Temperature cycles were most detrimental, reducing the capacity of the beams by 31% at 10,000 hours. Immersion of beams strengthened with GFRP produced an improvement in concrete compressive strength. This behavior was attributed to further wet curing of the concrete substrate. The authors believe that immersion may cause beneficial effects initially due to post curing of the polymers and further wet curing of concrete substrate, but at later times the degradation effects may overcome the beneficial effects of immersion in salt water. Pull out tests were used to provide comparative data on the effects of accelerated degradation on bond between FRP and concrete. The average result for GFRP strengthened slabs exposed to immersion in salt water and salt fog cycles, were 3.37 MPa and 3.58 MPa respectively, which were lower than the reference test results of 4.09 MPa. Failure occurred mainly in the concrete, with the exception of one case, when the failure occurred at the interface. In this isolated case, the specimen had been immersed in salt water for 10,000 hours, and this failure was associated to voids present between adhesive and concrete.

The hygrothermal effects in epoxy resins were investigated by Zhou et al. [35]. Fully cured epoxy samples were immersed in distilled water at different temperatures to determine the water uptake. The authors reported full saturation after 1530 hours of exposure, with no distinction due to the temperatures used. It is believed that initially water diffuses into the epoxy and breaks the inter chain Van der Waals forces, increasing mobility, swelling, and plasticizing the resin, but the water molecules can easily be removed by thermal desorption at lower temperatures. Longer exposure time, as well as higher exposure temperature, will result in residual water that cannot be easily removed due to the formation of bridges between chain segments resulting in secondary cross-linking (pseudo cross linking). In another study by Zhou et al. [36], the variation in  $T_g$  was associated to these two patterns of bound water, where the first one caused a large reduction in  $T_g$ , while the second one lessened the depression of  $T_g$ . It was also observed that the depression of  $T_g$  was greatest when epoxy first reached saturation, and post saturation time contributed to a gradual recovery of  $T_g$ .

Elarbi [11] has examined the effect of hygrothermal environmental conditions on the durability performance of FRP strengthened concrete beams, using 100°C and 180°C of temperature, and 0% or 100% relative humidity. In his studies, the behavior of the neat resin was also investigated. It was found that the flexural strength of Tyfo<sup>®</sup> S Saturant epoxy material improves when exposed to 100°C of temperature up to 250 cycles (500 hours), and decreases at 180°C. Coloration of epoxy beam specimens changed as they were conditioned, reaching the darkest color at 180°C and 0% relative humidity. No degradation occurred for any specimen that was strengthened by SikaWrap<sup>®</sup> Hex 113C CFRP and exposed to 100°C. At 180°C, both flexural and compressive strength decreased and FRP delamination was the dominant failure mode. It was concluded that both the deflection of the epoxy beam specimens, and the flexural strengths of the FRP strengthened beams at 250 cycles were higher at 0% relative humidity compared to 100% relative humidity for the same number of cycles.

## **2.4 Conclusion**

Long term exposure to environmental effects, such as high temperatures and humidity, seems to affect in a detrimental manner the bond interface between fiber and concrete substrate in a strengthening system. Bond quality and matrix durability are essential factors to ensure that FRP will perform well during its service life. Although many researchers have investigated the issues that may lead into deterioration of this interfacial region, due to the wide intrinsic variability in advanced composite materials, further data and confirmation of the trends obtained from previous research to all available materials seems to be imperative.

In order to create comparable data to Elarbi's [11] research, the main focus in this research was to expose CFRP strengthened beams to hygrothermal conditions and test their bond strength after conditioning using the pull-off test method. However, besides high temperatures and relative humidity, as used in Elarbi's work, the presence of water, both plain and salt water, was included in the experimental program developed herein.

## CHAPTER 3: EXPERIMENTAL STUDY

### 3.1 Test Specimens

This experimental program constitutes of 30 plain concrete beam specimens strengthened using the Sika carbon fiber, SikaWrap® Hex 113C, and the Fyfe epoxy, Tyfo® S Saturant Epoxy, and conditioned under cyclic temperature and constant humidity, as well as immersed in distilled water and salt water. Five aluminum dollies were attached to each beam after conditioning, which provided a total of 150 pull-off tests.

#### 3.1.1 Concrete Specimens Preparation and Properties

Concrete beams were cast using Type I Portland cement, ½" limestone, 3/8" P-stone and 2-NS sand in the same manner as in the previous research done at Wayne State University by A. M. Elarbi [11]. The intention was to give continuity and have similar parameters to create comparable results between the different testing methods used in this research and his research. Thus, the concrete mix design used was 1: 3.2: 1.95: 0.53 (cement: coarse aggregate: fine aggregate: water). Details of the design of this mix can be found in Elarbi's research titled "Durability Performance of FRP Strengthened Concrete Beams and Columns Exposed to Hygrothermal Environment" [11]. Table 1 was reproduced from his research and shows the mix compositions of concrete.

Concrete Material	Quantity (kg/m <sup>3</sup> )
Type I Portland cement	353
Crushed Lime-Stone (Coarse Aggregate)	566.75
P-Stone (Coarse Aggregate)	566.75
2-NS Sand (Fine Aggregate)	687.0
Water	187.0

Table 3.1: Mix compositions of concrete [11]

The procedures were followed cautiously to make sure that there was no difference in the concrete produced. Beams used in this research were made from four different batches. In the first two batches a small mixer with a revolving paddle was used, but as more beams were needed, extra molds had to be built to ensure that more specimens could be cast at one time. A larger mixer with a revolving drum was used for the last two batches. Mixing sequence and procedure did not vary from batch to batch.

Elarbi's [11] research and the ASTM C192 [44] were used as a reference to cast the concrete members. All concrete constituents were weighted using a digital scale. Dry components were first mixed for one minute before the addition of water [11]. Figures 3.1 and 3.2 shows the equipments used during concrete specimens' production.



Figure 3.1: digital scale (model # SL 3000) and table vibrator.

For easy handling, the size of the rectangular beam used was 65mm x 30mm x 300mm (2.5in x 1.25in x 12in). Minimum releasing agent (oil) was applied to coat the molds before use to avoid contamination. A table type external vibrator and a steel rod were used for compaction.

Specimens were vibrated until all air bubbles stop bursting up. A water storage tank was used to provide a wet-curing. Specimens were cured for 28 days. Figure 3.3 shows the molds used.



Figure 3.2: Concrete mixers used



Figure 3.3: Molds used for all beam specimens.

Standard compressive-strength tests of 4in diameter by 8in high cylindrical column samples were done using both a MTS-290 testing machine, and a Forney compression testing machine, as shown respectively in figures 3.4 and 3.5, to guarantee that the compressive strength matched Elarbi's average compressive strength of 38MPa (5502psi) at 28 days.





Figure 3.4: Compressive strength test using MTS-290 machine



Figure 3.5: Compressive strength test using Forney compression testing machine



### 3.1.2 FRP Application and Properties

Material selection was based on availability in the lab, and similarity with Elarbi's research. The carbon fiber used was from Sika Company, called SikaWrap® Hex 113C, while the epoxy used was from Fyfe Company, called Tyfo® S Saturant Epoxy. Both materials were used according to their respective manufacturer's recommendations.

SikaWrap® Hex 113C [13] is a bi-directional (0°/90°) carbon fiber fabric. The manufacturer recommends the use of this material for structural strengthening in locations where a load increase is needed due to a design or construction defects, or a change in structural system, such as a removal of a wall [13]. In addition to that, this fiber can be used where structural parts are damaged by impact, aging or fire, or to provide seismic strengthening. It is used for shear, flexural and confinement. This flexible and lightweight fabric is ideal for confined spaces, and can be wrapped around complex shapes. Besides its high strength, it is non corrosive, alkali resistant and creates a low aesthetic impact. The properties of this fiber are reproduced on table 3.2 from the Sika product data sheet no. H35113 [13].

Color	Black
Primary Fiber Direction	0°/90° (bi-directional)
Weight per square yard	196 g/m <sup>2</sup> (5.7 oz.)
Tensile strength of the fiber	3,450 MPa (5 x 10 <sup>5</sup> psi)
Tensile modulus of the fiber	230,000 MPa (33.4 x 10 <sup>6</sup> psi)
Elongation of the fiber	1.5 %
Density of the fiber	1.8 g/cc (0.065 lbs/in <sup>3</sup> )

Table 3.2: SikaWrap® Hex 113C fiber properties [13]

Tyfo® S Saturant Epoxy [14] is a two-component epoxy matrix material used for bonding applications in composite systems for strengthening structural members. Its high elongation and long working time are excellent properties in such applications. The components are mixed according to the manufacturer's recommendations at a ratio of 100.0 parts of component A to

42.0 parts of component B by volume, or 100 parts of component A to 34.5 parts of component B by weight. Table 3.3 shows the properties Tyfo<sup>®</sup> S Saturant Epoxy provided by the Fyfe Company [7], while Table 3.4 shows the cured laminate properties (with Sikadur<sup>®</sup> Hex 300 epoxy) from the SikaWrap<sup>®</sup> Hex 113C data sheet [13].

T <sub>g</sub>	82°C (180°F)
Tensile strength	72.4 MPa (10,500 psi)
Tensile modulus	3.18 GPa (461,000 psi)
Elongation	5.0 %
Compressive strength	86.2 MPa (12,500 psi)
Compressive modulus	3.2 GPa (0.465 x 10 <sup>6</sup> psi)
Flexural strength	123.4 MPa (17,900 psi)
Flexural modulus	3.12 GPa (452,000 psi)

Table 3.3: Tyfo<sup>®</sup> S Saturant Epoxy properties [14]

Tensile strength of laminate	456 MPa (66,000 psi)
Tensile modulus of laminate	41,400 MPa (6.0 x 10 <sup>6</sup> psi)
Elongation at break	1.2 %
Thickness	0.25 mm (0.010 in)

Table 3.4: Cured laminate properties from SikaWrap<sup>®</sup> Hex 113C [13]

The carbon fiber reinforced polymer (CFRP) was laminated using the wet lay-up process. Concrete specimens were allowed to air dry for 48 hours after removal from water tank. Concrete surface was prepared to ensure good bonding between concrete substrate and fiber. A clean and dry surface was required. Typically, a light sandblast or grinding is sufficient to prepare the surface for bonding. A Ryobi orbit palm sander and a wire brush were used to create the roughened texture necessary for bonding, as shown in figure 3.6. The surface was then cleaned to remove any dust [7].

The bi-directional carbon fiber fabric was cut according to the beam length using a heavy duty scissor. Figure 3.7 shows the SikaWrap® Hex 113C used.



Figure 3.6: Concrete surface preparation.

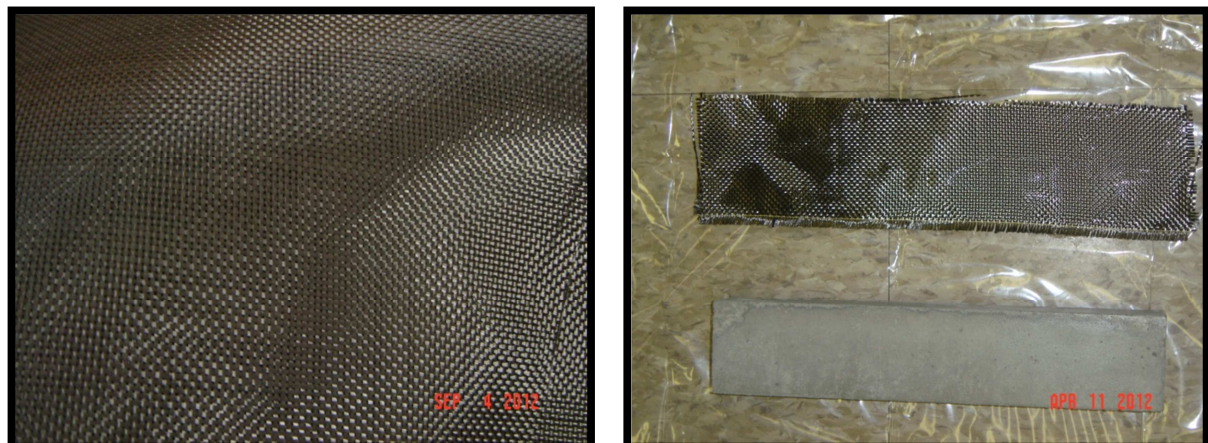


Figure 3.7: SikaWrap® Hex 113C used.

Each component of the Tyfo® S Saturant was measured by weight at a ratio of 100: 34.5 (A: B), and mixed together using a drill with a mixer beater on low speed for 5 minutes. The epoxy was applied to the concrete surface beam and the pre-cut fiber using a roller. Once saturated, the fabric was attached to the surface of the concrete. More epoxy was then applied on top, and another roller was used to smooth out air pockets and excess epoxy. A single layer of carbon fiber fabric was used. This CFRP laminate was cured in air at room temperature for

14 days. Figures 3.8 and 3.9 show the preparation and application of CFRP to the concrete specimen.



Figure 3.8: Mixing resin with drill.

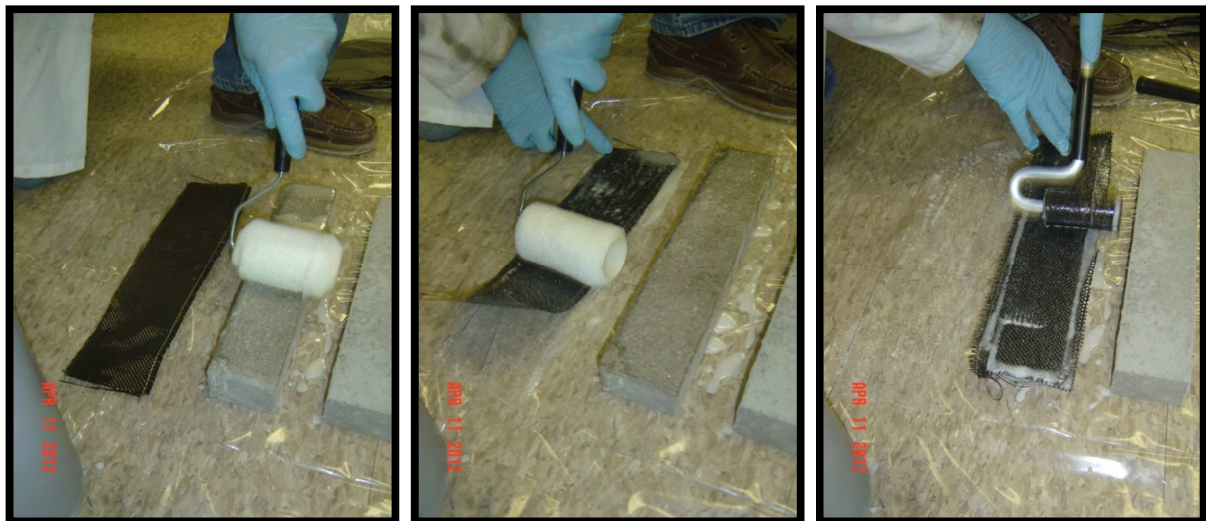


Figure 3.9: Application of carbon fiber to concrete beam.

### 3.2 Environmental Conditioning

Concrete strengthened with FRP composite sheets are subjected to environmental conditions during its service life that may affect their performance. Temperature, humidity, and the presence of water are expected to play a significant role on the durability of the system. Durability issues occur if the bond between concrete and FRP is deteriorated. In order to study

the degradation of this interfacial region, specimens were conditioned to high temperatures and humidity, and immersed in distilled water and salt water. These accelerated tests were carried out under conditions more severe than those expected under the most extreme service environments [27] to simulate the long term effects in a short period of time.

Initially, based on the higher bond degradation found at Elarbi's research, only the 180°C (356°F) temperature was going to be studied, however due to the large delamination found on the first specimens conditioned, reducing the possibility to acquire the necessary bond strength readings, 100°C was also added to this experimental program.

A Tenney environmental chamber was used to expose specimens to either 100°C (212°F) or 180°C (356°F) at 100% relative humidity, and a laboratory oven was used to subject the beams to 0% relative humidity at both temperatures. Figures 3.10 and 3.11 show both equipments used.



Figure 3.10: Tenney environmental chamber (model # T10RC-1.5SPL) used to provide high temperatures and 100% relative humidity.





Figure 3.11: Laboratory oven (Quincy Lab, model # 21-350) used to provide high temperatures and 0% relative humidity.

Even though Elarbi [11] has found no significant effect caused by the two cycle frequencies, cycles were carried out in this research to ensure compatibility to his previous work. The two hour thermal cycles consisted of 15 minute ramp time (from 25°C to the desirable temperature, either 100°C or 180°C), 75 minute constant temperature and 30 minute ramp down (back to 25°C). Relative humidity was kept constant throughout the cycle periods at either 100% or 0%. Figure 3.12 shows a summary of the conditions used in a chart format.

The same conditions were employed for 40, 100 and 250 cycles. Room temperature (77°F) and relative humidity (25%) conditions provided control samples. Besides temperature and humidity, specimens were immersed in plain (distilled) water and salt water (5% NaCl by mass).

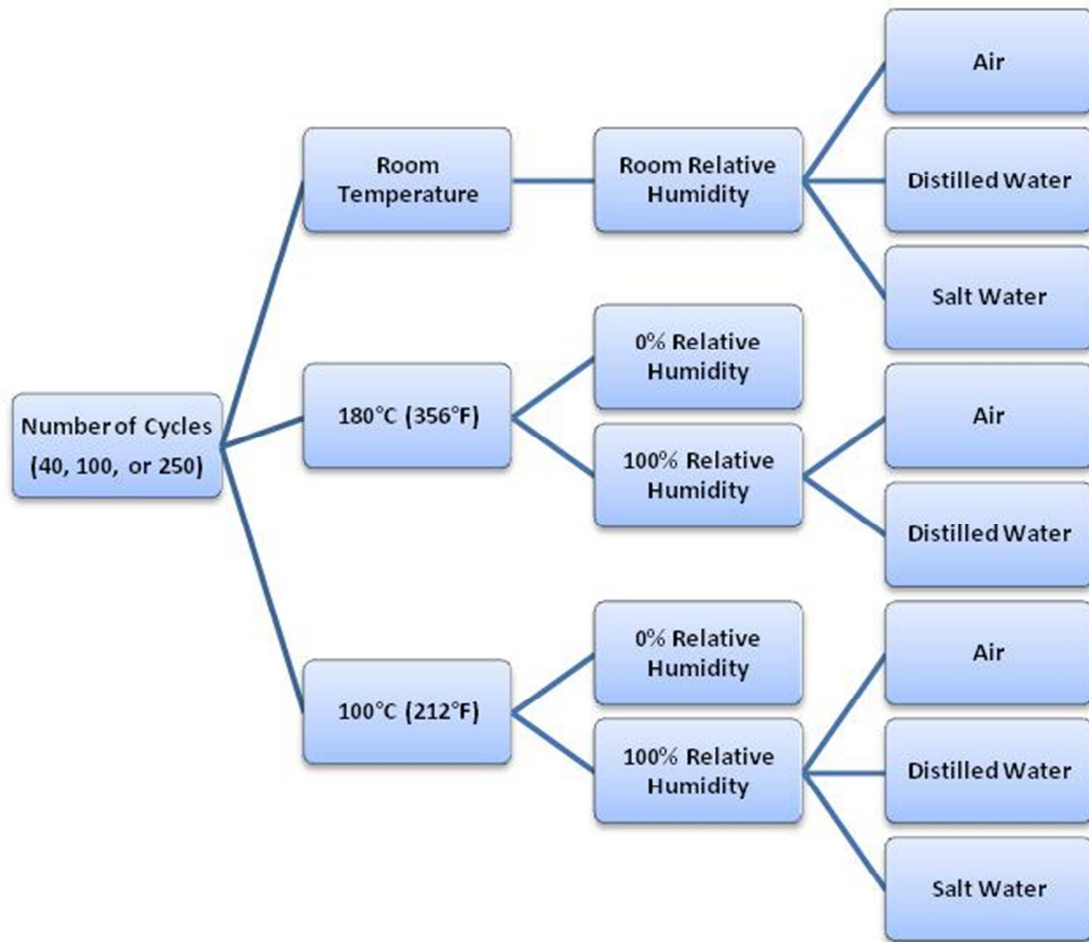


Figure 3.12: Conditioning performed during experimental program.

### 3.3 Test Procedures

As the goal of this experimental work was to study the bond strength between concrete and FRP laminate after exposure to detrimental conditions, the pull-off test method, using a Positest® Pull-off Adhesion Tester, was chosen to assess the adhesion strength between the CFRP and the existing concrete substrate of each conditioned beam specimen.

The pull-off test is a simple tensile bond test method, commonly used on site for quality control, and in the laboratory to evaluate the material properties and failure modes [34]. Failure occurs along the weakest plane within the system, which can be the concrete substrate, at the

bond interface, at the repair overlay, at the epoxy used to bond the dolly to the core, or as a combination of these failure modes [34, 41]. Figure 3.13 shows a simplified sketch of the possible failure locations.

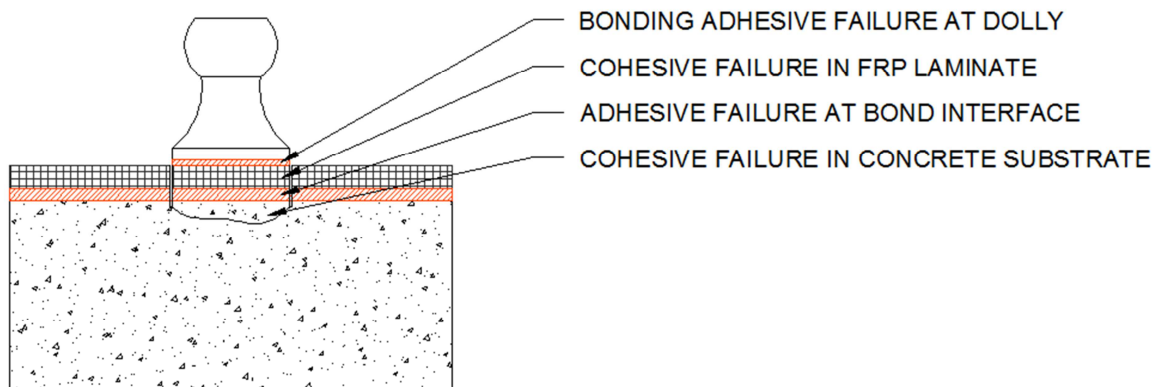


Figure 3.13: Failure locations.

The pull-off test provides the true bond strength when failure occurs at the adhesion material [34]. Thus, to conclude that there is a loss in bond between FRP and concrete substrate due to the environmental conditions applied in this research, this adhesive failure was expected. In practice, the desirable failure mode is a cohesive failure in the concrete substrate, which is expected to be the weakest link in the system, confirming that the FRP laminate used for repair is satisfactory.

ASTM provides standards to execute the pull-off test procedure. According to Malvar et al. [20], ASTM D 4541 [41] can be used for determining CFRP adhesion, evaluating concrete tensile strength, and studying the effect of contamination on the adhesion of a coating to the surface. [20] ACI 440.2R [16] recommends that tension adhesion testing of cored samples be conducted in bond-critical applications using the methods in ACI 503R, or ASTM D4541, or ACI 440.3R.[16] Other researchers, such as Silva & Biscaia [19] and Benzarti et al. [21] have used the European Standard EN 1542 for such tests. Nishizaki & Kato [22], on the other hand,



performed the pull-off tests as prescribed by ASTM D 7234 [42], while Gartner et al. [23] suggested the use of ASTM D 7522 [40]. In the current study, due to size limitation on the beam specimens, and the desire to increase the accuracy of readings, an automatic tester was chosen as recommended by ASTM D 4541.

ASTM D4541 specifies portable adhesion testers that can be used to find the greatest perpendicular force in tension that a surface area can bear before a plug of material is detached [41]. The pull-off test is performed by attaching a loading fixture (dolly) perpendicular to the surface of the coating with an adhesive. After the adhesive is cured, a testing apparatus is fastened to the loading fixture and aligned to apply gradual tension normal to the test surface. Pull-off strength results may vary when different devices are used. Measurements depend upon both material and instrumental parameters [41].

The self-aligning adhesion tester type V, per ASTM D4541 - test method E, used in this research is fabricated by Elkometer. This equipment is called Positest<sup>®</sup> pull-off Adhesion Tester AT-A. It has a pull-off pressure capacity of 20MPa (3,000 psi) for a 20mm (0.78 in) dolly, an accuracy of  $\pm 1\%$ , and a resolution of 0.01MPa (1 psi). Table 3.4 was extracted from the Positest<sup>®</sup> pull-off Adhesion Tester manual [45] and shows its capacity according to the dolly size.

<b>Adhesion Strength</b>	<b>Dolly Size (mm)</b>	<b>Max Pull-Off Pressure</b>
	10 mm	10,000 psi (70 MPa)
	14 mm	6,000 psi (40 MPa)
	20 mm	3,000 psi (20 MPa)
	50 mm*	500 psi (3.5 MPa)

\*requires optional 50 mm accessory kit

Table 3.5: Capacity of Positest<sup>®</sup> pull-off Adhesion Tester AT-A [45]

The Positest® pull-off Adhesion Tester AT-A is composed of an electronically controlled hydraulic pump that automatically applies continuous pressure at a specified rate of pull. This portable equipment, shown of figure 3.14, can be used to measure the adhesion of coatings to metals, wood, or concrete [37].

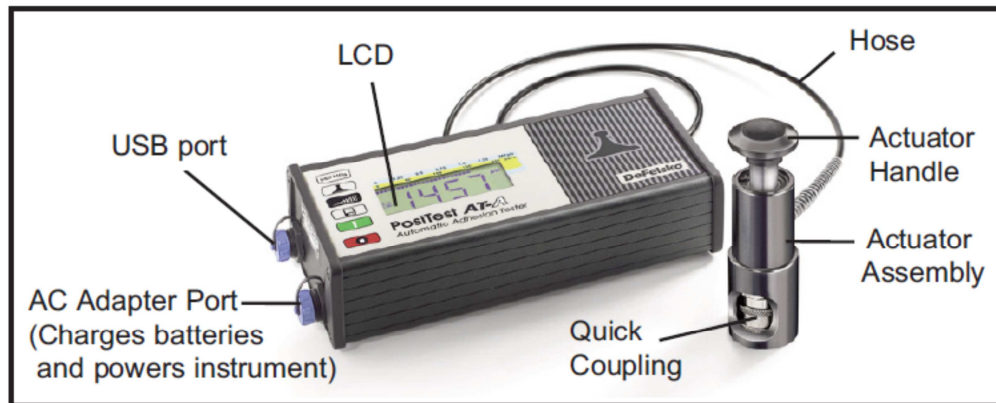


Figure 3.14: Positest® pull-off Adhesion Tester AT-A [45]

Before attaching the dollies, scoring was performed through the coating down to the surface of the concrete substrate. Specimens were cooled down completely into room temperature before the scoring procedure. The lack of scoring could lead into higher values of bond strength, since the effective test area is not defined [42]. Ideally, the core bit inside diameter should be equal to the diameter of the fixture, but since that was not available, the closest size available was used. The typical thickness of the FRP laminate measured with a caliper was 0.5 mm (0.02in). Initially, different depths of scoring, varying from 0.5 mm to 7.5 mm were studied in unconditioned samples. Among the 15 samples used, it was observed that all deeper scoring, such as 4 mm and 6 mm, produced a cohesive failure in the concrete substrate, which was not the desirable failure mode for this study. It is also believed that by increasing the drilling depth, more damage will be generated to the core since the vibration of the cutting drill machine increases [34]. Mixed failures were found in shallower scoring, which led to the selection of a scoring depth of 1 mm to be performed throughout this experimental program.

A drill press with a diamond tipped core bit with inside diameter of 19.5 mm, was used to create the perpendicular cut. The use of this equipment was preferred for reducing the chance of twist or torque in the test area, which could cause micro-cracking of the coating and the substrate, and lead to lower adhesion values. To minimize heat and suppress dust, air was blasted while scoring. Figure 3.15 shows the equipment used for scoring into the concrete. A template guide, as shown in figures 3.16 and 3.17, was created to locate where the cuts needed to be made. Each test site was separated by at least the distance needed to accommodate the detaching apparatus per ASTM D4541, avoiding measurements too close to the edge. Figure 3.18 shows the pre-cut test sites.

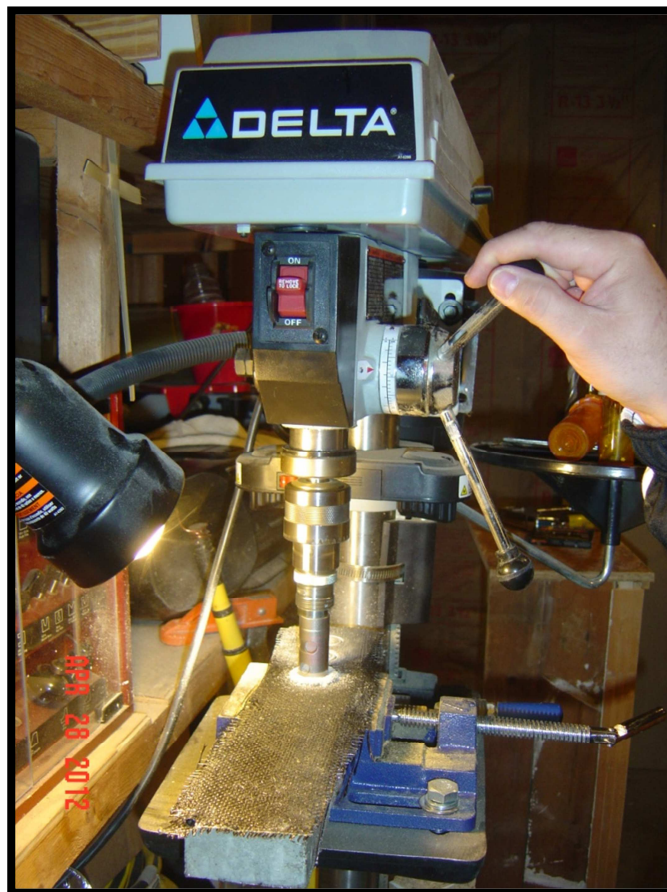


Figure 3.15: Delta drill press used for scoring the test sites.

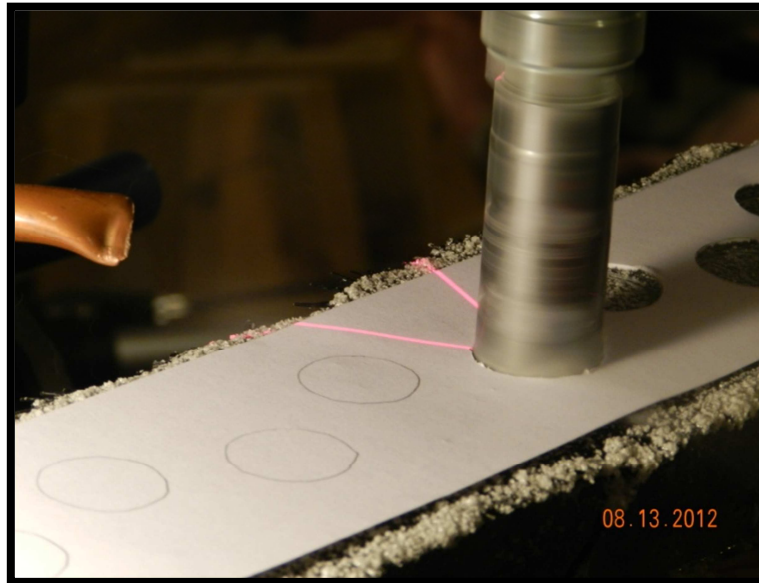


Figure 3.16: Scoring being performed showing air blaster



Figure 3.17: Scoring being performed showing template guide



Figure 3.18: Pre-cut site tests

Due to specimen size restriction, 20 mm (0.78in) single-use aluminum dollies were used, which is the standard dolly size per ASTM D4541. Dollies were attached using Loctite® 907™ Hysol® Epoxi-Patch® Adhesive as recommended by the manufacturer. Preparation of this two-part epoxy followed manufacturer's instructions. The FRP surface was cleaned by blowing air and with solvent (acetone) prior to applying the adhesive. The surface of the dolly was also prepared by roughening it with a 3M Scotch-Brite™ pad and removing any residue from dolly preparation using a dry paper towel. Figure 3.19 shows these supplies used. An even amount of resin and hardener were mixed, and a thin layer of this adhesive was spread over the disk area of the dolly. Dolly was pressed firmly to the FRP surface in a perpendicular position without any movement of twisting or rotation. Full cure properties were obtained in 3 days.





Figure 3.19: two-part epoxy used to attach dollies to beam

After curing, pull-off tests were performed at room temperature and relative humidity. First, the actuator assembly was placed over the dolly head and the quick coupling was engaged to the dolly. Once the settings were specified, such as pull-off pressure measurement unit (MPa), size of dolly (20 mm), and rate of pull (1MPa/s), the test was performed quickly, and the pull-off pressure was displayed to the user. No calculations were necessary. Typically, in most adhesion testers, the pull-off bond strength (pressure) needs to be calculated based on the pull-off force obtained from the test, and the dolly size ( $\text{Pressure} = \text{Force}/\text{area}$ ). Each pressure read in the LCD display was stored in the internal memory of the tester. The two major advantages in using this automatic tester were the elimination of operator error by twisting, pumping or cranking, and compensation of any uneven surface to be tested. This equipment, as being self-aligning, ensures that the perpendicular pull-off force is evenly distributed over the area tested. The pressure reacted by the loading fixture is the same as the pressure in the actuator (co-axial forces) and is transmitted directly to the pressure gauge. Figure 3.20 shows the equipment used and 3.21 shows its self-aligning feature. Figures 3.22 through 3.25 show a few tests being performed.



Figure 3.20: Positest<sup>®</sup> pull-off Adhesion Tester AT-A used in this research

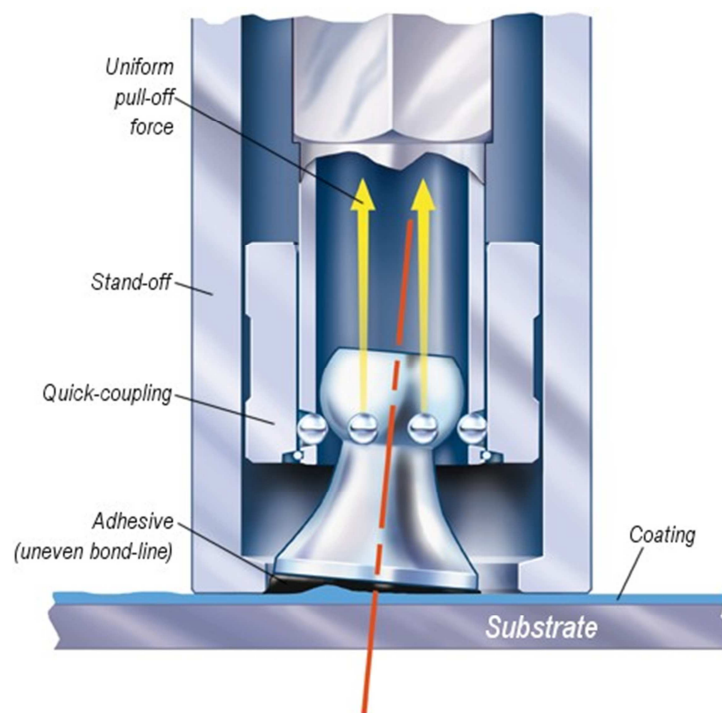


Figure 3.21: self-alignment feature of Positest<sup>®</sup> pull-off Adhesion Tester AT-A [46]



Figure 3.22: Actuator assembly over the dolly head and the quick coupling engaged



Figure 3.23: Pull-off test being performed for B32





Figure 3.24: Pull-off test being performed for B24

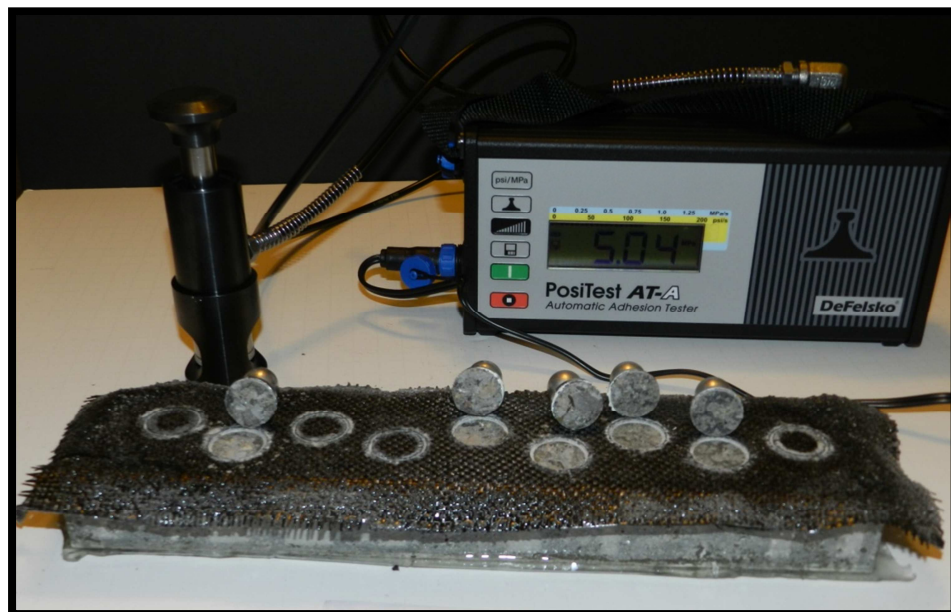


Figure 3.25: Pull-off test performed in five specimens

## CHAPTER 4: EXPERIMENTAL RESULTS

### 4.1 Introduction

In situ testing of concrete using the pull-off test allows an immediate assessment of the concrete strength and durability before it goes into service [15]. In this experimental study, 30 beams were subjected to accelerated environmental conditions and tested using the pull-off test method. The pull-off strength of a bonded FRP system is a performance property used in specifications, and for assessing the quality of an application [40]. Five pull-off values were obtained from each type of environmental condition.

ASTM D7522 [40] specifies the possible failure modes due to environmental degradation as being adhesive failure at either adhesive interface, or less likely, cohesive failure in adhesive. Environmental conditions could also lead to a cohesive failure in FRP laminate, which would represent a degradation of the FRP material itself, but this failure mode is usually expected when fibers were not completely wet-out. The most common and desirable failure on site is the cohesive failure in concrete substrate, and it represents sound FRP- adhesive system [40]. Mixed failures are also frequently found in pull-off tests. This failure is expected to start cohesively in the concrete substrate, and propagate through the interface, becoming adhesively [40]. Per ASTM D4541, the nature of the failure must be described as adhesive or cohesive in accordance to the percentage of each and their respective locations [41]. Failures observed in this research were classified as cohesive in concrete substrate, mixed, and adhesive at the interface.

Pull-off strength was obtained directly from the Positest<sup>®</sup> pull-off Adhesion Tester AT-A (test method E of ASTM D4541). According to ASTM D4541 [41], the maximum recommended difference for results obtained by the same operator using only method E is 27.8%. The average coefficient of variation (standard deviation/ average pull-off strength) was calculated for each condition to evaluate this precision.

## 4.2 Experimental Results

All beams were scored following the same pattern. Only five pull-off tests were done in each beam, but nine scoring locations were created in case more pull-off tests were needed afterward. ASTM D4541 recommends at least three replications to statistically characterize the test area [41]. An attempt to obtain five pull-off tests of each condition was made. However, delaminated beams, for example, only provided four test sites. Locations were selected based on the representativeness of the area. Areas with any visible local defect were rejected. Figure 4.1 shows how the pull-off locations were numerated.

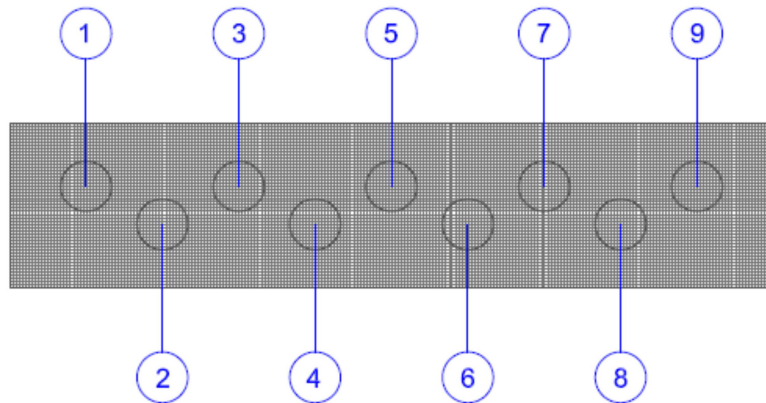


Figure 4.1: Pull-off locations.

### 4.2.1 Beam conditioned to room temperature and relative humidity (in air)

Control samples were obtained from beams exposed to room temperature and relative humidity.

#### 4.2.1.1 Beam conditioned to room temperature and relative humidity: 40 cycles

After 40 cycles (80 hours) of conditioning, the predominant failure mode, as expected, was cohesive in concrete substrate, and the average pull-off strength was 5.72 MPa. Table 4.1

shows the results for this conditioning. Figures 4.2 through 4.4 show respectively the conditioned beam, the partial damage caused by the pull-off test, and all five dollies detached.

Conditioning: Room Temperature and Relative Humidity								
# Cycles	Dolly #	Pull-off Strength		Average		Std. dev.	CV (%)	Failure Mode
		MPa	psi	MPa	psi			
40	35-1	4.72	684	5.72	829	0.632	11.04	mixed/cohesive
40	35-2	5.53	802					cohesive
40	35-4	5.88	853					cohesive
40	35-7	6.19	898					cohesive
40	35-9	6.28	911					cohesive

Table 4.1: Results for 40 cycles of room temperature and relative humidity

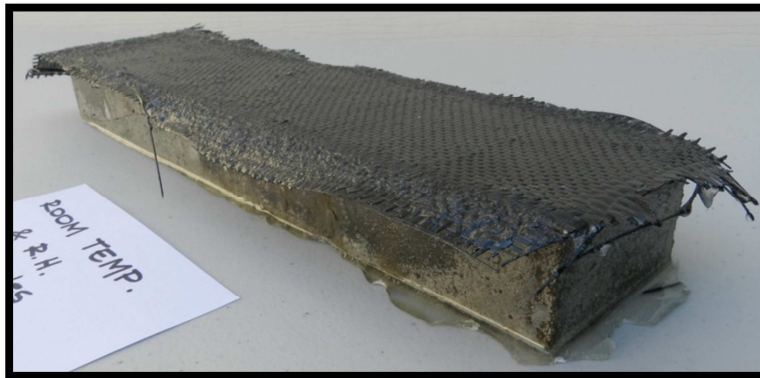


Figure 4.2: Beam conditioned to 40 cycles (80 hours) of room temperature and relative humidity



Figure 4.3: Partial damage caused by the pull-off test.

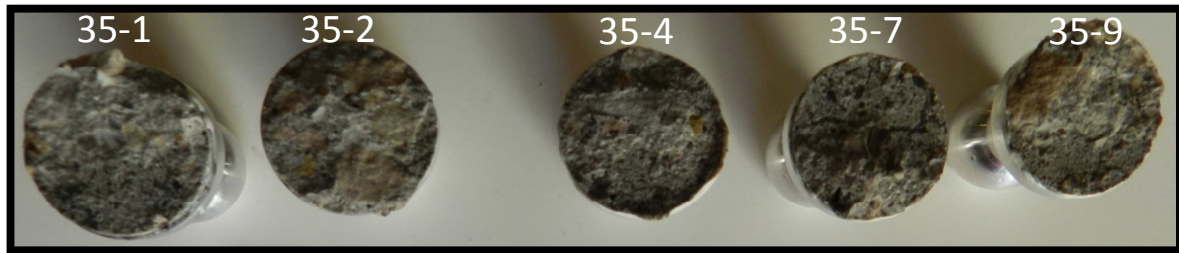


Figure 4.4: Dollies detached by the pull-off test after 40 cycles of room temperature and relative humidity

#### 4.2.1.2 Beam conditioned to room temperature and relative humidity: 100 cycles

After 100 cycles (200 hours) of conditioning, no changes in failure mode or pull-off strength were observed. Failure was cohesive in concrete substrate, and the average pull-off strength was 5.75 MPa. Table 4.2 shows the results for 100 cycles. Figures 4.5 and 4.6 show the conditioned beam and the pull-off tests done.

Conditioning: Room Temperature and Relative Humidity								
# Cycles	Dolly #	Pull-off Strength		Average		std. dev.	CV (%)	Failure Mode
		MPa	psi	MPa	psi			
100	36-3	6.68	969	5.75	833	0.871	15.16	cohesive
100	36-4	5.41	784					cohesive
100	36-6	5.41	784					mixed/cohesive
100	36-7	6.59	956					cohesive
100	36-8	4.64	673					cohesive

Table 4.2: Results for 100 cycles of room temperature and relative humidity

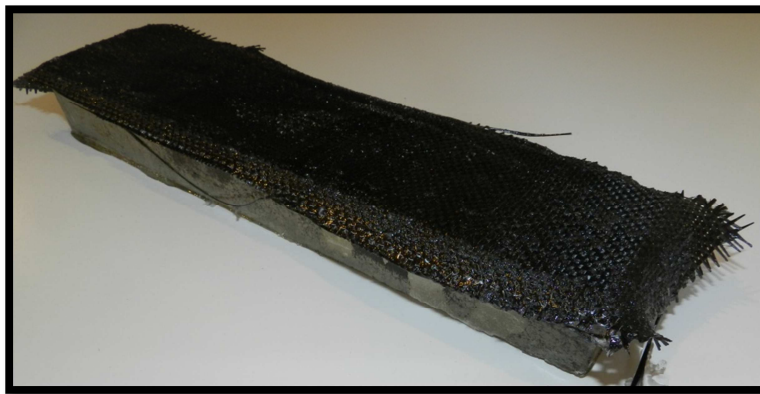


Figure 4.5: Beam conditioned to 100 cycles (200 hours) of room temperature and relative humidity



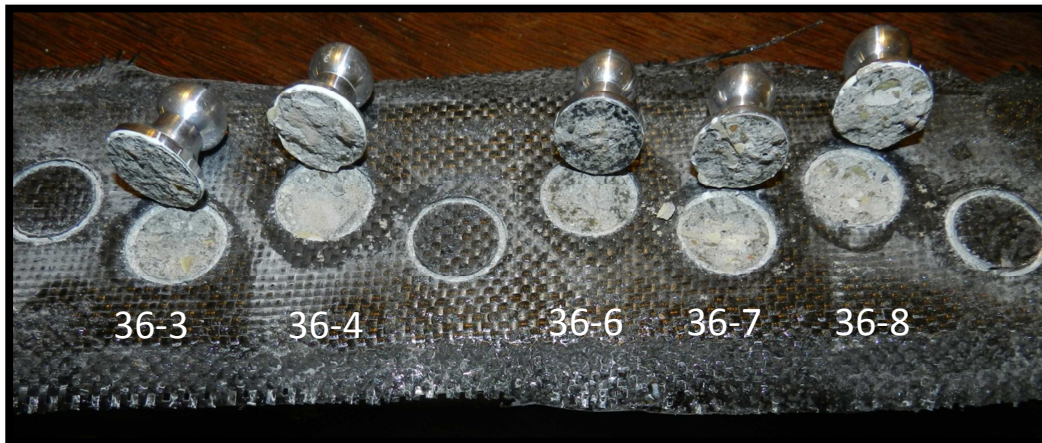


Figure 4.6: Pull-off tests on beam after 40 cycles of room temperature and relative humidity

#### 4.2.1.3 Beam conditioned to room temperature and relative humidity: 250 cycles

After 250 cycles (500 hours) of conditioning, still no significant changes were observed. Failure was mostly cohesive in concrete substrate, and the average pull-off strength was 6.26 MPa. Table 4.3 shows the results for 250 cycles. Figure 4.7 shows the conditioned beam, while figures 4.8 and 4.9 show the failure plane in each dolly.

Conditioning: Room Temperature and Relative Humidity								
# Cycles	Dolly #	Pull-off Strength		Average		std. dev.	CV (%)	Failure Mode
		MPa	psi	MPa	psi			
250	18-2	7.74	1122	6.26	908	1.229	19.63	cohesive
250	18-3	5.44	789					cohesive
250	18-7	7.22	1047					cohesive
250	18-8	4.76	690					mixed
250	18-9	6.15	892					cohesive

Table 4.3: Results for 250 cycles of room temperature and relative humidity

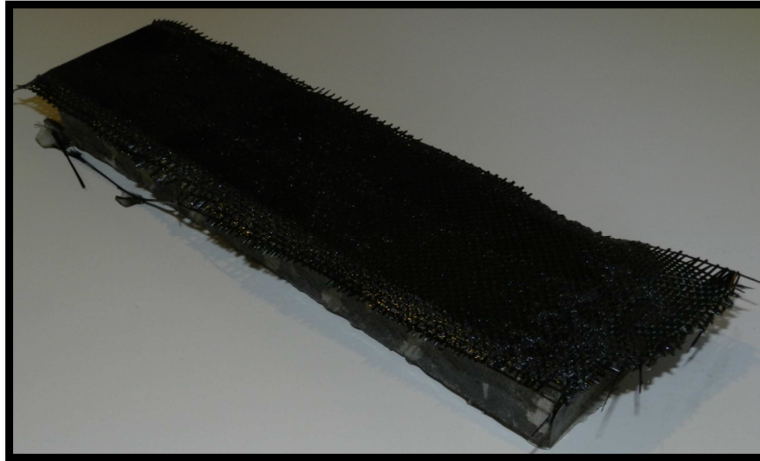


Figure 4.7: Beam conditioned to 250 cycles (500 hours) of room temperature and relative humidity



Figure 4.8: Pull-off tests on beam after 250 cycles of room temperature and relative humidity

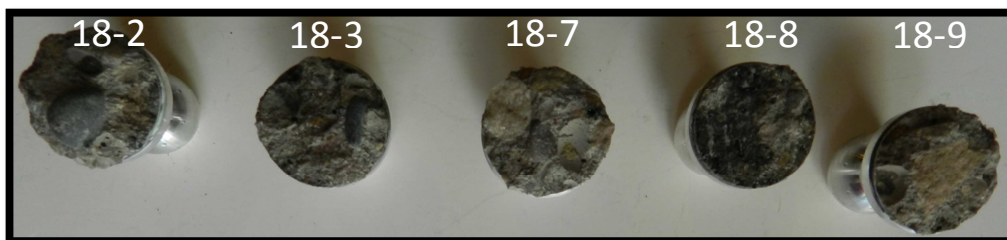


Figure 4.9: Dolies show cohesive failures and single mixed failure after 250 cycles of room temperature and relative humidity



#### 4.2.2 Beam conditioned to room temperature and immersion in distilled water

A second set of control samples was created at room temperature and immersion in distilled water. Cycles started once beams were immersed in water.

##### 4.2.2.1 Beam conditioned to room temperature and immersion in distilled water: 40 cycles

After 40 cycles, all pull-off failures occurred in concrete, and the average pull-off strength was 6.12 MPa. Table 4.4 shows the results for this conditioning. Figure 4.10 shows the conditioned beam. Figure 4.11 shows the pull-off test results being performed in this beam, and figure 4.12 shows the beam after testing with all five detached dollies.

Conditioning: Room Temperature and Immersion in Distilled Water								
# Cycles	Dolly #	Pull-off Strength		Average		Std. dev.	CV (%)	Failure Mode
		MPa	psi	MPa	psi			
40	32-1	7.03	1019	6.12	887	0.527	8.61	cohesive
40	32-2	6.05	877					cohesive
40	32-4	5.90	856					cohesive
40	32-5	5.93	860					cohesive
40	32-6	5.68	824					cohesive

Table 4.4: Results for 40 cycles of room temperature and immersion in distilled water

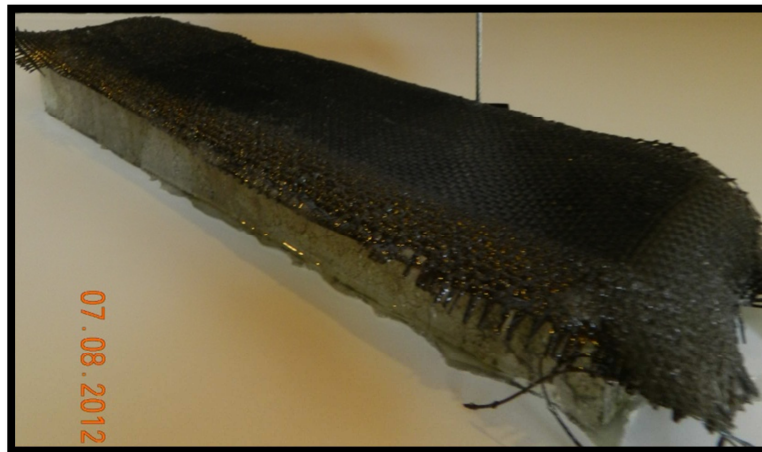


Figure 4.10: Beam conditioned to 40 cycles (80 hours) of room temperature and distilled water



Figure 4.11: Pull-off test being performed on beam conditioned to 40 cycles of room temperature and distilled water

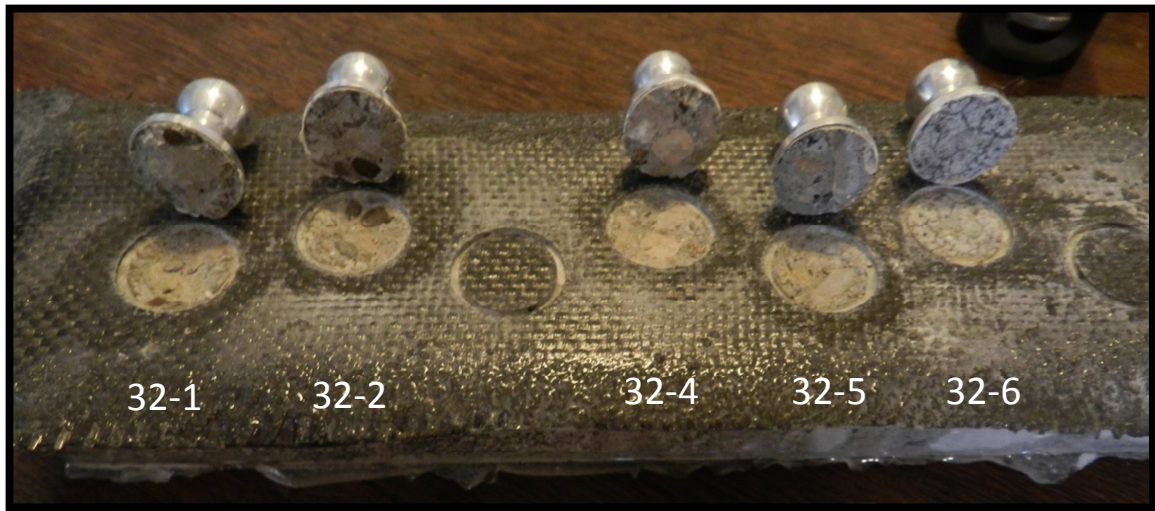


Figure 4.12: Dollies detached during pull-off tests.

#### **4.2.2.2 Beam conditioned to room temperature and immersion in distilled water: 100 cycles**

Pull-off test results for the beam conditioned to 100 cycles (200 hours) of room temperature and immersion in distilled water have shown no major deterioration. Most failures occurred in concrete, and the average pull-off strength was 4.98 MPa. The coefficient of variation, though, was above the expected 27.8%, due to the low value of one of the two mixed failures. No apparent reason for this difference was detected in this specific location.

Table 4.5 shows the results for this conditioning. Figure 4.13 shows the conditioned beam. Figure 4.14 shows the beam after testing with all five detached dollies.

Conditioning: Room Temperature and Immersion in Distilled Water								
# Cycles	Dolly #	Pull-off Strength		Average		Std. dev.	CV (%)	Failure Mode
		MPa	psi	MPa	psi			
100	16-3	2.57	373	4.98	722	1.615	32.46	mixed
100	16-5	6.12	887					cohesive
100	16-7	6.46	937					cohesive
100	16-8	4.12	597					mixed
100	16-9	5.61	813					cohesive

Table 4.5: Results for 100 cycles of room temperature and immersion in distilled water



Figure 4.13: Beam conditioned to 100 cycles of room temperature and distilled water



Figure 4.14: Beam after testing with detached dollies

#### 4.2.2.3 Beam conditioned to room temperature and immersion in distilled water: 250 cycles

Results for the pull-off tests on the beam conditioned to 250 cycles (500 hours) of room temperature and distilled water are shown on table 4.6. Most failures occurred cohesively in concrete, and the average pull-off strength was 5.76 MPa. Figures 4.15 and 4.16 show the conditioned beam before and after testing.

Conditioning: Room Temperature and Immersion in Distilled Water								
# Cycles	Dolly #	Pull-off Strength		Average		Std. dev.	CV (%)	Failure Mode
		MPa	psi	MPa	psi			
250	17-2	6.18	896	5.76	835	0.373	6.47	cohesive
250	17-3	5.50	798					mixed
250	17-7	5.64	818					cohesive
250	17-8	6.13	889					cohesive
250	17-9	5.36	777					mixed

Table 4.6: Results for 250 cycles of room temperature and immersion in distilled water



Figure 4.15: Beam conditioned to 250 cycles (500 hours) of room temperature and distilled water



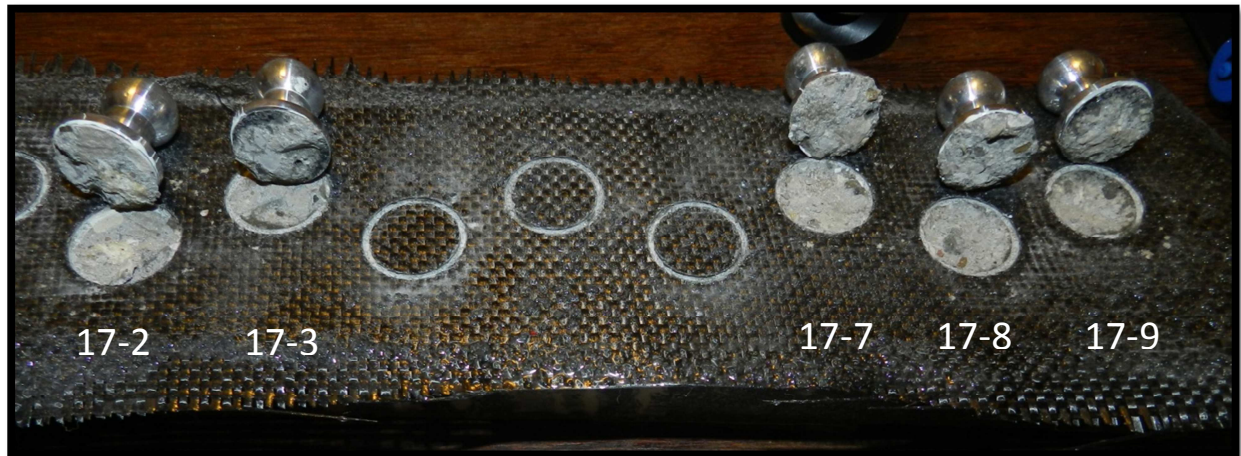


Figure 4.16: Pull-off on beam after 250 cycles of room temperature and distilled water

#### **4.2.3 Beam conditioned to room temperature and immersion in salt water**

The last set of control samples were produced at room temperature and immersion in five percent of salt water by mass. Similarly to the immersion in distilled water, cycles started once beams were immersed in salt water.

##### **4.2.3.1 Beam conditioned to room temperature and immersion in salt water: 40 cycles**

Specimens obtained after 40 cycles (80 hours) of room temperature and salt water showed cohesive failures and average pull-off strength of 4.53 MPa, as shown in table 4.7. Figures 4.17 and 4.18 show the beam used in for this condition.

Conditioning: Room Temperature and Immersion in Salt Water								
# Cycles	Dolly #	Pull-off Strength		Average		Std. dev.	CV (%)	Failure Mode
		MPa	psi	MPa	psi			
40	60-1	5.19	753	4.53	657	0.783	17.29	cohesive
40	60-2	4.02	583					cohesive
40	60-3	4.23	613					cohesive
40	60-4	5.52	800					cohesive
40	60-5	3.70	537					cohesive

Table 4.7: Results after 40 cycles of room temperature and immersion in salt water

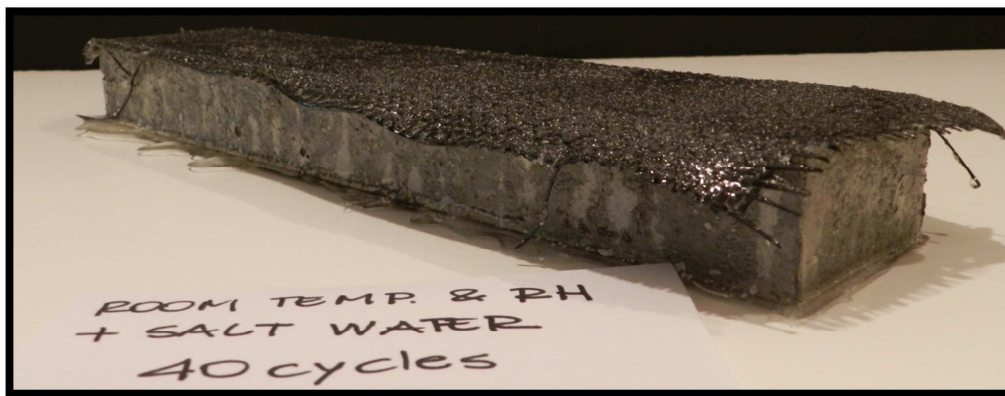


Figure 4.17: Beam conditioned to 40 cycles (80 hours) of room temperature and salt water

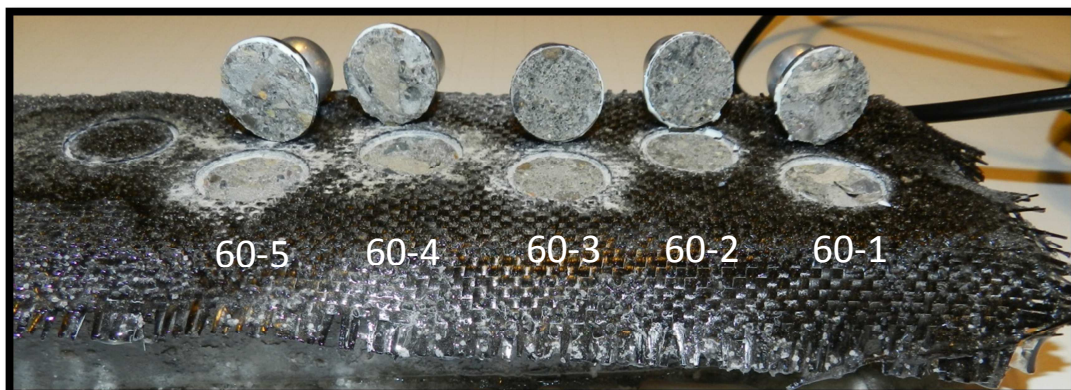


Figure 4.18: Beam tested after 40 cycles in room temperature and salt water

#### 4.2.3.2 Beam conditioned to room temperature and immersion in salt water: 100 cycles

After 100 cycles (200 hours) of room temperature and salt water failures were cohesive and average pull-off strength of 4.27 MPa, as shown in table 4.8. Figures 4.19 and 4.20 show the beam before and after testing.

Conditioning: Room Temperature and Immersion in Salt Water								
# Cycles	Dolly #	Pull-off Strength		Average		Std. dev.	CV (%)	Failure Mode
		MPa	psi	MPa	psi			
100	61-1	4.19	608	4.27	619	0.683	16.00	cohesive
100	61-2	5.15	747					cohesive
100	61-3	3.84	557					cohesive
100	61-4	3.44	499					cohesive
100	61-6	4.73	686					cohesive

Table 4.8: Results after 100 cycles of room temperature and immersion in salt water

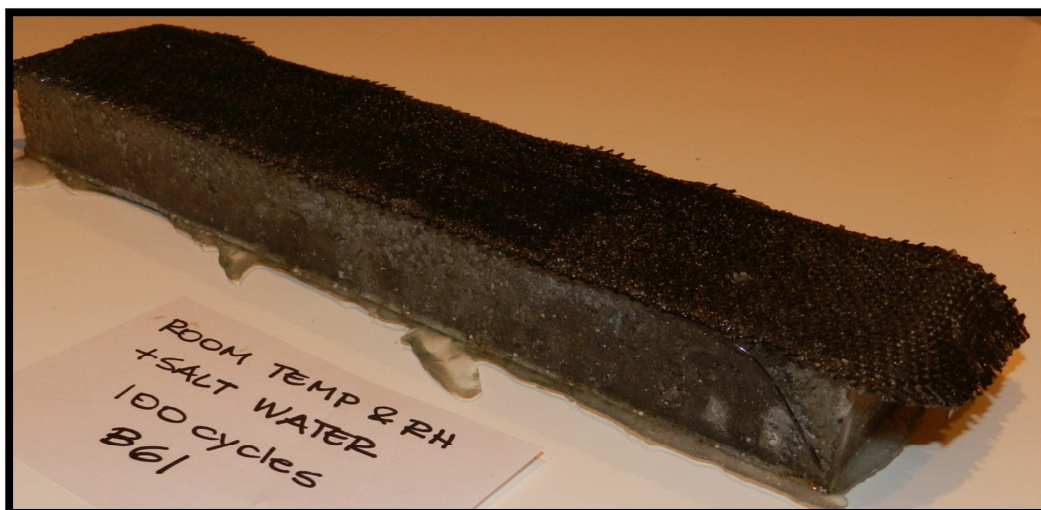


Figure 4.19: Beam conditioned to 100 cycles (200 hours) of room temperature and salt water



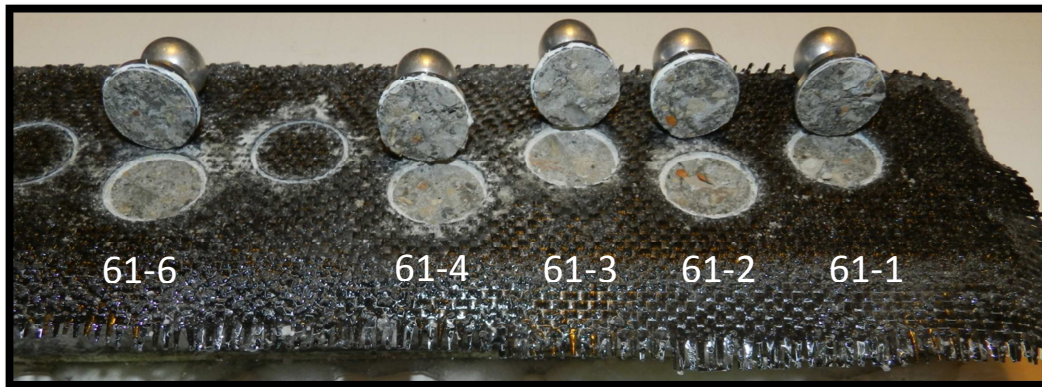


Figure 4.20: Pull-off tests performed in beam conditioned to 100 cycles of room temperature and salt water

#### 4.2.3.3 Beam conditioned to room temperature and immersion in salt water: 250 cycles

After 250 cycles (500 hours) of room temperature and salt water failures were cohesive and average pull-off strength of 5.74 MPa. Compared to 40 and 100 cycles, at 250 cycles bond strength showed an increase, but failure remained cohesive in the concrete substrate, which may indicate that concrete properties have improved, possibly due to further wet cure provided by the immersion [17].

The adhesive failure shown in table 4.9 was not included in the calculation of the average strength. This value is not considered valid, since it showed a failure in the epoxy adhesive at the dolly, indicating an error in affixing this fixture. Figures 4.21 and 4.22 show the beam before and after testing.

Conditioning: Room Temperature and Immersion in Salt Water								
# Cycles	Dolly #	Pull-off Strength		Average		Std. dev.	CV (%)	Failure Mode
		MPa	psi	MPa	psi			
250	62-1	6.00	870	5.74	832	0.590	10.29	cohesive
250	62-2	5.67	822					cohesive
250	62-3	4.80	696					adhesive at dolly
250	62-4	6.33	918					cohesive
250	62-5	4.95	718					cohesive

Table 4.9: Results after 250 cycles of room temperature and immersion in salt water

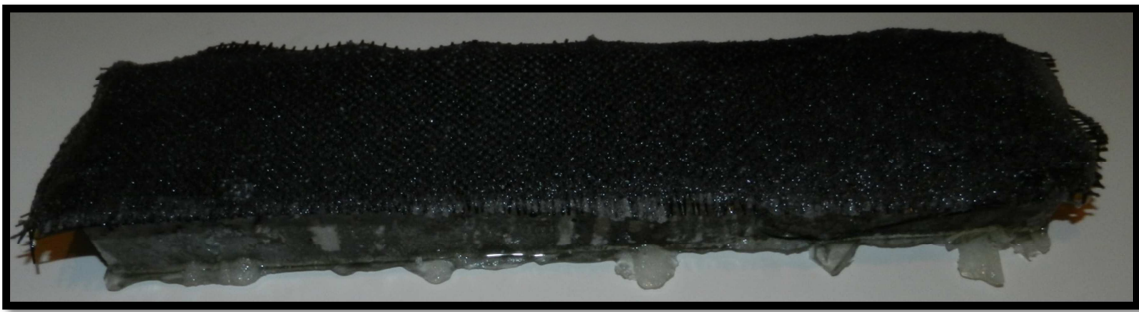


Figure 4.21: Beam after 250 cycles (500 hours) of conditioning under room temperature and salt water

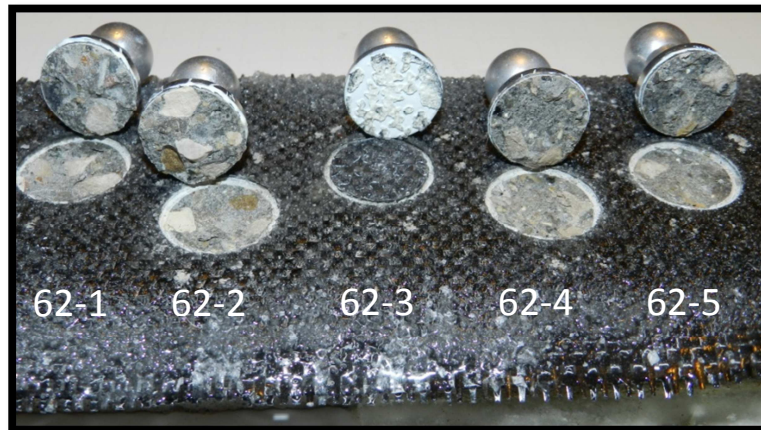


Figure 4.22: Beam tested after 250 cycles of conditioning under room temperature and salt water. An error in the fixture attachment produced an invalid result, observed by an adhesive failure at the dolly.

#### **4.2.4 Beam conditioned to 180°C and 0% relative humidity**

Initially, beams were going to be conditioned only to 180°C, but due to the large delamination found, 100°C was added to this research. The first set of beams conditioned to 180°C with the use of the oven in the laboratory had a relative humidity of 0%.

##### **4.2.4.1 Beam conditioned to 180°C and 0% relative humidity: 40 cycles**

Due to the large delamination seen after 40 cycles (80 hours) of exposure to 180°C of temperature and 0% relative humidity, a second beam had to be conditioned to obtain enough replications. The first beam only provided two values, and consequently was disregarded, while the second one provided four pull-off results, which are shown in Table 4.10. All failures were mixed, and the average bond strength was under the minimum determined by ACI 440 of 1.4 MPa (200psi). Besides that, the coefficient of variation obtained was above the 27.8% recommended by ASTM D4541, which may be attributed to the large delamination found.

Figure 4.23 shows the beam after 40 cycles of 180°C of temperature and 0% relative humidity. Figure 4.24 shows the delamination in this beam, and the dollies pulled can be seen in figure 4.25.

Conditioning: 180°C and 0% Relative Humidity								
# Cycles	Dolly #	Pull-off Strength		Average		Std. dev.	CV (%)	Failure Mode
		MPa	psi	MPa	psi			
40	78-1	0.95	138	0.91	132	0.271	29.86	mixed
40	78-2	1.26	183					mixed
40	78-3	0.62	90					mixed
40	78-4	0.80	116					mixed
40	78-5	0	0					delaminated

Table 4.10: Results after 40 cycles of 180°C of temperature and 0% relative humidity



Figure 4.23: Beam after 40 cycles (80 hours) of 180°C of temperature and 0% relative humidity





Figure 4.24: Delamination in beam after 40 cycles of 180°C of temperature and 0% relative humidity

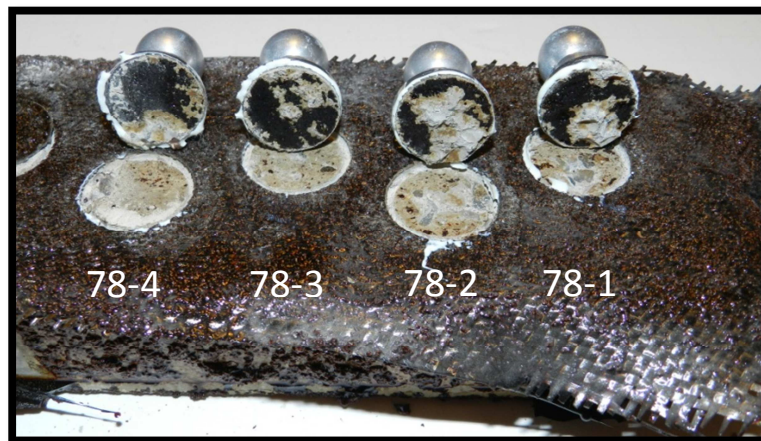


Figure 4.25: Dollies from beam exposed to 40 cycles of 180°C of temperature and 0% relative humidity

#### 4.2.4.2 Beam conditioned to 180°C and 0% relative humidity: 100 cycles

Delamination was also present in the beam exposed to 100 cycles (200 hours) of 180°C of temperature and 0% relative humidity. During scoring, five of the locations had the fiber completely detached from the beam, and only four values were obtained. Failures were either mixed or adhesive, and the average bond strength was 1.87 MPa. A large coefficient of

variation was obtained, which indicates the localized characteristic of the pull-off test. Pull-off results are shown in Table 4.11. Figures 4.26, 4.27, and 4.28 show respectively, the conditioned beam, the locations from where the results were obtained, and dollies pulled.

Conditioning: 180°C and 0% Relative Humidity								
# Cycles	Dolly #	Pull-off Strength		Average		Std. dev.	CV (%)	Failure Mode
		MPa	psi	MPa	psi			
100	29-1	2.59	376	1.87	270	0.736	39.45	mixed
100	29-2	1.14	165					adhesive
100	29-3	2.40	348					mixed
100	29-9	1.33	193					mixed
100	29-5	0	0					delaminated

Table 4.11: Results after 100 cycles of 180°C of temperature and 0% relative humidity



Figure 4.26: Beam exposed to 100 cycles of 180°C of temperature and 0% relative humidity



Figure 4.27: Pull-off tests locations in beam exposed to 100 cycles of 180°C of temperature and 0% relative humidity

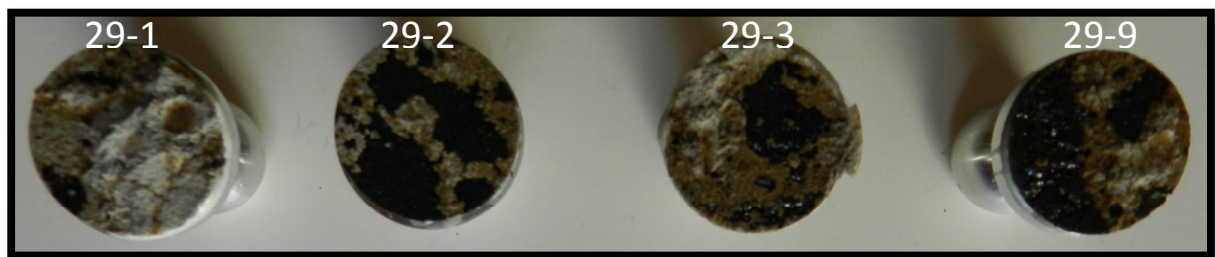


Figure 4.28: Dolies pulled after 100 cycles of 180°C of temperature and 0% relative humidity

#### 4.2.4.3 Beam conditioned to 180°C and 0% relative humidity: 250 cycles

Visibly deterioration was observed in the beam exposed to 180°C of temperature and 0% relative humidity. After 250 cycles (500 hours) of exposure all failures were adhesive and one of the dolies was pulled by hand. The average bond strength was 0.50 MPa.

The coefficient of variation was very large, as can be seen in Table 4.12. Figures 4.29, 4.30, and 4.31 show the conditioned beam, the locations from where the results were obtained, and dolies pulled.

Conditioning: 180°C and 0% Relative Humidity								
# Cycles	Dolly #	Pull-off Strength		Average		Std. dev.	CV (%)	Failure Mode
		MPa	psi	MPa	psi			
250	30-3	0	0	0.50	73	0.382	76.45	pulled by hand
250	30-4	0.30	44					adhesive
250	30-5	1.06	154					adhesive
250	30-6	0.42	61					adhesive
250	30-9	0.22	32					adhesive

Table 4.12: Results after 250 cycles of 180°C of temperature and 0% relative humidity



Figure 4.29: Beam exposed to 250 cycles of 180°C of temperature and 0% relative humidity





Figure 4.30: Beam after pull-off tests were performed.



Figure 4.31: Dollies from beam exposed to 250 cycles of 180°C of temperature and 0% relative humidity

#### 4.2.5 Beam conditioned to 180°C and 100% relative humidity (in air)

Beams were exposed 180°C and 100% relative humidity using the Tenney chamber. However due to a malfunction of the chamber before 250 cycles were reached, the test had to be redone using the laboratory oven. The humidity in this case was provided artificially using water tubs. 100% humidity was provided most of the time, with the exception of three days of lab closure, which represents about 36 cycles. This issue was present for both beams conditioned for 250 cycles at 180°C and 100% relative humidity, including the one immersed in distilled water.

#### 4.2.5.1 Beam conditioned to 180°C and 100% relative humidity: 40 cycles

After 40 cycles (80 hours) of exposure to 180°C of temperature and 100% relative humidity, failures occurred mostly cohesively in concrete, as shown in table 4.13, and the average pull-off strength was 3.44 MPa. Figure 4.32 shows the beam after exposure, and figures 4.33, 4.34, and 4.35 shows, respectively, the locations used for testing, the dollies pulled from each location and failure planes of the dollies.

Conditioning: 180°C and 100% Relative Humidity								
# Cycles	Dolly #	Pull-off Strength		Average		Std. dev.	CV (%)	Failure Mode
		MPa	psi	MPa	psi			
40	24-5	3.91	567	3.44	498	0.858	24.96	cohesive
40	24-6	2.08	302					mixed/adhesive
40	24-7	3.46	502					cohesive
40	24-8	3.36	487					cohesive
40	24-9	4.37	634					cohesive

Table 4.13: Results after 40 cycles of 180°C of temperature and 100% relative humidity

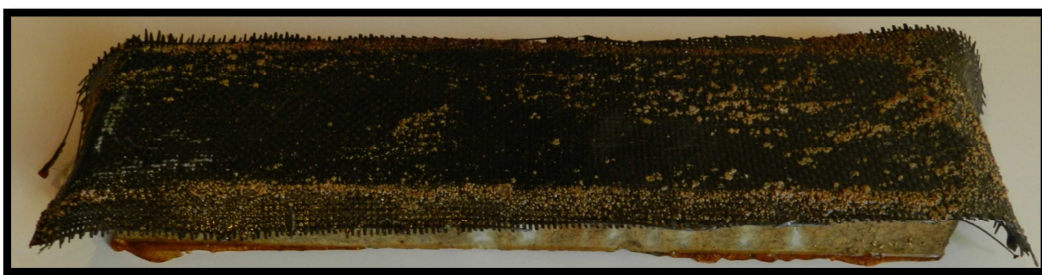


Figure 4.32: Beam after exposure to 40 cycles of 180°C of temperature and 100% relative humidity



Figure 4.33: Pull-off testing locations on beam exposed to 40 cycles of 180°C of temperature and 100% relative humidity



Figure 4.34: Pulled dolies at their respective testing locations.

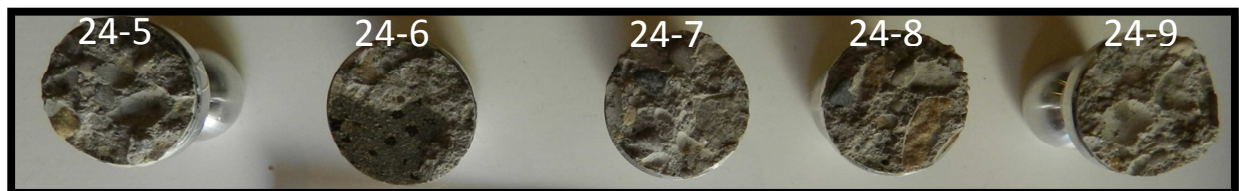


Figure 4.35: Failure planes on each dolly for 40 cycles of 180°C of temperature and 100% relative humidity exposure.

#### 4.2.5.2 Beam conditioned to 180°C and 100% relative humidity: 100 cycles



100 cycles (80 hours) of exposure at 180°C of temperature and 100% relative humidity, produced failures mostly cohesively in concrete, and the average pull-off strength was 4.50 MPa, as shown in table 4.14. Figure 4.36 shows the beam after exposure and figure 4.37 shows dollies pulled from this conditioned beam.

Conditioning: 180°C and 100% Relative Humidity								
# Cycles	Dolly #	Pull-off Strength		Average		Std. dev.	CV (%)	Failure Mode
		MPa	psi	MPa	psi			
100	21-3	4.76	690	4.50	652	1.045	23.25	cohesive
100	21-5	4.48	650					cohesive
100	21-7	2.79	405					mixed/cohesive
100	21-8	5.63	816					cohesive
100	21-9	4.82	699					cohesive

Table 4.14: Results after 100 cycles of 180°C of temperature and 100% relative humidity

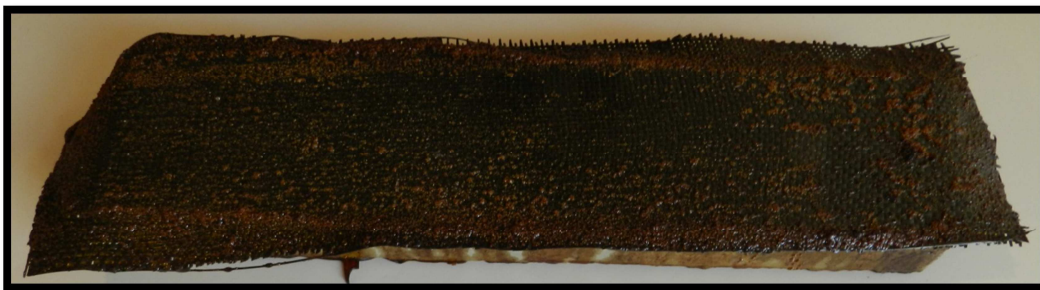


Figure 4.36: Beam after exposure to 100 cycles of 180°C of temperature and 100% relative humidity

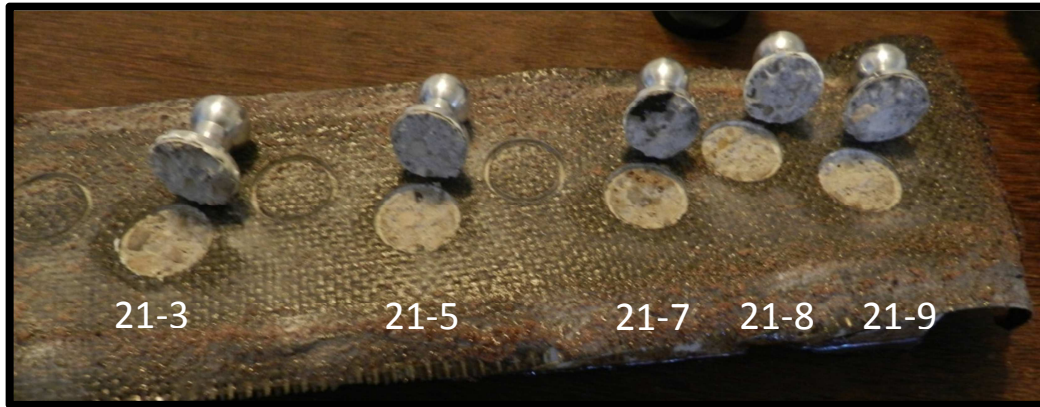


Figure 4.37: Dollies pulled after 100 cycles of 180°C of temperature and 100% relative humidity

#### 4.2.5.3 Beam conditioned to 180°C and 100% relative humidity: 250 cycles

An increase in the coefficient of variation was seen in the results from the beam exposed to 250 cycles of 180°C of temperature and 100% relative humidity. Very low values of bond strength were obtained, including two values below the minimum recommended by ACI 440. Table 4.15 shows that the average pull-off strength was 1.77 MPa and failures were mostly adhesive. The three days without humidity may have contributed to a certain extent to the deterioration, but the humidity clearly improved the strength in comparison to the results from the beams exposed to the same 180°C of temperature and dry air (0% relative humidity).

Figure 4.38 shows the beam after exposure to 250 cycles of 180°C of temperature and 100% relative humidity, while figure 4.39 shows the dollies pulled at their respective locations on the beam.

Conditioning: 180°C and 100% Relative Humidity								
# Cycles	Dolly #	Pull-off Strength		Average		Std. dev.	CV (%)	Failure Mode
		MPa	psi	MPa	psi			
250	47-1	1.62	235	1.77	256	0.611	34.55	mixed/ adhesive
250	47-2	1.75	254					adhesive
250	47-3	2.81	407					adhesive
250	47-4	1.35	196					mixed/ adhesive
250	47-5	1.31	190					adhesive

Table 4.15: Results after 250 cycles of 180°C of temperature and 100% relative humidity



Figure 4.38: Beam after exposure to 250 cycles of 180°C of temperature and 100% relative humidity

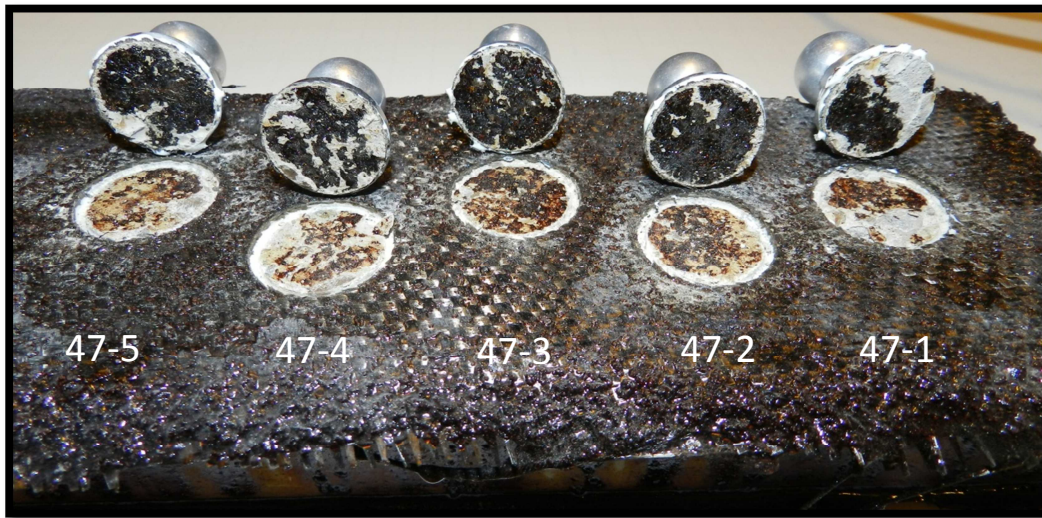


Figure 4.39: Dollies pulled at their respective locations on the beam exposed to 250 cycles of 180°C of temperature and 100% relative humidity.

#### **4.2.6 Beam conditioned to 180°C and distilled water**

Similarly to the beams conditioned to a temperature of 180°C and 100% relative humidity, the Tenney chamber was used to condition the beams to 180°C and immersion in distilled water. The test was also redone using the laboratory oven for the beam exposed to 250 cycles, since the chamber had a malfunction before 250 cycles were reached.

##### **4.2.6.1 Beam conditioned to 180°C and distilled water: 40 cycles**

The results from the beam exposed to 40 cycles of 180°C and immersion in distilled water shows great variability and large coefficient of variation. Very low bond strength was obtained from one of the dollies. It was observed that this dolly presented the most adhesive failure among all others in this beam, but no specific local defect was associated to this result, which can be attributed to a localized deterioration.

Figure 4.40 shows the beam after exposure, figure 4.41 shows the dollies at their testing locations, and figure 4.42 shows a closer view of the failure plane at these dollies.

Conditioning: 180°C and Immersion in Distilled Water								
# Cycles	Dolly #	Pull-off Strength		Average		Std. dev.	CV (%)	Failure Mode
		MPa	psi	MPa	psi			
40	19-4	3.30	479	3.25 (3.88)*	471	1.484	45.65 (14.85)*	mixed/ adhesive
40	19-5	4.63	671					cohesive
40	19-6	0.75	109					mixed/ adhesive
40	19-7	3.59	521					mixed/ adhesive
40	19-8	3.98	577					mixed/ adhesive

\*excluding sample 19-6.

Table 4.16: Results after 40 cycles of 180°C and immersion in distilled water

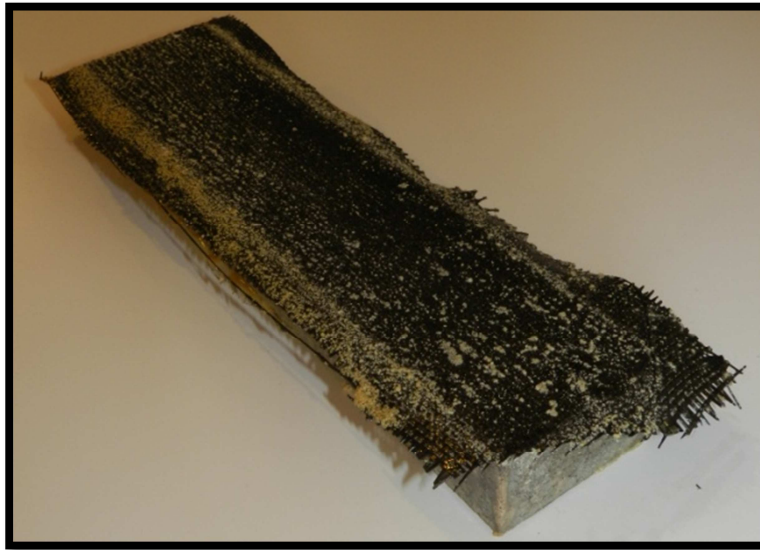


Figure 4.40: Beam exposed to 40 cycles of 180°C of temperature and immersion in distilled water.





Figure 4.41: Dollies at their testing locations on beam exposed to 40 cycles of 180°C of temperature and immersion in distilled water.

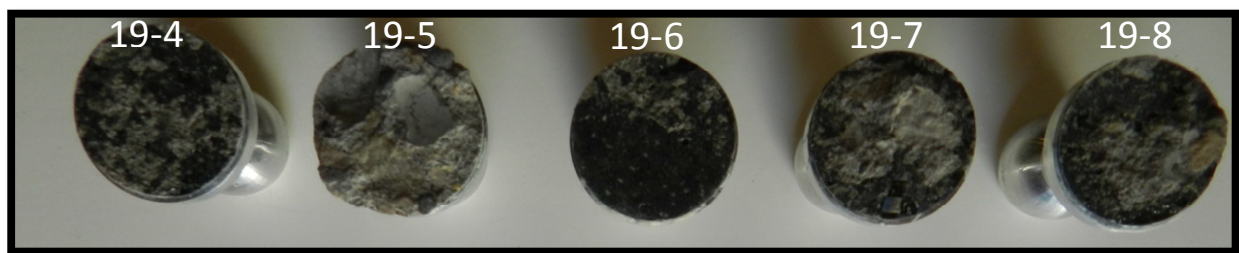


Figure 4.42: View of the failure plane at dollies from the beam exposed to 40 cycles of 180°C of temperature and immersion in distilled water.

#### 4.2.6.2 Beam conditioned to 180°C and distilled water: 100 cycles

After 100 cycles of 180°C of temperature and immersion in distilled water, failures had a great variability, ranging from cohesive in concrete substrate to adhesive at the interface. Variability was also seen on the bond strength results, and the coefficient of variation was higher than expected. The lowest value for the adhesive strength did not reach the minimum required by ACI 440, and showed true adhesive bond deterioration with a full adhesive failure face. Still, the average of 3.91 MPa was over the acceptable value of 1.40 MPa. Figure 4.43

shows the beam exposed to 100 cycles of 180°C of temperature and immersion in distilled water. Figure 4.44 shows the dollies at their testing locations, while figure 4.45 shows the wide variability in failure modes at the dollies.

Conditioning: 180°C and Immersion in Distilled Water								
# Cycles	Dolly #	Pull-off Strength		Average		Std. dev.	CV (%)	Failure Mode
		MPa	psi	MPa	psi			
100	20-1	6.61	958	3.91 (4.80)*	567	2.486	63.59 (36.25)*	cohesive
100	20-2	4.87	706					mixed/ cohesive
100	20-3	0.37	54					adhesive
100	20-4	2.44	354					mixed/ adhesive
100	20-5	5.26	763					cohesive

\*excluding sample 20-3.

Table 4.17: Results after 100 cycles of 180°C and immersion in distilled water



Figure 4.43: Beam exposed to 100 cycles of 180°C of temperature and immersion in distilled water.



Figure 4.44: Dollies at their testing locations on beam exposed to 100 cycles of 180°C of temperature and immersion in distilled water.

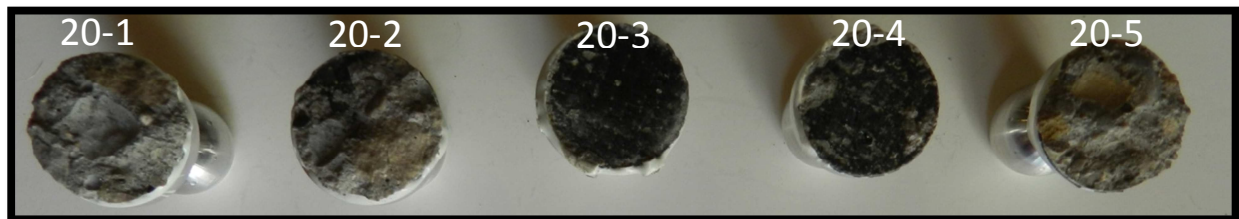


Figure 4.45: Variability in failure modes at dollies from the beam exposed to 100 cycles of 180°C of temperature and immersion in distilled water.

#### 4.2.6.3 Beam conditioned to 180°C and distilled water: 250 cycles

After 250 cycles of 180°C of temperature and immersion in distilled water, the coefficient of variation was also higher than the 27.8% recommended by ASTM D4541. Once again, only one of the pull-off strength values did not reach the minimum of 1.40 MPa. The average pull-off strength was 2.39 MPa, and all failures were mixed. Figures 4.46 and 4.47 show the beam after exposure and figure 4.48 shows the dollies at their testing locations.

Conditioning: 180°C and Immersion in Distilled Water								
# Cycles	Dolly #	Pull-off Strength		Average		Std. dev.	CV (%)	Failure Mode
		MPa	psi	MPa	psi			
250	48-1	2.92	423	2.39 (2.78)*	347	1.003	41.91 (21.69)*	mixed/ cohesive
250	48-3	0.86	125					mixed/ adhesive
250	48-5	2.46	357					mixed/ adhesive
250	48-7	2.17	315					mixed/ adhesive
250	48-9	3.55	515					mixed/ cohesive

\*excluding sample 48-3.

Table 4.18: Results after 100 cycles of 180°C and immersion in distilled water



Figure 4.46: Beam after exposure to 250 cycles of 180°C of temperature and immersion in distilled water.





Figure 4.47: Closer view of the beam exposed to 250 cycles of 180°C of temperature and immersion in distilled water.

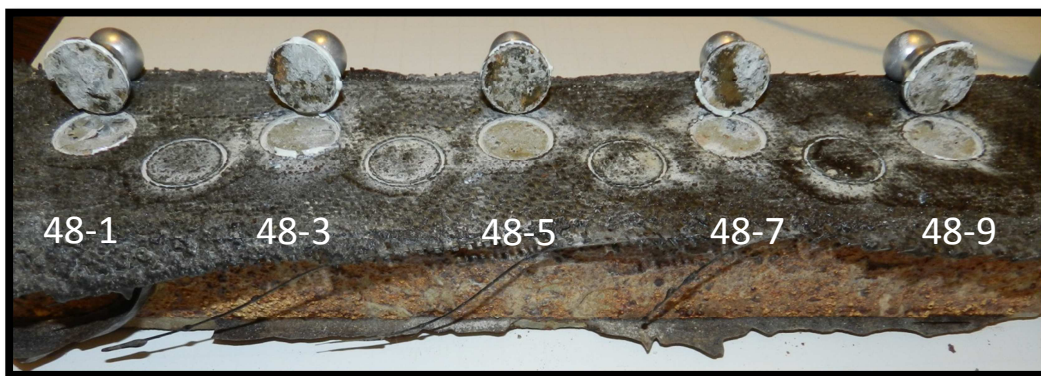


Figure 4.48: Dollies at their respective test locations showing mixed failures.

#### 4.2.7 Beam conditioned to 100°C and 0% relative humidity

After the 180°C systems were complete, the first set of beams conditioned at 0% relative humidity and 100°C of temperature were placed in the laboratory oven.

##### 4.2.7.1 Beam conditioned to 100°C and 0% relative humidity: 40 cycles

After 40 cycles (80 hours) of conditioning, all dollies pulled from the beam showed a cohesive failure in the concrete substrate and the average pull-off strength was 3.11 MPa. The

coefficient of variation was above the recommended by ASTM D4541 due to the high variability between values obtained. Table 4.19 shows the testing results and figures 4.49 and 4.50 show the conditioned beam before and after testing.

Conditioning: 100°C and 0% Relative Humidity								
# Cycles	Dolly #	Pull-off Strength		Average		Std. dev.	CV (%)	Failure Mode
		MPa	psi	MPa	psi			
40	43-1	3.87	561	3.11	451	0.928	29.85	cohesive
40	43-2	3.30	479					cohesive
40	43-4	4.07	590					cohesive
40	43-8	2.33	338					cohesive
40	43-9	1.97	286					cohesive

Table 4.19: Results after 100 cycles of 100°C and 0% relative humidity



Figure 4.49: Beam exposed to 40 cycles of 100°C of temperature and 0% relative humidity  
before testing

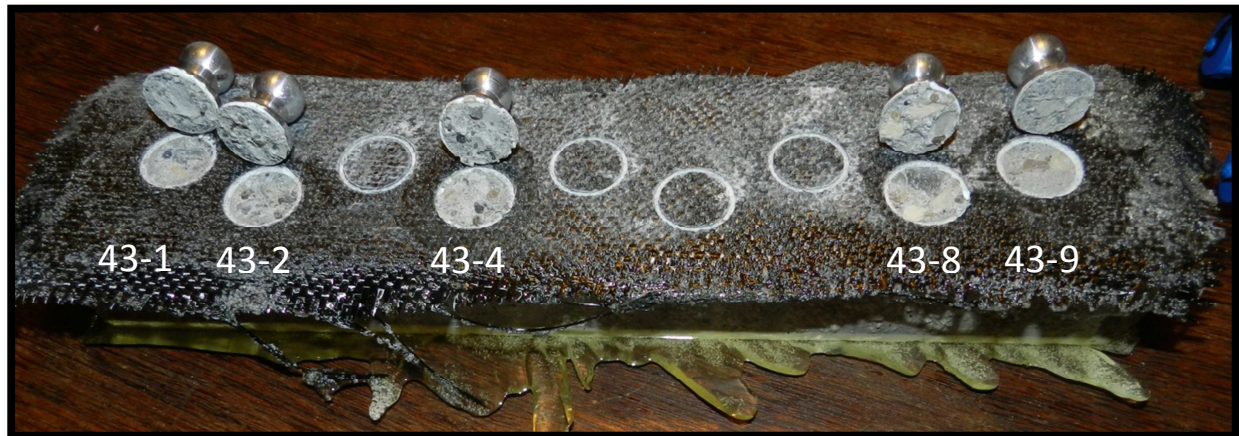


Figure 4.50: Beam exposed to 40 cycles of 100°C of temperature and 0% relative humidity after testing

#### 4.2.7.2 Beam conditioned to 100°C and 0% relative humidity: 100 cycles

After 100 cycles (200hours), the specimens showed mostly cohesive failures with low coefficient of variation and average pull-off strength of 3.85 MPa. Table 4.20 shows these results. Figures 4.51 and 4.52 show the conditioned beam before and after testing.

Conditioning: 100°C and 0% Relative Humidity								
# Cycles	Dolly #	Pull-off Strength		Average		Std. dev.	CV (%)	Failure Mode
		MPa	psi	MPa	psi			
100	44-2	3.39	492	3.85	558	0.595	15.44	cohesive
100	44-4	4.76	690					cohesive
100	44-5	3.26	473					cohesive
100	44-6	4.01	581					mixed
100	44-8	3.83	555					mixed

Table 4.20: Results after 100 cycles of 100°C and 0% relative humidity





Figure 4.51: Beam exposed to 100 cycles of 100°C and 0% relative humidity before testing

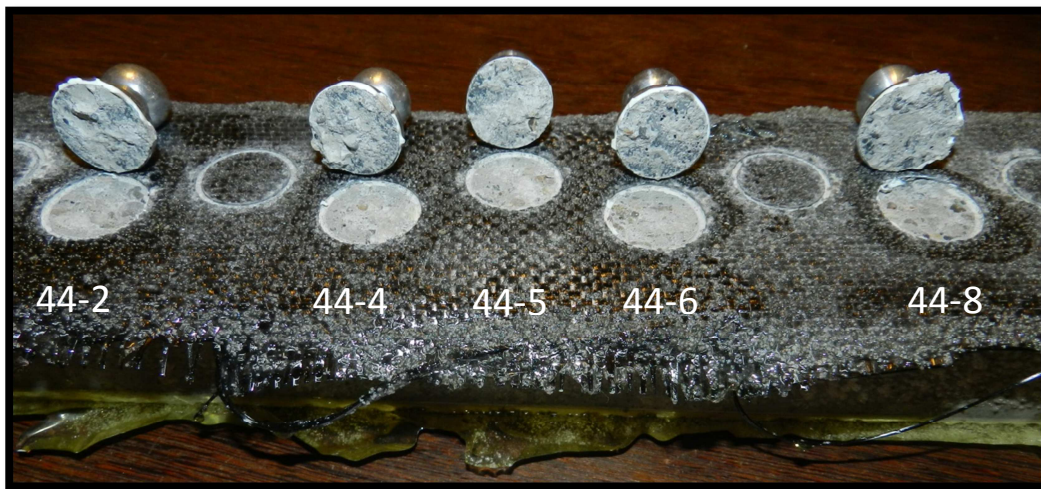


Figure 4.52: Beam exposed to 100 cycles of 100°C and 0% relative humidity after testing

#### 4.2.7.3 Beam conditioned to 100°C and 0% relative humidity: 250 cycles

After 250 cycles (500 hours) under 100°C and 0% relative humidity, failures were still mostly cohesive and average pull-off strength was 3.91 MPa. Table 4.21 shows these results. Figures 4.53 and 4.54 show the conditioned beam before and after testing.



Conditioning: 100°C and 0% Relative Humidity								
# Cycles	Dolly #	Pull-off Strength		Average		Std. dev.	CV (%)	Failure Mode
		MPa	psi	MPa	psi			
250	45-1	3.92	568	3.91	567	0.964	24.64	mixed
250	45-3	5.37	779					mixed
250	45-4	4.17	605					cohesive
250	45-8	3.19	463					cohesive
250	45-9	2.91	422					cohesive

Table 4.21: Results after 250 cycles of 100°C and 0% relative humidity



Figure 4.53: Beam exposed to 250 cycles of 100°C and 0% relative humidity before testing



Figure 4.54: Beam exposed to 250 cycles of 100°C and 0% relative humidity after testing

#### 4.2.8 Beam conditioned to 100°C and 100% relative humidity (in air)

The 100% relative humidity and 100°C of temperature used was provided by the Tenney chamber.

##### 4.2.8.1 Beam conditioned to 100°C and 100% relative humidity: 40 cycles

After 40 cycles, all failures were cohesive in the concrete substrate, and the average pull-off strength was 5.08MPa. Table 4.22 shows these results. Figure 4.55 shows the conditioned beam, and figure 4.56 shows the beam with the dollies pulled.

Conditioning: 100°C and 100% Relative Humidity								
# Cycles	Dolly #	Pull-off Strength		Average		Std. dev.	CV (%)	Failure Mode
		MPa	psi	MPa	psi			
40	74-3	6.07	880	5.08	736	0.623	12.26	cohesive
40	74-4	4.83	700					cohesive
40	74-5	4.44	644					cohesive
40	74-6	4.81	697					cohesive
40	74-9	5.24	760					cohesive

Table 4.22: Results after 40 cycles of 100°C and 100% relative humidity



Figure 4.55: Beam exposed to 40 cycles of 100°C and 100% relative humidity

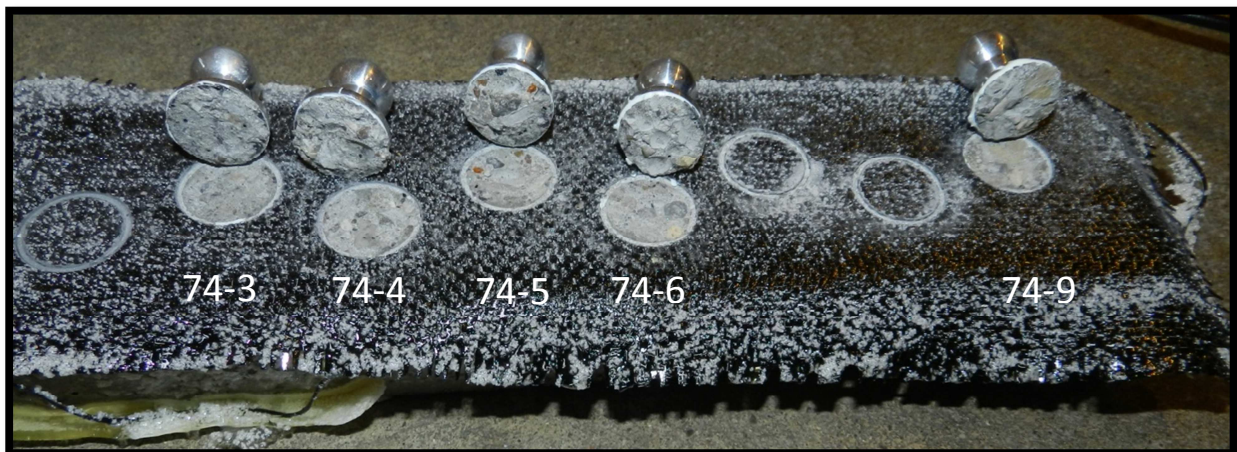


Figure 4.56: Dollies pulled from beam exposed to 40 cycles of 100°C and 100% relative humidity

#### 4.2.8.2 Beam conditioned to 100°C and 100% relative humidity: 100 cycles

Failures after 100 cycles of conditioning were mostly cohesive in the concrete substrate, and the average pull-off strength was 4.93MPa.

Table 4.23 shows these results. Figure 4.57 shows the conditioned beam, and figure 4.58 shows the pull-off tests done on this beam.



Conditioning: 100°C and 100% Relative Humidity								
# Cycles	Dolly #	Pull-off Strength		Average		Std. dev.	CV (%)	Failure Mode
		MPa	psi	MPa	psi			
100	75-1	5.96	864	4.93	715	1.246	25.26	cohesive
100	75-2	2.97	431					cohesive
100	75-3	4.46	647					mixed
100	75-5	5.42	786					cohesive
100	75-6	5.85	848					cohesive

Table 4.23: Results after 100 cycles of 100°C and 100% relative humidity



Figure 4.57: Beam exposed to 100 cycles of 100°C of temperature and 100% relative humidity

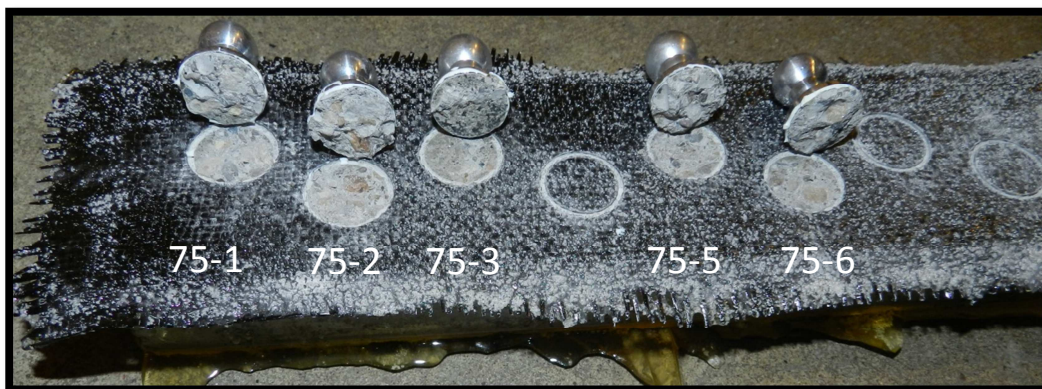


Figure 4.58: Pull-off tests on beam exposed to 100 cycles of 100°C and 100% relative humidity

#### 4.2.8.3 Beam conditioned to 100°C and 100% relative humidity: 250 cycles

Mixed failures started to be seen after 250 cycles of exposed to 100°C of temperature and 100% relative humidity. Still, failures were very cohesive. The average pull-off strength was 4.46MPa. Table 4.24 shows these results, and figure 4.59 and 4.60 shows the conditioned beam before and after testing. Figure 4.61 shows the dolies failure face.

Conditioning: 100°C and 100% Relative Humidity								
# Cycles	Dolly #	Pull-off Strength		Average		Std. dev.	CV (%)	Failure Mode
		MPa	psi	MPa	psi			
250	76-1	4.80	696	4.46	647	1.001	22.43	cohesive
250	76-4	5.13	744					mixed/cohesive
250	76-5	5.01	726					mixed/cohesive
250	76-6	2.70	392					mixed/cohesive
250	76-7	4.66	676					mixed/cohesive

Table 4.24: Results after 250 cycles of 100°C and 100% relative humidity



Figure 4.59: Beam exposed to 250 cycles of 100°C and 100% relative humidity

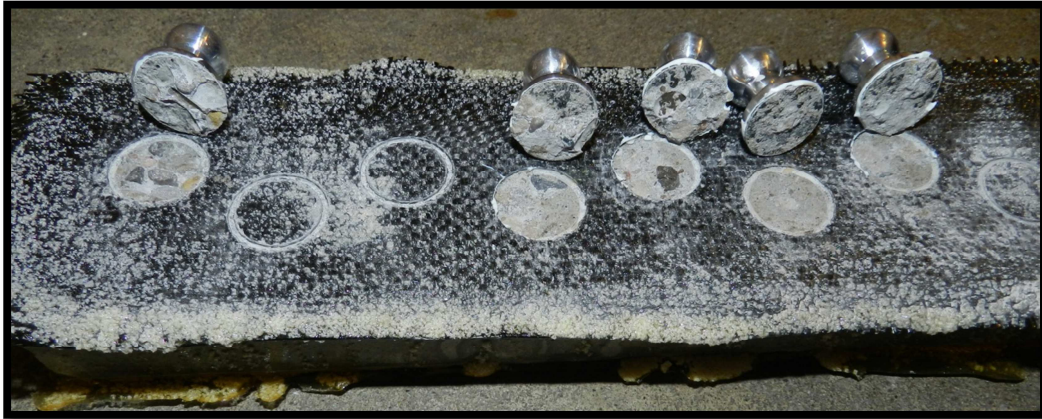


Figure 4.60: Pull-off tests on beam exposed to 250 cycles of 100°C and 100% relative humidity



Figure 4.61: Failure modes on dolies after 250 cycles of 100°C and 100% relative humidity

#### 4.2.9 Beam conditioned to 100°C and distilled water

Similarly to the 100% relative humidity and 100°C of temperature condition, the Tenney chamber was used to create the environmental exposure of 100°C of temperature and immersion in distilled water.

##### 4.2.9.1 Beam conditioned to 100°C and distilled water: 40 cycles

After 40 cycles of 100°C and immersion in distilled water, failures were mixed, and average pull-off strength was 2.55 MPa. A high coefficient of variation was obtained, as shown in table 4.24. Figure 4.62 shows the beam tested after conditioning, while figure 4.63 shows the dolies failure faces.



Conditioning: 100°C and Immersion in Distilled Water								
# Cycles	Dolly #	Pull-off Strength		Average		Std. dev.	CV (%)	Failure Mode
		MPa	psi	MPa	psi			
40	79-3	2.17	315	2.55	369	1.569	61.56	mixed
40	79-4	1.15	167					mixed
40	79-6	1.07	155					mixed
40	79-8	4.54	658					mixed
40	79-9	3.81	552					mixed

Table 4.25: Results after 40 cycles of 100°C and immersion in distilled water

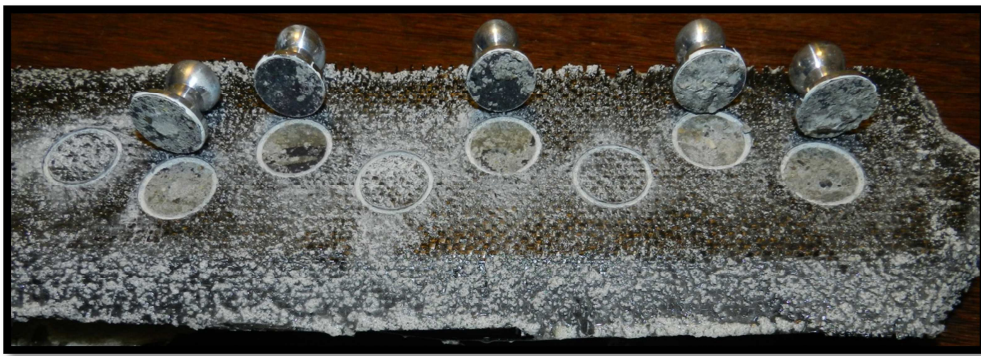


Figure 4.62: Beam tested after exposure to 40 cycles of 100°C and immersion in distilled water.



Figure 4.63: Dollies from testing the beam subjected to 40 cycles of 100°C and immersion in distilled water

#### 4.2.9.2 Beam conditioned to 100°C and distilled water: 100 cycles

The beam exposed to 100 cycles of 100°C and immersion in distilled water showed either mixed or adhesive failure modes. The average pull-off strength was 2.44 MPa, with a coefficient of variation larger than the 27.8% desired. Two out of the five pull-off values were lower than the minimum required by ACI 440, which shows the deterioration caused by the environmental conditions experienced. Table 4.25 shows these results.

Figures 4.64, 4.65, and 4.66 show respectively, the exposed beam, the tested dollies close to their testing locations, and the view of the faces of the dollies.

Conditioning: 100°C and Immersion in Distilled Water								
# Cycles	Dolly #	Pull-off Strength		Average		Std. dev.	CV (%)	Failure Mode
		MPa	psi	MPa	psi			
100	80-1	4.64	673	2.44	354	1.661	68.09	mixed
100	80-2	3.75	544					mixed
100	80-3	1.66	241					mixed
100	80-4	1.35	196					adhesive
100	80-5	0.80	116					adhesive

Table 4.26: Results after 100 cycles of 100°C and immersion in distilled water





Figure 4.64: Beam exposed to 100 cycles of 100°C and immersion in distilled water.



Figure 4.65: Beam exposed to 100 cycles of 100°C and immersion in distilled water with the tested dollies close to their testing locations.



Figure 4.66: Face of dollies removed from beam exposed to 100 cycles of 100°C and immersion in distilled water

#### 4.2.9.3 Beam conditioned to 100°C and distilled water: 250 cycles

Most failures in the beam exposed to 250 cycles of 100°C and immersion in distilled water were adhesive. The average pull-off strength was 2.06 MPa, with a coefficient of variation very larger. Table 4.26 shows the testing results for this condition.

Figure 4.67 shows the exposed beam, while figures 4.68 and 4.69 show the tested dollies close to their testing locations, and the view of the faces of the dollies.

Conditioning: 100°C and Immersion in Distilled Water								
# Cycles	Dolly #	Pull-off Strength		Average		Std. dev.	CV (%)	Failure Mode
		MPa	psi	MPa	psi			
250	81-1	3.66	531	2.06	298	1.518	73.74	mixed
250	81-2	0.64	93					adhesive
250	81-4	3.61	523					mixed
250	81-6	1.79	260					adhesive
250	81-8	0.59	86					adhesive

Table 4.27: Results after 250 cycles of 100°C and immersion in distilled water



Figure 4.67: Beam exposed to 250 cycles of 100°C and immersion in distilled water.



Figure 4.68: Dolliers from the beam exposed to 250 cycles of 100°C and immersion in distilled water.



Figure 4.69: Faces of dolliers removed from beam exposed to 250 cycles of 100°C and immersion in distilled water.

#### 4.2.10 Beam conditioned to 100°C and salt water

Beams were also exposed to 100°C of temperature and immersed in five percent of salt water by mass.

##### 4.2.10.1 Beam conditioned to 100°C and salt water: 40 cycles

After 40 cycles under 100°C of temperature and immersed in salt water, all specimens showed a cohesive failure in concrete substrate, and the average pull-off strength was 5.31 MPa. Table 4.27 shows the test results. Figure 4.70 shows the beam after conditioning, and figure 4.71 shows the tested dolliers close to their testing locations.



Conditioning: 100°C and Immersion in Salt Water								
# Cycles	Dolly #	Pull-off Strength		Average		Std. dev.	CV (%)	Failure Mode
		MPa	psi	MPa	psi			
40	68-1	5.48	795	5.31	770	1.002	18.86	cohesive
40	68-2	6.34	919					cohesive
40	68-3	6.19	898					cohesive
40	68-4	4.21	610					cohesive
40	68-5	4.34	629					cohesive

Table 4.28: Test results after 40 cycles of 100°C and salt water



Figure 4.70: Beam after conditioning.

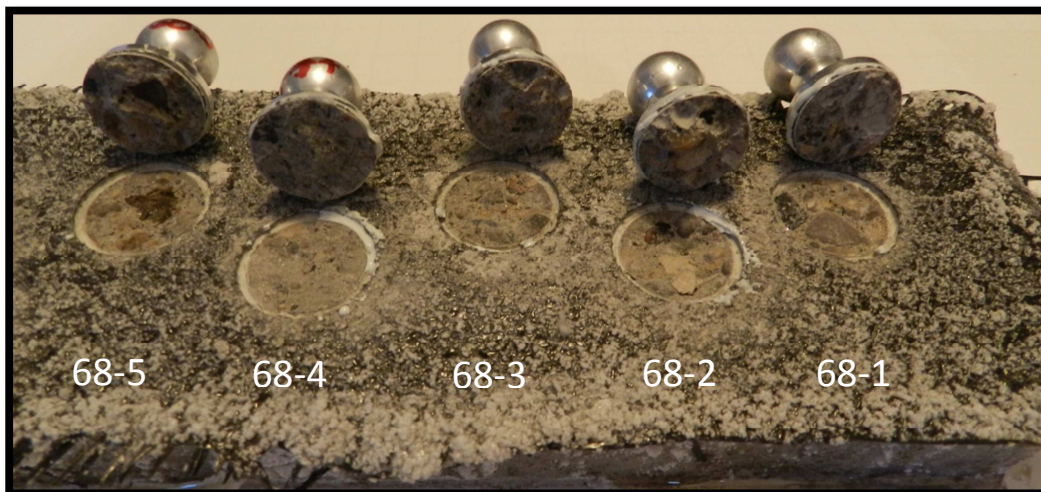


Figure 4.71: Conditioned and tested beam with dollies close to their testing locations.

#### 4.2.10.2 Beam conditioned to 100°C and salt water: 100 cycles

After 100 cycles of 100°C of temperature and immersion in salt water, the cohesive in concrete substrate was still the predominant mode of failure. The average pull-off strength was 4.51 MPa, as shown in table 4.28. Figure 4.72 shows the beam after conditioning, and figure 4.73 shows the dollies removed during testing.

Conditioning: 100°C and Immersion in Salt Water								
# Cycles	Dolly #	Pull-off Strength		Average		Std. dev.	CV (%)	Failure Mode
		MPa	psi	MPa	psi			
100	69-1	4.70	682	4.51	655	0.587	13.00	mixed
100	69-2	4.54	658					cohesive
100	69-3	3.84	557					cohesive
100	69-6	5.37	779					cohesive
100	69-8	4.12	597					cohesive

Table 4.29: Test results after 100 cycles of 100°C and salt water.



Figure 4.72: Beam after conditioning.

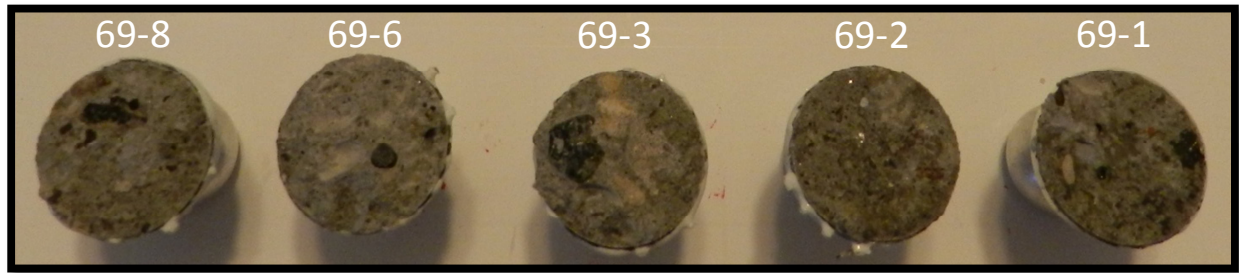


Figure 4.73: Dollies from beam exposed to 100 cycles of 100°C and salt water.

#### 4.2.10.3 Beam conditioned to 100°C and salt water: 250 cycles

After 250 cycles of 100°C of temperature and immersion in salt water, only four specimens could be tested due to the delamination of the fiber on the remaining of the beam. Since the composite was visibly deteriorated, failures were predominantly adhesive, and the coefficient of variation was very high. The average pull-off strength was 2.10 MPa, but two out of the four values obtained were under the minimum required by ACI440. One of the pull-off tests had a high strength compared to the others adjacent to it, which confirms the limitation of the pull-off test for each localized test site.

Table 4.29 shows the testing results. Figure 4.74 shows the beam after conditioning, and figure 4.75 shows a closer view of the delamination. Figures 4.76 and 4.77 show the dollies removed during testing at each test site and the failure faces of each dolly.

Conditioning: 100°C and Immersion in Salt Water								
# Cycles	Dolly #	Pull-off Strength		Average		Std. dev.	CV (%)	Failure Mode
		MPa	psi	MPa	psi			
250	70-1	4.99	724	2.10	304	2.044	97.58	mixed
250	70-2	0.72	104					adhesive
250	70-3	2.08	302					adhesive
250	70-4	0.59	86					adhesive
250	70-5	0	0					delaminated

Table 4.30: Test results after 250 cycles of 100°C and salt water



Figure 4.74: Beam after conditioning.



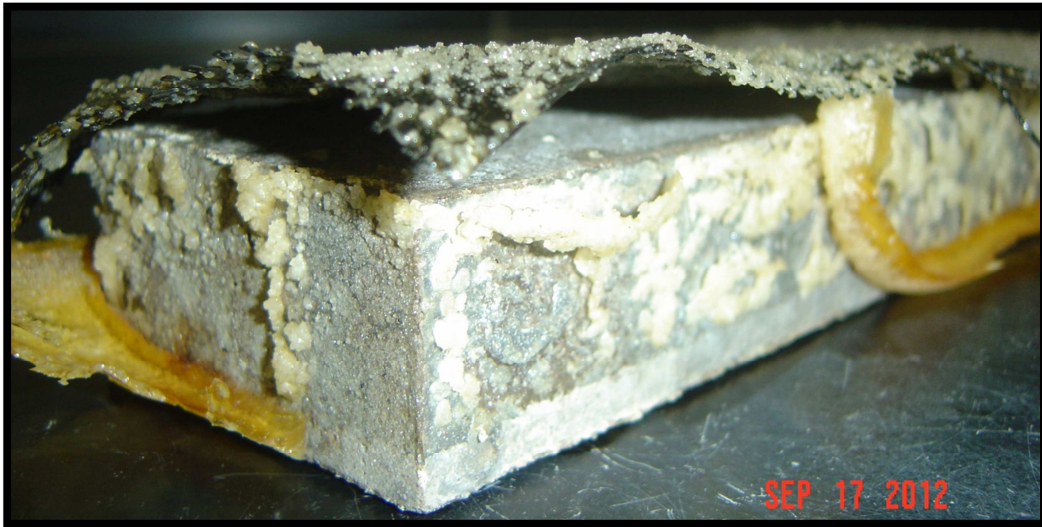


Figure 4.75: Visible delamination of fiber after beam was exposed to 250 cycles of 100°C and immersed in salt water.



Figure 4.76: Dollies removed during testing at each test site



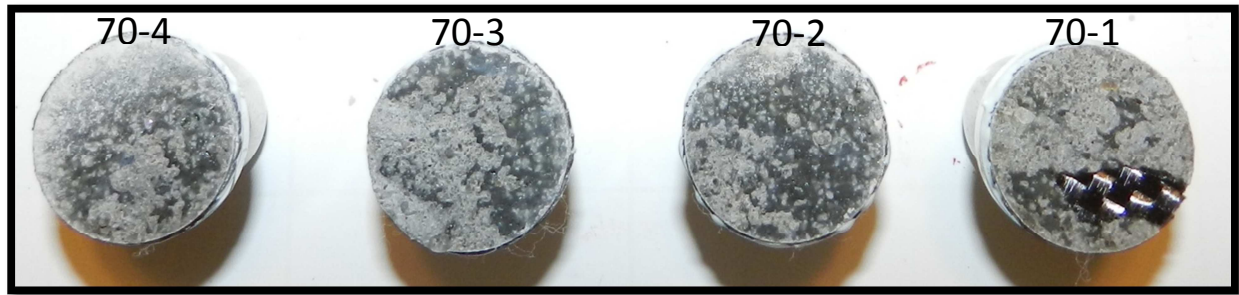


Figure 4.77: Dollies showing the failure modes from beam exposed to 250 cycles of 100°C and immersed in salt water.

#### 4.3 Observations

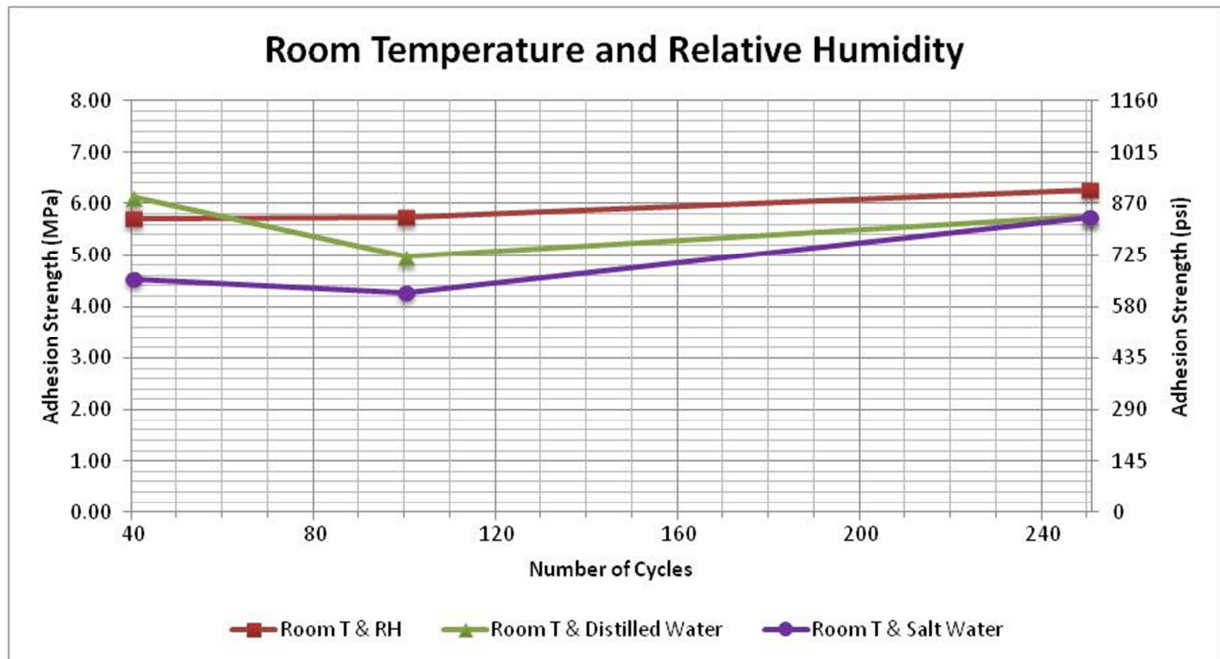


Figure 4.78: Comparison of average pull-off strength values for all conditions at room temperature and relative humidity.

Figure 4.78 can be used to compare the progression of the pull-off strength values for all conditions at room temperature and relative humidity (in air). Average bond strength values obtained for beams conditioned to room temperature and relative humidity, both in air and in salt

water, showed a slight improvement in strength with time. Beams immersed in distilled water at room temperature and relative humidity, however, did not show the same improvement, which might be associated to the large scatter obtained. The coefficient of variation for 100 cycles of room temperature and distilled water, for example, was 32.36%, which is larger than the 27.8% recommended by ASTM D4541. Overall, the addition of either distilled water or salt water did not characterize a significant reduction in strength when compared to the results in air at the same room temperature and relative humidity. All average strength values were above the minimum of 1.40 MPa required by ACI 440. Regarding the failure modes, there was no visible degradation, and failure remained cohesive in the concrete substrate.

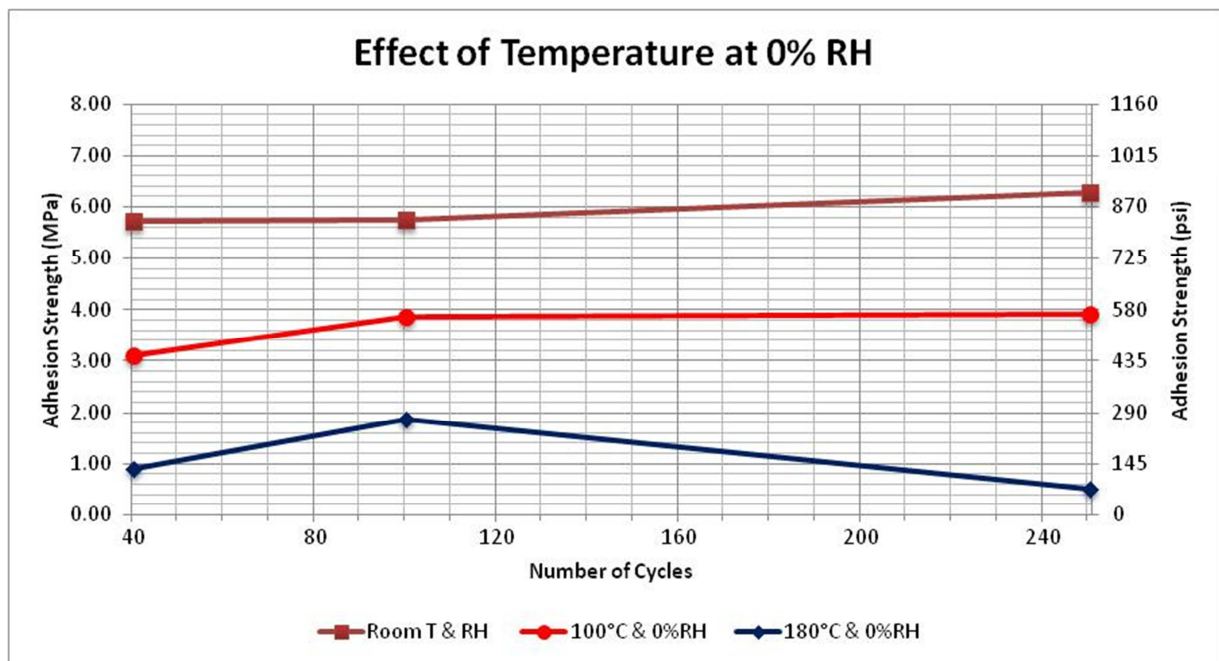


Figure 4.79: Average pull-off strength values at 0% relative humidity.

Using figure 4.79, it is possible to evaluate the effect of temperature at 0% relative humidity on the bond strength. Comparing the average pull-off strength at 100°C and 180°C at 0% relative humidity to the control sample, clearly the higher the temperature was, the lower was the bond strength. At 100 cycles, both averages at 100°C and at 180°C, showed an

increase in strength compared to the 40 cycles of exposure of each temperature. Typically, an initial increase in strength is attributed to the completion of the curing process of the resin with the elevation of the temperature, but strength values were still not higher than the control sample values. In contrast to the failure modes found in the 100°C specimens, which was mostly cohesive in the concrete substrate, a large delamination was found in the 180°C specimens, and adhesive failures were predominant. None of the strength values at 100°C and 0% relative humidity was below ACI 440 requirement of 1.40 MPa, however as expected due to the large deterioration, strength at 180°C and 0% relative humidity did reach unacceptable values.

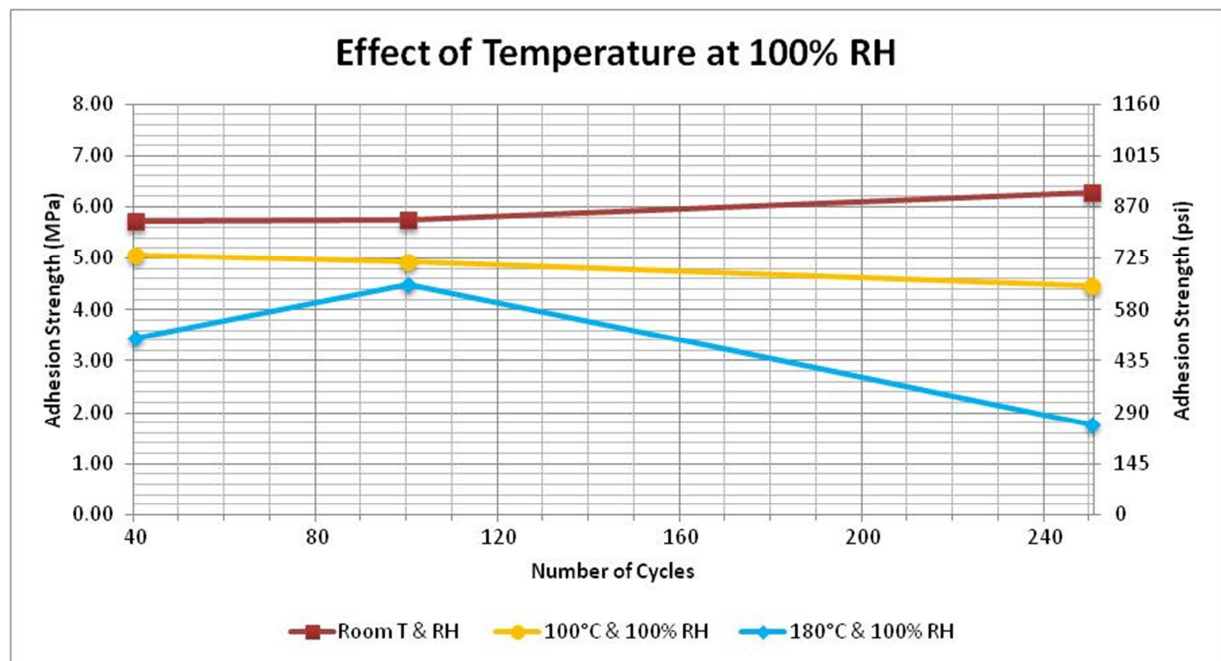


Figure 4.80: Average pull-off strength values at 100% relative humidity (in air).

Figure 4.80 shows the effect of temperature at 100% relative humidity on the bond strength. Comparing the average pull-off strength values at 100% relative humidity to the control sample, the higher temperature was more detrimental to the bond. At 100°C, strength decreased slightly over time, while the average at 180°C showed an increase in strength from

40 cycles to 100 cycles of exposure, before a continuing decrease after 100 cycles. Comparing all the data used in figure 4.80, a large coefficient of variation was only found at 180°C and 250 cycles. A large deterioration was also present at 180°C, 100% relative humidity and 250 cycles, which may be attributed to the chamber malfunction issue found at this specific condition. However it is not believed that this issue has impaired completely the results, since such an increase in temperature shows a higher decrease in strength when compared to the control sample, and in comparison to the 100°C pattern, even lower values were expected at this higher temperature, concluding that such issues may only have aggravated the values obtained and not affected the trend.

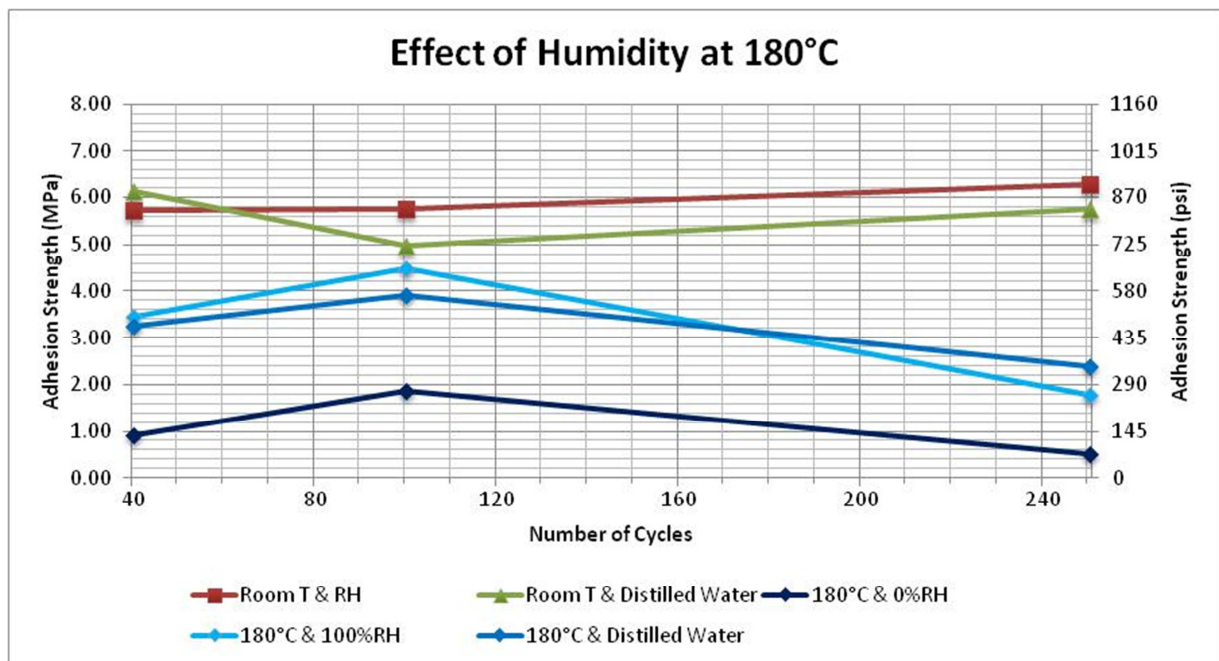


Figure 4.81 Average pull-off strength values at 180°C of temperature

Figure 4.81 shows the effect of humidity at 180°C of temperature on the bond strength. It was observed that the dry air (0% relative humidity) produced the lowest average pull-off strength values, and higher deterioration at 180°C, which was consistent to the flexural strength results found in Elarbi's [11] research. Similar results were obtained for both the 100% relative

humidity (in air) and immersion in distilled water. All average pull-off strength values were lower than the control sample values.

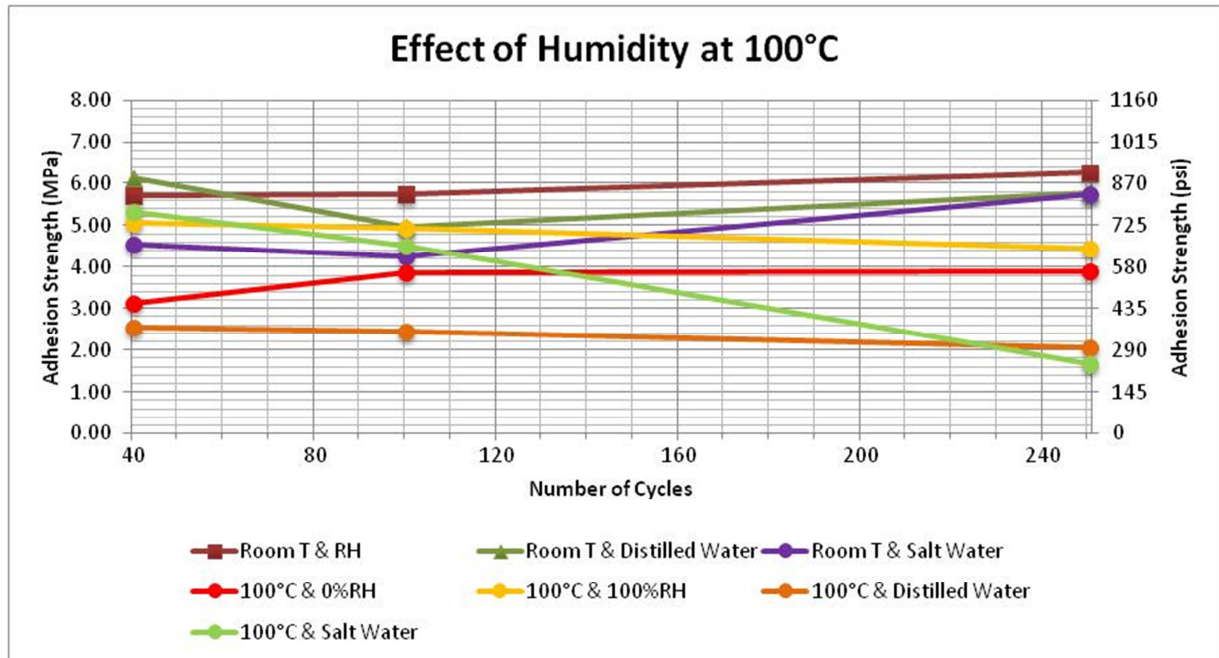


Figure 4.82: Average pull-off strength values at 100°C of temperature

The effect of humidity at 100°C of temperature on the bond strength can be evaluated from figure 4.82. It was observed that at 100°C both, the 100% relative humidity in air and immersed in distilled water followed the same trend of slight reduction in strength over time, with the specimens immersed in distilled water showing higher reduction in strength in comparison to the control samples, which might be attributed to the higher moisture uptake by the resin and consequently plasticization [24, 35]. The dry air (0% relative humidity) exposure at 100°C showed a slight increase in strength over time, consistent to Elarbi's results, but a strength reduction in comparison to the control sample smaller than that produced by the immersion in distilled water.

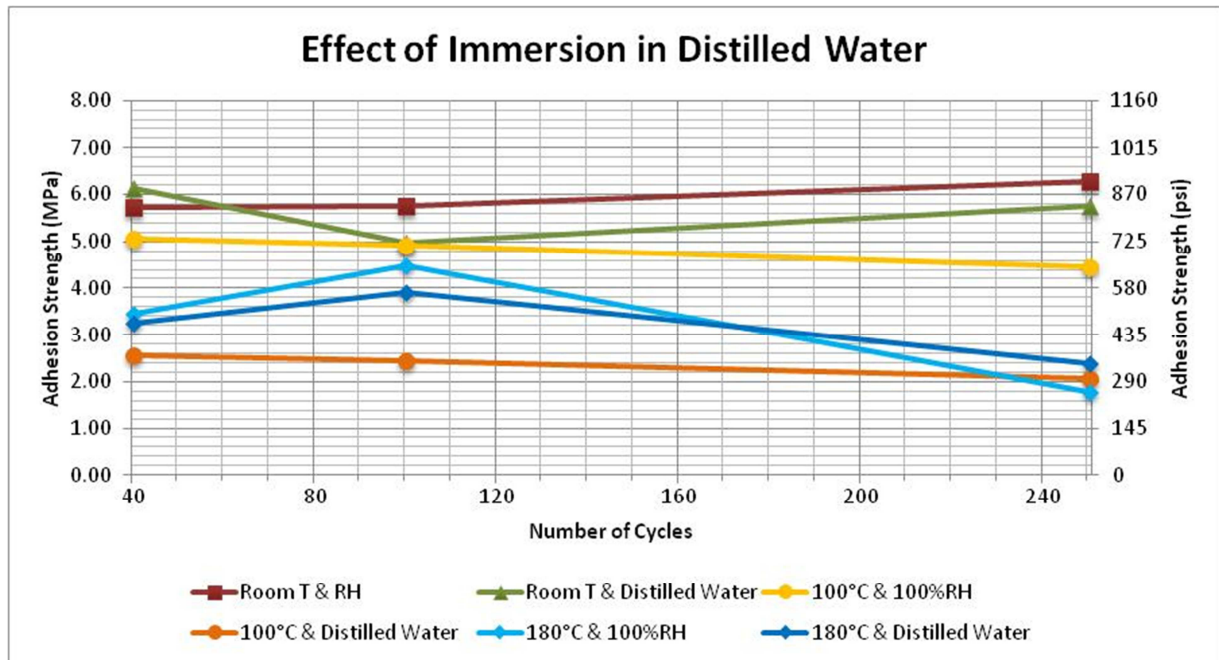


Figure 4.83: Average pull-off strength values showing the effect of immersion in distilled water

Figure 4.83 combines the results from both temperatures, 100°C and 180°C, the control samples, with 100% relative humidity in air or with immersion in distilled water. It can be observed that mainly during the first 100 cycles of exposure, immersion in distilled water caused a reduction in bond strength in comparison to the control samples higher than just exposure to 100% relative humidity, which might be attributed to the fully saturation of the resin followed by its plasticization [24, 35]. It was interesting to note that the lowest bond strength values were obtained at 100°C with immersion in distilled water, which might be explained by the formation of secondary cross linking (pseudo cross linking) at the higher temperature of 180°C [35]. However, the large scattering found on the experimental data indicates the need for further testing.



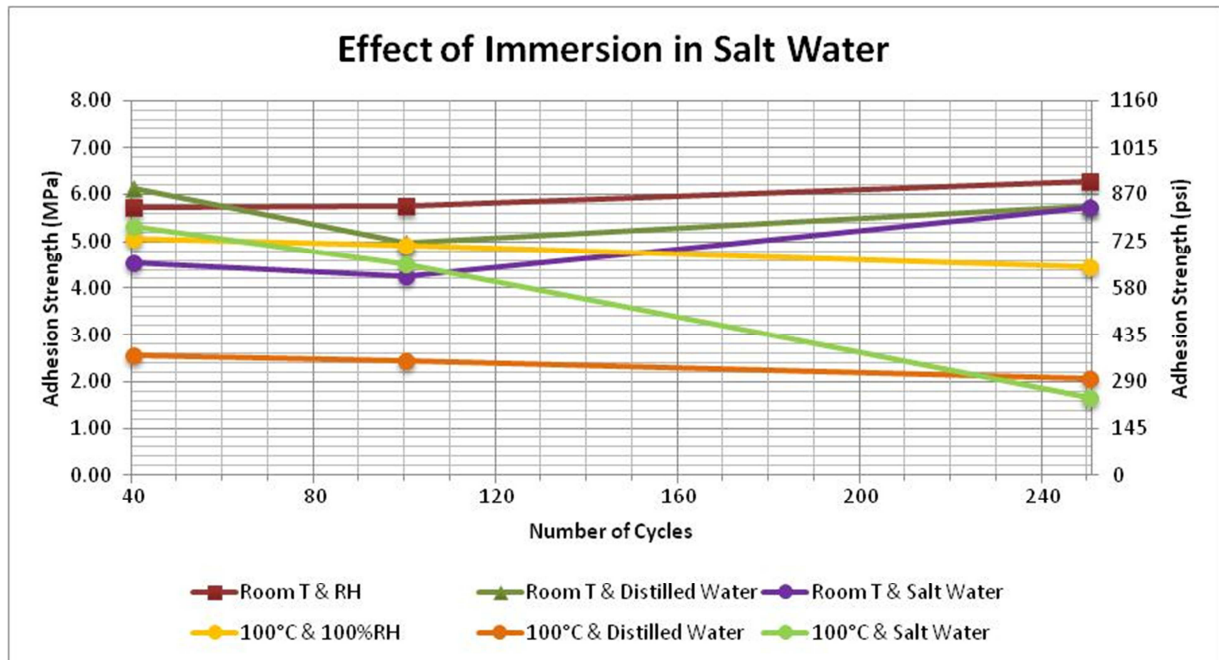


Figure 4.84: Average pull-off strength values showing the effect of immersion in salt water

Salt water was only used at 100°C. Figure 4.84 shows all room temperature conditions and all 100°C with 100% relative humidity conditions studied, including in air, in distilled water and in salt water. The addition of salt water showed to be detrimental only at 250 cycles, but further evaluation of the data obtained from all specimens immersed in salt water lead to the observation that a large delamination and large coefficient of variation was only found at 250 cycles. All failure modes for the samples immersed in salt water, with the exception of the 250 cycles, showed a cohesive failure in the concrete substrate, which reflects the tensile strength of the concrete, concluding that initially; the immersion might have contributed to further wet curing of the concrete substrate [17].

## **CHAPTER 5: CONCLUSIONS**

### **5.1 Conclusions**

In this experimental study, concrete beam specimens were cast, strengthened with a single ply of CFRP in a hand layup installation and exposed to cyclic hygrothermal (temperature and humidity) conditions, as well as immersed in distilled and salt water. The intention in this research was to study the effect of long term environmental exposure on the bond strength at the interface between concrete and FRP laminate, and to investigate the use of pull-off testing to develop comparable data on the CFRP bond degradation. The development of a continuation and comparison to Elarbi's research performed at Wayne State University was also intended.

Pull-off strength of a bonded FRP system is a performance property used in specifications, and for assessing the quality of an application [40]. Even though, in practice, the substrate failure is typically the desired failure mode, in order to evaluate the long-term performance of the adhesive bond, adhesive failure was the target failure mode in this study [23]. In general, as degradation occurred over time, not only the adhesive strength was reduced, but the failure mode also progressed from cohesive towards an adhesive failure, indicating the reduction in bond strength is faster than in concrete strength. In this research, large scatter commonly found in pull-off tests, was mainly associated to an uneven deterioration, mostly in beams with visible delamination and adhesive failure modes.

#### **5.1.1 Effect of High Temperatures**

According to the literature review, it was expected that high temperatures would cause degradation of the bond between CFRP and concrete substrate. Elarbi [11] has found no degradation on CFRP upon an increase in temperature to 100°C with flexural strength results higher than the control sample values, and an improvement in epoxy until 250 cycles (500 hours) at 100°C. An initial improvement in strength as temperature rises is typically associated

to the post curing process of the resin, which may not have been completely cured under ambient temperature [17]. In Elarbi's study, the 180°C of temperature produced a large deterioration in both CFRP and epoxy, evidenced by the partial melt of the epoxy resin, its change in color, and the delamination of the fiber [11].

In this study, the effect of temperature was clearly observed. Comparing the average pull-off strengths at 100°C and 180°C to the control sample, pull-off strength showed a reduction as temperature increased, concluding that the higher the temperature, the higher the bond degradation, and consequently, the lower the pull-off strength. All bond strength values were lower than the control sample values, still an improvement from 40 to 100 cycles was observed, which was consistent to Elarbi's results for 100°C. After 250 cycles, though, the 180°C temperature showed a very detrimental effect on the bond, also observed by Elarbi [11]. The thermal expansion mismatch between fiber, matrix and concrete, may have contributed to the deterioration by creating residual stresses, and thus micro-cracks at the interface as temperature changed [11, 39].

Regarding failure modes, in contrast to the primarily cohesive in concrete failure modes found at room temperatures and the cohesive/ mixed at 100°C specimens, the predominant failure mode found in specimens exposed to 180°C was adhesive, mainly due to the extensive delamination present, which was also reported by Elarbi. In the highly delaminated specimens, pull-off tests typically showed a large scatter.

The effect of the high temperature at 0% relative humidity was most damaging. The average adhesive strength, after 250 cycles (500 hours) of conditioning, for instance, dropped from 3.91 MPa at 100°C with mixed/ cohesive failure to 0.50 MPa at 180°C and adhesive failure, reaching values that are not acceptable according to ACI 440. It should be noted that the

bond strength of the control sample at the same age was 6.26 MPa, and failure occurred in the concrete substrate, which reflects the tensile strength of the concrete substrate.

### **5.1.2 Effect of Humidity**

In fully cured epoxy specimens, moisture exposure is expected to cause degradation of the mechanical properties of FRP, including the  $T_g$  value, due to the plasticization of the resin, but higher exposure temperatures and longer exposure time result in the formation of secondary cross-linking, lessening the depression of  $T_g$  [27, 36].

As indicated by Elarbi, and also found in the present research, humidity influences the strength of the system, especially at 180°C. In Elarbi's research, flexural strength values were lower at 0% relative humidity than at 100% relative humidity, and humidity caused a larger deflection in epoxy beams at 0% humidity. In this research, it was also found that 0% relative humidity condition produced lower pull-off strength values than the 100% relative humidity.

### **5.1.3 Effect of Immersion in Distilled Water**

Moisture absorption results in the development of residual stress and plasticization of the resin. [24] Depression of  $T_g$ , for instance, is expected to be the greatest once epoxy first reach saturation under hygrothermal exposure [36]. On the other hand, higher exposure temperature and longer exposure time result in the formation of secondary cross-linking, which lessen the depression of  $T_g$ . [35, 36]

In comparison to the control samples, the reduction in bond strength caused by immersion in distilled water was larger than the exposure to 100% relative humidity, especially at 100°C. Immersion in distilled water might have provided for a full moisture saturation of the specimen and plasticization of the resin at this temperature.

While failure modes of specimens immersed in distilled water at room temperature remained cohesive in concrete substrate and the strengths were not significantly affected, the higher temperatures might have contributed to accelerate the water diffusion process and deterioration of the FRP, since more mixed and adhesive failures were present [24]. Once the failure is initiated, crack propagation occurs in the weakest part of the bonded assembly, which becomes progressively the weakened epoxy interface due to moisture diffusion, leading to a change in failure mode [17, 21].

It was noticed that a large coefficient of variation was obtained for all cycles of specimens immersed in distilled water both at 100°C and 180°C, but not for the specimens immersed in distilled water at room temperature.

#### **5.1.4 Effect of Immersion in Salt Water**

While immersion in salt water solution at room temperature showed a gradual improvement in bond strength with time, such immersion at elevated temperature (100°C) has clearly shown a reduction in bond strength. After 250 cycles at 100°C and salt water solution, the beam specimen was about 60% delaminated and only four bond strength values could be obtained. Further evaluation of the data obtained lead to the observation that a large coefficient of variation was only found at 250 cycles. Initially, though, the salt immersion at 100°C showed better results when compared to immersion in distilled water at the same temperature or immersion in salt water at room temperature. All failure modes for the samples immersed in salt water, with the exception of the 250 cycles, showed a cohesive failure in the concrete substrate, which reflects the tensile strength of the concrete, concluding that the immersion might have contributed to further wet curing of the concrete substrate at initial exposure [17].

## 5.2 Future Work

This study has evaluated the effect of environmental exposure on the bond strength of CFRP and concrete using pull-off testing. Measurements from pull-off methods are considered to be dependent on the material and device used, as well as instrumental parameters and procedures, which create results not directly comparable [40]. Still, the use of pull-off testing was considered to be satisfactory for this research, since it allowed the drawing of trends and comparison to previous research observations as aimed. Additional research, though, can add a greater number of beams in each condition, and include different substrates. Beams can be immersed in water previously to start cycles to achieve saturation of the FRP layers and allow test results to predict much longer time of degradation [24]. Furthermore, measurements of the degree of cure of epoxy can be performed.

Future research can also be done on matrix durability to develop a deeper understanding of the failure mechanisms considering both physical and chemical changes in the system, and how they affect the properties of the materials involved. The impact of the intrinsic variability of FRP on the long term performance of this material under environmental exposure can then be completely understood.

It is important to emphasize that even with the complete understanding of the long term durability performance of any material, all materials age, and maintenance and inspection should be encouraged to guarantee the expected performance during its service life. The adhesive strength is affected by environmental exposure, such as temperature, humidity and presence of water. Long term exposure may be very detrimental, and the minimum of 10 year record suggested by ACI-503 should be followed to ensure that the material is performing well in every single job site.



## REFERENCES

1. Nawy, E. G. "Concrete Construction Engineering Handbook.", second edition, CRC Press, 2008. <<http://www.crcnetbase.com/doi/pdf/10.1201/9781420007657.fmatt>>
2. Neville, A.M. "Properties of concrete.", fourth edition, England: Pearson Education, Prentice Hall, 2012.
3. Wight, J. K., and MacGregor, J. G. "Reinforced Concrete: Mechanics and Design.", sixth edition, New Jersey: Pearson Education, Prentice Hall, 2012.
4. Kett, I. "Engineered Concrete Mix Design and Test Methods." CRC Press, LLC, 2000.<<http://www.crcnetbase.com/isbn/9781420049831>>
5. Woodson, R. D. "Concrete Structures: Protection, Repair and Rehabilitation.", Elsevier, Inc. , 2009. <<http://www.sciencedirect.com/science/book/9781856175494>>
6. Page, C. L., and Page, M. M., "Durability of Concrete and Cement composites." CRC Press LLC, 2007.
7. Fyfe Product Data Sheet: Tyfo<sup>®</sup> S Saturant Epoxy, Fyfe Co. LLC, May 2011. <<http://www.fyfeco.com/products/pdf/tyfosepoxy.pdf>>
8. Sika<sup>®</sup> Carbodur Composite Strengthening Systems. "Section 03 01 30.72: Strengthening of Concrete with FRP (Fiber Reinforced Polymer) Reinforcement." <<http://usa.sika.com/dms/getdocument.get/b352cd28-0f57-3c1f-afbf-6bedb4226d3e/sc-cpd-CarboDurSikaWrap-us.pdf>>
9. Wu, H. "Advanced Composite Materials for Civil Infrastructure." Lecture. September 2009.
10. Bank, L. C. "Composites for construction: structural design with FRP materials." New Jersey: John Wiley & Sons, 2006.

11. Elarbi, A. M. "Durability Performance of FRP Strengthened Concrete Beams and Columns Exposed to Hygrothermal Environment". PhD Dissertation. Wayne State University, 2011.
12. Epoxy Technology. "Epoxy Adhesive Application Guide." 32- 37. 2012  
<<http://www.epotek.com/SSCDocs/BrochuresandSelectorGuides/Brochures/AdhesiveApplicationGuide.pdf>>
13. Sika® Product Data Sheet: SikaWrap® Hex 113C., edition July 2008.  
<<http://us01.webdms.sika.com/files/show.do?documentID=324>>
14. Epoxy Technology. "Understanding Mechanical Properties of Epoxies For Modeling, Finite Element Analysis (FEA)." Tech Tip 19. 2011.  
<<http://www.epotek.com/SSCDocs/techtips/Tech%20Tip%2019%20-%20Understanding%20Mechanical%20Properties%20of%20Epoxies%20for%20FEA.pdf>>
15. Malhotra, V. M., and Carino, N. J., "Handbook on Nondestructive Testing of Concrete.", second edition, CRC press, 2003.
16. ACI 440.2R-08. "Guide for the Design and Construction of Externally Bonded FRP Systems for Strengthening Concrete Structures." 2008. Reported by ACI Committee 440.
17. Silva, M. A. G., and Biscaia, H. 2007. "Degradation of bond between FRP and RC beams.", Composite Structures, Volume 85, Issue 2, September 2008, 164-174, March 26, 2011.,  
<<http://www.sciencedirect.com/science/article/pii/S0263822307002516>>
18. Grace, N. F. "Concrete Repair with CFRP." Concrete International. May 2004. October 13, 2011,  
<<http://www.financialaid.ltu.edu/cm/attach/B6FC1930-05B0-447D-98A2-05ACB25736D1/CI2605Grace.pdf>>

19. Silva, M. A. G., and Biscaia, H. 2010. "Effects of exposure to saline humidity on bond between GFRP and concrete." *Composite Structures*, Volume 93, Issue 1, December 2010, 216-224, October 13, 2011.
  
20. Malvar, L. J., ASCE, M., Joshi, N.R., Beran, J. A., and Novinson, T. 2003. "Environmental Effects on the Short-Term Bond of Carbon Fiber-Reinforced Polymer (CFRP) Composites." *Journal of Composites for Construction*. May 11, 2011, 58-63  
<<http://ascelibrary.org/doi/pdf/10.1061/%28ASCE%291090-0268%282003%297%3A1%2858%29>>
  
21. Benzarti, K., Chataigner, S., Quiertant, M., Marty, and C., Aubagnac, C. 2010. "Accelerated ageing behavior of the adhesive bond between concrete specimens and CFRP overlays." *Construction and Building Materials*. May 23, 2011, <[http://ac.els-cdn.com/S095006181000423X/1-s2.0-S095006181000423X-main.pdf?\\_tid=b1dc5afc-0e32-11e2-9b6e-00000aab0f26&acdnat=1349362347\\_8d9433afbb7726bc2aa4133e67af6449](http://ac.els-cdn.com/S095006181000423X/1-s2.0-S095006181000423X-main.pdf?_tid=b1dc5afc-0e32-11e2-9b6e-00000aab0f26&acdnat=1349362347_8d9433afbb7726bc2aa4133e67af6449)>
  
22. Nishizaki, I., and Kato, Y. 2010. "Durability of the adhesive bond between continuous fibre sheet reinforcements and concrete in an outdoor environment." *Construction and Building Materials*. <[http://ac.els-cdn.com/S0950061810002151/1-s2.0-S0950061810002151-main.pdf?\\_tid=e1af64e0-0e32-11e2-b49b-00000aab0f26&acdnat=1349362427\\_d1a55318b689041da9f23f7447f15ef3](http://ac.els-cdn.com/S0950061810002151/1-s2.0-S0950061810002151-main.pdf?_tid=e1af64e0-0e32-11e2-b49b-00000aab0f26&acdnat=1349362427_d1a55318b689041da9f23f7447f15ef3)>
  
23. Gartner, A., ASCE, M., Douglas, E. P., Dolan, C. W., and Hamilton, H. R. 2011. "Small Beam Bond Test Method for CFRP Composites Applied to Concrete. *Journal of Composites for Construction*." June 03, 2011, <<http://ascelibrary.org/doi/pdf/10.1061/%28ASCE%29CC.1943-5614.0000151>>
  
24. Li, G., Pang, S., Helms, J. E., Mukai, D., Ibekwe, S. I. and Alaywan, W. 2002. "Stiffness Degradation of FRP Strengthened RC Beams Subjected to Hygrothermal and Aging

- Attacks.” Journal of Composite Materials. February 02, 2012, <<http://jcm.sagepub.com/content/36/7/795.full.pdf>>
25. McSweeney, B. M., and Lopez, M. M. “FRP-Concrete Bond Behavior: A Parametric Study Through Pull-off Testing.” June 03, 2011, <<http://www.quakewrap.com/frp%20papers/FRP-ConcreteBondBehaviorAParametricStudyThroughPull-OffTesting.pdf>>
26. Myers, J. J., and Ekenel, M. “Effect of Environmental Conditions on Bond Strength between CFRP Laminate and Concrete Substrate.” June 03, 2011, <<http://www.quakewrap.com/frp%20papers/EffectofEnvironmentalConditionsonBondStrengthbetweenCFRPLaminateandConcreteSubstrate.pdf>>
27. Jones, R. H., “Environmental Effects on Engineered Materials.” first edition, CRC Press, 2001.
28. Abanilla, M. A., Li, Y., and Karbhari, V. M. 2005. “Durability Characterization of Wet layup graphite/epoxy composites used in external strengthening.” Composite Part B: engineering. February 02, 2012, <[http://ac.els-cdn.com/S135983680500082X/1-s2.0-S135983680500082X-main.pdf?\\_tid=de184ca6-0e33-11e2-bbe0-00000aacb360&acdnat=1349362850\\_0703111ca1252b3100b0311e90185cf2](http://ac.els-cdn.com/S135983680500082X/1-s2.0-S135983680500082X-main.pdf?_tid=de184ca6-0e33-11e2-bbe0-00000aacb360&acdnat=1349362850_0703111ca1252b3100b0311e90185cf2)>
29. Chin, J. W., Nguyen, T., and Aouadi, K. 1998. “Sorption and Diffusion of Water, Salt Water, and Concrete Pore Solution in Composite Matrices.” February 02, 2012, <<http://fire.nist.gov/bfrlpubs/build99/PDF/b99004.pdf>>
30. Y. Kato, M. Quiertant, K. Benzarti, S. Chataigner, I. Nishizaki, and C. Aubagnac, 2008. “Durability of CFRP strengthened concrete structures under accelerated or environmental ageing conditions.” Concrete Repair, Rehabilitation and Retrofitting. Taylor & Francis Group,

London. CRC Press. 421- 422.  
[<http://www.crcnetbase.com/doi/pdf/10.1201/9781439828403.ch167>](http://www.crcnetbase.com/doi/pdf/10.1201/9781439828403.ch167)

31. Raupach, M., and Wolff, L., 2008. "Durability of adhesion of epoxy coatings on concrete; causes of delamination and blistering." Concrete Repair, Rehabilitation and Retrofitting. Taylor & Francis Group, London. CRC Press. 337- 338  
[<http://www.crcnetbase.com/doi/pdf/10.1201/9781439828403.ch129>](http://www.crcnetbase.com/doi/pdf/10.1201/9781439828403.ch129)
  
32. Wu, H., and Yan, A. 2011. "Time-dependent deterioration of FRP bridge deck under freeze/thaw conditions." Composites Part B: Engineering. March 23, 2011 [<http://ac.els-cdn.com/S1359836811000837/1-s2.0-S1359836811000837-main.pdf?\\_tid=3363ca04-0e35-11e2-9b0f-00000aacb35d&acdnat=1349363423\\_c33f88f027c05f728c89747a3d82d016>](http://ac.els-cdn.com/S1359836811000837/1-s2.0-S1359836811000837-main.pdf?_tid=3363ca04-0e35-11e2-9b0f-00000aacb35d&acdnat=1349363423_c33f88f027c05f728c89747a3d82d016)
  
33. Bissonnette, B., Nuta, A., Morency, M., Marchand, J., and Vaysburd, A. M., 2008. "Concrete repair and interfacial bond: Influence of surface preparation." Concrete Repair, Rehabilitation and Retrofitting. 2009. Taylor & Francis Group, London. CRC Press. 345- 346  
[<http://www.crcnetbase.com/doi/pdf/10.1201/9781439828403.ch132>](http://www.crcnetbase.com/doi/pdf/10.1201/9781439828403.ch132)
  
34. Bonaldo, E., Barros, J.A.O., Lourenço, P.B., "Bond characterization between concrete substrate and repairing SFRC using pull-off testing.", International Journal of Adhesion and Adhesives, Volume 25, Issue 6, December 2005, 463-474,  
[<http://www.sciencedirect.com/science/article/pii/S0143749605000096>](http://www.sciencedirect.com/science/article/pii/S0143749605000096)
  
35. Zhou, J., Lucas, J.P. "Hygrothermal effects of epoxy resin. Part I: the nature of water in epoxy.", Polymer, Volume 40, Issue 20, September 1999, 5505-5512,  
[<http://www.sciencedirect.com/science/article/pii/S0032386198007903>](http://www.sciencedirect.com/science/article/pii/S0032386198007903)

36. Zhou, J., Lucas, J.P., "Hygrothermal effects of epoxy resin. Part II: variations of glass transition temperature", Polymer, Volume 40, Issue 20, September 1999, 5513-5522, <<http://www.sciencedirect.com/science/article/pii/S0032386198007915>>
37. Positest® Pul-off Adhesion Tester Literature. Defelsko.< <http://www.defelsko.com/adhesion-tester/PosiTestAT.pdf>>
38. Williams, M.E., Bouadi, H., and Choudhuri, D. "FRP Retrofit Solutions." Structures Magazine online. 2008.<<http://www.structuremag.org/Archives/2008-1/C-BB-FRP-Retrofit-WPMoore-Jan08.pdf>>
39. ACI 503R- 93 "Use of epoxy compounds with concrete." Reported by committee 503. 1993. <<http://www.cargill.com/wcm/groups/public/@ccom/@ps/@industrial/@winter/documents/document/cdt-safelane-aci-531-tech-data.pdf>>
40. ASTM D7522/D7522M – 09. "Standard Test Method for Pull-off Strength for FRP Bonded to Concrete Substrate." 2009.
41. ASTM D4541 – 09. "Standard Test Method for Pull-off Strength Using Portable Adhesion Testers." 2009.
42. ASTM D7234 – 05. "Standard Test Method for Pull-off Adhesion Strength of Coatings on Concrete Using Portable Pull-off Adhesion Testers." 2005.
43. ASTM C39/C39M – 09a. "Standard Test Method for Compressive Strength of Cylindrical Concrete Specimens." 2009.
44. ASTM C192/C192M – 07. "Standard Practice for Making and Curing Concrete Test Specimens in the Laboratory." 2007.



45. DeFelsko® Corporation. Positest® Pull-off Adhesion Tester: Instruction Manual v. 4.0. 2011.<<http://www.defelsko.com/manuals/download/at/PosiTestAT-v4.0.pdf>>
46. DeFelsko® Corporation Website. Positest® Pull-off Adhesion Tester. 2012. <<http://www.defelsko.com/adhesion-tester/features.htm#selfalign>>
47. MDA Composites. "Why use FRP composites?" American Composites Manufacturers Association, 2004.<[http://www.mdacomposites.org/mda/why\\_frp.html](http://www.mdacomposites.org/mda/why_frp.html)>

**ABSTRACT****FRP BOND STRENGTH DEGRADATION: AN EXPERIMENTAL STUDY USING PULL-OFF TESTING**

by

**CLARISSE MACHADO MIKAMI**

December 2012

**Advisor:** Dr. Hwai-Chung Wu**Major:** Civil Engineering**Degree:** Master of Science

Fiber reinforced polymer (FRP) is an advanced composite material that has been employed efficiently to rehabilitate deteriorated concrete structures. Environmental factors, however, affect the durability performance of FRP. As bond at the interfacial region between FRP and concrete is essential to the overall integrity of the system, the focus of this thesis is on bond deterioration due to hot weathering conditions.

In this study, an experimental program was developed to investigate the effect of long-term environmental exposure on bond strength. During this program, concrete beam specimens were cast, strengthened with a single ply of CFRP in a hand layup installation method and exposed to accelerated tests in the laboratory, such as cyclic hygrothermal (temperature and humidity) conditions, and immersion in distilled and salt water. Pull-off testing was used to generate quantitative data on the CFRP bond degradation, which allowed as aimed, the drawing of trends, conclusions and a comparison to previous work performed at Wayne State University. Future research was also recommended to further enlighten this issue.

**AUTOBIOGRAPHICAL STATEMENT****CLARISSE MIKAMI**

Clarisse Mikami received her Bachelor of Science in Civil Engineering in 2001 from the Escola de Engenharia de Piracicaba, Piracicaba, Brazil. She has been studying towards her master degree in Civil Engineering at Wayne State University since 2009. Her research interests include concrete technology, retrofit of concrete structures using fiber reinforced polymer composites (FRP), and materials testing.